Structural behaviour of tapered steel plate girders subjected to shear

Doctoral Thesis by
Agnieszka Bedynek

Supervised by
Prof. Esther Real Saladrigas
Prof. Enrique Mirambell Arrizabalaga

Barcelona, February 2014

Universitat Politècnica de Catalunya, Barcelona Tech
Departament d´Enginyeria de la Construcció

DOCTORAL THESIS

Acknowledgements

After nearly six years since I had arrived in Spain and started my PhD experience not only my professional life has changed. During my studies I had to learn new languages, understand and adapt to a new environment and culture, what meant - create my world from the beginning. Since the first days of my stay here, Esther and Quique have not only been my supervisors but also they have been substituting my family. Thank you Esther for you brilliant ideas and willingness to be always ready in supporting me in both - personal and professional life and you Quique - for your clear and critical advice and always constructive point of view.

I would like to express my gratitude to the Spanish Ministry of Science and Innovation for financial support provided as a part of the Research Project BIA2008-01897 and for a doctoral scholarship awarded for four years. Additionally, I wish to thank the Universitat Politècnica de Catalunya for the grant awarded in 2009 which helped me to complete the first stage of my studies.

I am very grateful for the help provided by the staff of the Laboratory of Structural Technology of Universitat Politècnica de Catalunya in both Experimental Campaigns, especially to my technician Carlos Hurtado for his peculiar sense of humour and to Jordi Cabrerizo for his creativity and willingness to share with me his innovative solutions.

Also I would like to thank my colleagues who were working with me in the laboratory - Lorena, Marcos and Carles, for sharing with me all hard moments and their undisputed positive influence on the final form of my thesis. Also I wish to thank Cefe – our great cameraman for his involvement in our work.

I have to give great thanks to my workmates, to Denise – for her every-single-day company and to Rolando, for his advice and for sharing with me his experience, especially in the beginning phase of my studies.

I wish to say "thank you" to my parents - for their unconditional love, for inculcating me the passion for science and especially for respecting my decisions.

And finally, I would like to give the most sincerely thanks and dedicate this work to Jordi, my partner and my best friend, for his immense support and being with me every day, his love and understanding, patience and most of all for everlasting "positive energy" passed on to me especially in the most difficult moments.

Thank you all

Summary

Tapered plate girders often form part of large-scale structures such as long continuous bridges or industrial buildings where due to considerable loads the higher resistance is required. There are several important reasons choosing non-prismatic girders. First of all, their tapered shape with gradually changing inertia allows for more effective stress distribution inside the web-panel and contributes to steel reduction and thereby to decrease the overall cost of the structure. Trapezoidal shape of such panels also may be desirable in structures with non-standard shape for example where pre-formed service openings are needed.

In this thesis several important issues related to tapered steel plate girders subjected to shear were studied. The main objective of this work was development of the reliable design tool to assess the ultimate shear resistance of non-prismatic plate girders. As the research was progressing some new interesting problems and unknowns appeared and had to be solved.

Although rectangular plate girders were studied in many occasions in last few decades, the latest investigations have shown that the structural behaviour of tapered panels is much more complex and there are new factors which should be studied and taken into account in design process. Apart from the instability problem which is common to all structures with higher slenderness, the new one is related to the additional force appearing in the inclined flange. It has been proved that vertical component of this axial force can positively or negatively influence the ultimate shear resistance of the tapered web-panel. This phenomenon is known as the Resal effect and also was widely studied in this thesis.

Above mentioned instability problems often can be solved with the design of transversal and/or longitudinal stiffeners. Dividing the web-panel into one or more sub-panels also the slenderness of each of them is reduced and automatically the critical shear load of whole panel increases. In case of tapered plate girders this improvement not always is correlated directly with the increase of the ultimate shear strength. Nevertheless, the reduction of the slenderness would be recommended to avoid web-breathing. This phenomenon can be caused by an application of the in-plane repeated loads (whose level rises above the critical load) and significant out-of-plane displacements of the web may appear. As a consequence, failure may be caused by fatigue of welded junctions between the flange-web-stiffener. In fact, to protect the structure against web-breathing, it is necessary to know an exact value of the critical shear load. Even though EN 1993-2 provides the additional specification for very slender rectangular plate girders, there are no rules to assess the actual value of the critical shear load for tapered elements. In this thesis an attempt of improvement this situation also was done.

In spite of a few references in the worldwide bibliography dealing with the issue of tapered plate girders subjected to shear, the current design code EN 1993-1-5 does not provide detailed specification for tapered members when the angle of the inclined flange is greater than 10˚.

Studies on all previously mentioned issues helped to understand the behaviour of tapered panels and to define the principal goal of this research - searching for simple analytical solution for assessment of the ultimate shear resistance of tapered plate girders, valid for different geometric parameters and structural situations.

The main body of the thesis is composed of four independent publications where each of them summarizes different phase of the investigation. The most important issues related to tapered panels discussed in the papers were: the critical shear load in tapered simple-supported plates, the influence of the geometrical and structural imperfections, the optimal position of the longitudinal stiffener and finally the ultimate shear resistance of stiffened and unstiffened tapered plate girders.

The methodology applied in the research consists of the following stages: study of the bibliography and initial theoretical research, development of a numerical model, two experimental campaigns, parametric studies, analysis of the experimental and numerical results against the EN 1993-1-5 and finally - development of a new design proposal for the assessment of the ultimate shear resistance for tapered steel plate girders.

In the initial stage of the PhD period, as a result of numerous approaches and verifications, the numerical model was developed. The optimum between its simplicity and accuracy had to be found. The numerical model was defined with use of finite shell elements, which are especially suitable in non-linear analysis where large rotations and displacements are expected. Full 3D model of a symmetric tapered steel plate girder with realistic boundary conditions was very useful in predicting of behaviour of such members in experimental tests and allowed placing the measure equipment in the most efficient way.

The PhD research was supported by two experimental programs focused on the structural behaviour of tapered plate girders. In the first part, the transversally stiffened members subjected to shear and shear-bending interaction, were tested. The second experimental campaign was focused on longitudinally stiffened tapered plate girders under shear. The complex measure equipment used in tests allows controlling the full strain-state at the interesting points, the out-of-plane displacements of the web-panel and the maximum deflection of the girders measured at the mid-span.

Results obtained from the experimental tests were used in the verification of the numerical model. Plate girders reveal tendency to possess a significant post-buckling resistance. This phenomenon can be observed as a diagonal tension field developing within the web-panel. In both, experimental and numerical tests this characteristic behaviour was observed. A good agreement between qualitative and quantitative outcomes obtained from the numerical studies and experimental tests allowed concluding that the numerical model was defined correctly and could be used in further numerical simulations conducted for tapered panels varying the most relevant geometric parameters.

Once verified the numerical model, it was used to carry out a parametric study for a large number of tapered plate girders. All numerical results presented in this research were compared with those obtained according to EN 1993-1-5 rules. The differences between them were deeply discussed, highlighting inconsistencies between the two above-mentioned procedures – the numerical model and EN 1993-1-5.

Finally, a new design method for the assessment of the ultimate shear resistance of tapered steel plate girders was presented. The new design proposal is based on the currently valid - Rotated Stress Field Method. The procedure maintains its simplicity and improves considerably results obtained for non-prismatic panels. This new reliable design tool, valid for any geometry and any typology of tapered steel plate girders, provides a solution of the principal objective defined in this research.

***Keywords*:** tapered steel plate girders; critical shear load; ultimate shear resistance; design code, EN1993-1-5, instability; FE model; nonlinear analysis; experimental tests; imperfections; residual stresses; Resal effect; transversal and longitudinal stiffeners; shear-bending interaction.

Summary

Table of Contents

1. Introduction

1.1. Background of the problem

In many structures such as industrial buildings or long-span continuous steel and composite bridges, tapered plate girders become the most efficient solution from the economic and structural point of view. The most common is the situation where plates with varying depth are situated in the structure according to the distribution of internal forces. In this way, the largest cross-sections should be applied in places where the greatest internal forces are expected what allows reducing consumption of steel used in the structure and its cost. Consequently, the smallest cross-sections should be situated in those parts of the structure where internal forces are not excessive. **Fig. 1.1** illustrates this situation.

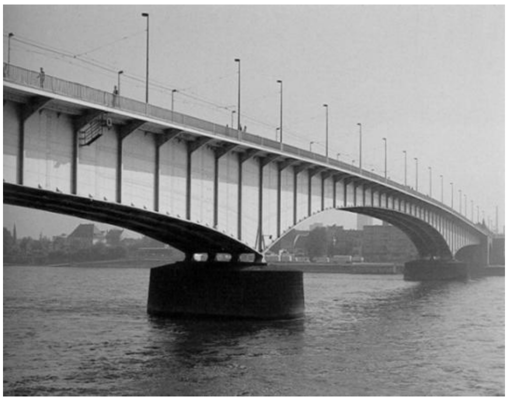

Fig. 1.1. Tapered plate girders in long continuous bridge over The Rhine River, Colonia-Deuz, Germany (photo: Leonhardt, 1986)

Other example of an application of tapered plate girders may be the Bullring Shopping Centre in Birmingham, UK (**Figs. 1.2a-b**). Inside the building plate girders incorporating service openings facilitated integration of services with the structure. Services could run in the void provided by the structural form (**Fig. 1.2a**) or in the pre-formed service openings (**Fig. 1.2b**).

Images taken from http://www.newsteelconstruction.com/wp/the-new-bullring-shopping-centre.

Fig. 1.2. The Bullring Shopping Centre in Birmingham in UK.
a) Bespoke plate girders **b)** Plate girders with provision for services in the web.

Apart from the undisputed advantages of tapered plate girders such as less self-weight, modern look and high slenderness, there are also some disadvantages which should be taken into consideration in the design of this kind of structures.

The high slenderness of the web-panels may cause the most frequent problem which is their global instability. Often, in order to limit the slenderness and avoid excessive deformation of the web, additional transversal and longitudinal stiffeners are required. Obviously, the use of additional stiffening increases the overall cost of fabrication so it is very important to make earlier optimisation between material and manufacture costs and expected improvement of the strength. Often large-scale structures are subjected to complex interaction of the internal forces and their distribution may determine the most efficient position of the longitudinal stiffeners. Therefore, for example in case of rectangular plate girders subjected to shear the most favourable position would be at the mid-depth of the web-panel. On the other hand, if significant interaction shear-bending takes place, the longitudinal stiffener should be designed in the part of web, where additional compressive stressed caused by bending moment appear. In tapered plate girders, the stress-state in the web is often too complex to find without an additional analysis the best position of the longitudinal stiffener in an unambiguous way.

Next issue related to tapered plates is their shear buckling resistance. Although the fact of existence of the post-critical shear resistance in tapered plate girders is well known since many years, often not only the ultimate shear strength plays a crucial role in design process. Tapered plate elements are very often used as part of structures subjected to dynamic loads, such as highway or railway bridges. To fulfil safety requirements, additional conditions should be checked. The higher slenderness of these panels can make them susceptible to a phenomenon called web breathing. This may be caused by repeated application of in-plane loading (the level of which rises above the critical load) and the large out-of-plane deformation of the web accompanying them. As a consequence, failure may be caused by fatigue of welded junctions between the flange-web-stiffener. Thus, to check the structure against web-breathing, it is necessary to know a precise value of the critical shear load. EN 1993-2 (2006) provides the additional specification for very slender rectangular plate girders, however there are no rules to assess the actual value of the critical shear load for tapered elements.

Trapezoidal shape of tapered plate girders makes the behaviour of such panels much more complex compared to the rectangular ones. With time it was observed that in the inclined flange of tapered plate girders subjected to shear a new axial force appears. In the next years, it was proved that the vertical component of that force may influence the ultimate shear resistance of the girder. Increase or decrease of the ultimate shear resistance caused by this vertical force is called the Resal effect. Positive or negative influence of this effect depends on the particular geometry of the tapered girder and should be taken into account in design of non-prismatic girders.

1.2. State of the art

The behaviour of rectangular steel plates subjected to shear load was deeply studied during last century and different theories were developed in order to describe and analyse the mechanisms that take place during the post-buckling state and finally, to determine their ultimate shear capacity. Some of them were taken as a reference and evolved in time and other ones were implemented in design codes. The most important methods to be mentioned are: Basler's model (1960), Chern and Ostapenko (1969), the Rotated Stress Field Model developed by Höglund (1971, 1997) and Tension Field Model developed in Cardiff and Prague by Porter et al. (1975) and Rockey and Škaloud (1972).

In most cases, the models are based on the assumption of simply supported rectangular plate and do not consider actual boundary conditions existing in the flange–web junctions and in the stiffener–web junctions neither the geometry of the tapered steel plate girder. In the last years, some researchers, among others Lee et al. (1996), Mirambell and Zárate (2000), Estrada et al. (2008) have demonstrated the importance of these effects.

Almost all ultimate shear strength models for tapered plate girders proposed in literature are based on the previous presented models for rectangular plate girders. Several models for tapered girders have been developed by: Falby and Lee (1976), Davies and Mandal (1979), Takeda and Mikami (1987), Roberts and Newmark (1997), Zárate and Mirambell (2004) and Shanmugam and Min (2007). Recently, some other numerical studies have been published by Abu-Hamd M. and Abu-Hamd I. (2011).

Here, also it is important to point out that all above-mentioned models demonstrate various limitations. In this way, the model presented by Falby and Lee based on the Basler's theory assumes that for tapered plate girders with significant angle of the inclined flange, the critical shear load may be calculated according to the classic theory as for simple supported rectangular plates, but using the average depth of the trapezoidal panel. This method seems to give more realistic results for the ultimate shear resistance of tapered members compared to those ones obtained according to the theory for rectangular plates, however it does not take into account the contribution from the flanges in resisting the shear load.

In the method developed by Davies and Mandal for tapered plate girders, the simplified truss model loaded within the tip was used. This model assumes that the ultimate shear capacity may be calculated as a superposition of two tensional states: buckling and post-critical shear reserve. However the critical shear load is calculated in the same way like it was proposed by Falby and Lee, the model takes into account the contribution from the flanges and the so-called Resal effect and generally gave satisfactory results. On the other hand, the researchers admitted that all tested cases were conducted for a small range of the geometric parameters and with the same slope of the inclined flange, so it was recommended to verify the model with experimental tests conducted for various geometries of tapered panels.

The next model for assessment the ultimate shear resistance of tapered plate girders was proposed by Takeda and Mikami and based on the Chern's and Ostapenko's theory for prismatic members. Also this approach assumes the ultimate shear resistance as a superposition of the pre-critical and post-critical states. The difference comparing to the previously mentioned methods is in assessment of the critical shear load. In this case the critical stress is calculated with use of formulae derived from Finite Element Theory applied to instability analysis of trapezoidal plates. Also this model discards contribution from the flanges in carrying the shear force what is opposite to the hypothesis stated before by Davies and Mandal.

Some experimental tests on tapered aluminium girders conducted by Roberts and Newmark (1997) allow them to observe that collapse mechanisms of tapered steel and aluminium girders are drastically different and existing theories for steel plates cannot be copied and adopted in easy way for aluminium.

Also last decade brought several attempts of solving the problem of the ultimate shear resistance of tapered steel plate girders. One of them was proposed by Zárate and Mirambell (2004). The method takes into account actual boundary conditions and trapezoidal shape of tapered plate girders in both pre-buckling and post-buckling phases. The proposal is based on the Tension Field Method and on the results obtained from numerical studies conducted with use of Finite Element Method. In order to obtain the ultimate shear resistance the iterative process has to be carried out. However the analytical model is valid for various geometric parameters of tapered panel and offers a very good approach for non-prismatic members; it can be used only for one of four possible structural situations where the tension field is developed on the shortest diagonal of the web-panel and the inclined flange is under compression. A new element introduced in this method is the consideration of the influence of the Resal effect.

Apart from the several above-mentioned approaches to assess the ultimate shear resistance of tapered steel plate girders, there are no specific rules for tapered plate girders in current codes. For calculating ultimate strength of such members, EN 1993-1-5 suggests to use the expressions for prismatic plates without any changes if the angle of the inclined flange is not greater than 10°. In other cases, it is recommended to calculate a tapered plate as a rectangular one with its larger depth. Unfortunately, this method cannot be used for some cases of tapered panels because overestimates the ultimate strength and thereby does not satisfy the safety requirements.

1.3. Objective of the thesis

The main goal of the thesis is the development of the theory and design tools allowing predicting the ultimate shear resistance of tapered steel plate girders subjected to shear. It was important to develop a new proposal as simply as possible, taking into consideration the most significant factors at the same time.

To achieve this goal some intermediate tasks had to be done.
The most important tasks to be mentioned are:

- ✓ studies of the bibliography and existing models;
- ✓ preparation of the most realistic numerical model;
- ✓ design of the experimental specimens (dimensions of the girders and their resistance, range of the applied loads, suitable measure equipment, strategic points based on the numerical model);
- ✓ preparation of the specimens and development of the experimental tests;
- ✓ renewed verification of the numerical model with its possible modifications;
- ✓ parametric studies in a wide range of geometrical parameters;
- ✓ comparison of the numerical results with those obtained according to EN 1993-1-5;
- ✓ development of a new proposal based on the existing formulae.

In this work, all numerical simulations are based on the previous laboratory tests, and the numerical model was always verified before its application in parametrical studies. Moreover, all results obtained as a result of the computer analysis were checked against the current European design code EN 1993-1-5, compared and discussed. For many cases some modifications in EN 1993-1-5 are proposed in order to adopt the existing procedure for prismatic plates also for those members which have a non-prismatic shape.

1.4. Methodology

The main body of the thesis is composed of four publications (chapters 2-5) submitted to international journals with high impact factors such as Engineering Structures (1 - published), ICE Structures and Buildings (2 - published) and The Journal of Constructional Steel Research (3, 4 – under revision). Moreover, two additional chapters: *Introduction* and *Conclusions* were added in order to explain the relationship between the individual papers and to help the reader to understand the meaning of the whole research.

The objective of the chosen form for the doctoral thesis as a collection of published articles was reaching the widest range of readers and triggering a debate off. The problems discussed in all papers exhausted the wide-range of structural issues established at the very beginning, whose common denominator is tapered steel plate girders subjected to shear. Nevertheless, each chapter can be read and understood independently.

The main issues discussed in the thesis are:

- ✓ the critical shear load of simply-supported tapered plates;
- ✓ the ultimate shear resistance of tapered steel plate girders with transversal stiffeners subjected to shear;
- ✓ the ultimate shear resistance of tapered steel plate girders with transversal stiffeners subjected to shear-bending interaction;
- ✓ the ultimate shear resistance of tapered steel plate girders with longitudinal stiffeners subjected to shear;

The overall structure of the PhD thesis is composed of six chapters where:

Chapter 1

Introduction – includes background of the problem, a brief description of the state of art, the objectives of the thesis, the methodology applied in research and an extended summary of the four papers;

Chapters 2-5

The main body of the thesis – consists of four publications, where the experimental and numerical results of partial studies on tapered plate girders are presented and discussed;

Chapter 6

Conclusions and future work – includes a general discussion of the results and the overall evaluation of the research and its importance, final conclusions and suggestions for further development;

To make easier navigation between the chapters, a structure of the whole document is illustrated in graphical way (**Fig. 1.3**):

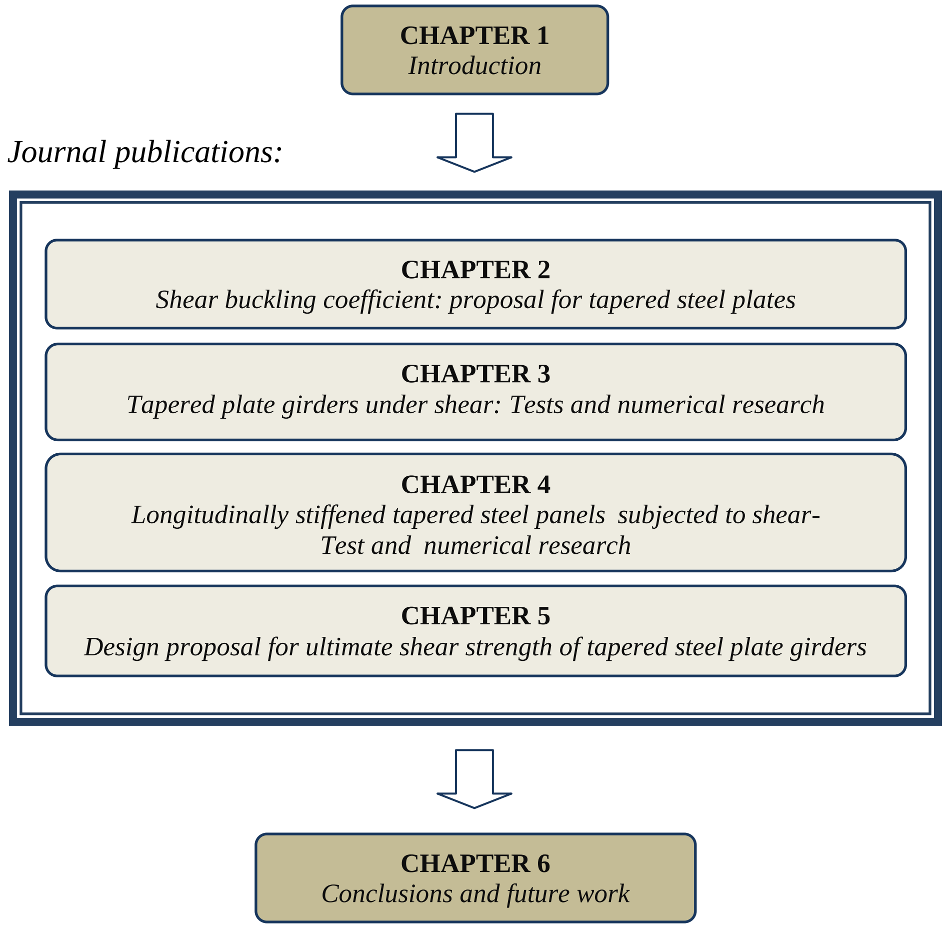

Fig. 1.3. Structure of the thesis

Next, an extended abstract with the main contribution of each paper in entire research is presented:

Paper no: 1;

Title: Shear buckling coefficient for simply-supported tapered plates subjected to shear.

Authors: A. Bedynek, E. Real, E. Mirambell;

Journal: ICE Structures and Buildings 166 (2013), Issue SB1;

Impact factor: 0.609;

Status: published;

Summary:

In this paper results of numerical research carried out on the critical shear load of simply-supported tapered plates subjected to pure shear are presented. Content of the document is focused on the searching for the shear buckling coefficient for simply-supported non-prismatic plates. In buckle analyses influence of the following geometrical parameters such as: an aspect ratio, slope of the inclined flange and web thickness was studied. Results obtained from over 500 numerical tests for four different typologies of tapered plates allowed developing a new proposal for the shear buckling coefficient. After some simplifications four analytical expressions for each typology were presented. Significant improvement was achieved comparing to the classic solution for rectangular simply-supported plates.

This work can be treated as a separated research due to its objective. The results presented in this document can be used in assessment of the real values of the critical shear load of tapered plates. For very slender web panels of steel structures such as highway and railway bridges postcritical plate buckling may induce out-of-plane deflections. When this kind of structure is subjected to repeated live loads, the repeated out-of-plane deflections produce secondary bending stresses at the web-flange- and web-stiffener junctions. The high ranges of the secondary bending stresses may lead to a severe fatigue problem. In order to verify this fatigue problem – web-breathing – in accordance with EN 1993-2 (2006), it is necessary to know the linear elastic buckling coefficient of the tapered web panel.

Paper no: 2;

Title: Tapered plate girders under shear: Tests and numerical research.

Authors: A. Bedynek, E. Real, E. Mirambell;

Journal: Engineering Structures 46 (2013), 350-385;

Impact factor: 1.713;

Status: published;

Summary:

The main applications for tapered plate girders in large-scale building and civil engineering structures make them very susceptible to shear buckling. Although this phenomenon has been widely studied for prismatic plates, there are very few theoretical and experimental investigations conducted on the structural response of tapered steel plate girders under increasing shear load up to failure. The current design code for plated structural elements, EN 1993-1-5 proposes to determine the ultimate shear resistance of tapered plate girders as prismatic ones. In order to evaluate this simplification, some experimental tests and a wide parametric study with different geometries of tapered plate girders were conducted.

This paper presents an experimental and numerical research on tapered steel plate girders subjected to shear. The first part is devoted to the test on four small-scale tapered steel plate girders with transversal stiffeners. Based on the experimental results, a numerical model was verified successfully and a numerical research with parametric studies on various geometries of tapered panels was done. The analysed parameters were: the panel aspect ratio, the slope of the inclined flange, the web and the flange slenderness.

Numerical simulations allowed distinguishing four various typologies (**Fig. 1.4**) of tapered plate girders which should be designed separately. Different structural response within each typology of tapered girders depends on the stress state in the inclined flange and on the direction of the tension field. These differences are also influenced by the Resal effect, where the vertical component of the axial force in the inclined flange may increase or decrease the ultimate shear capacity of the tapered panel.

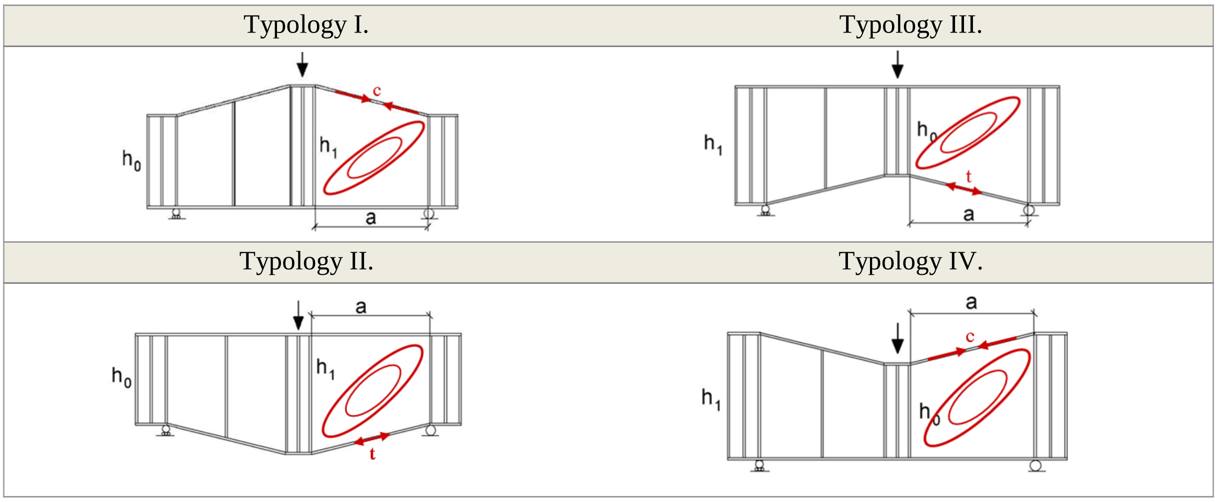

Fig. 1.4. Four typologies of tapered plate girders.

Verification of the simplified procedure for tapered plates proposed in Eurocode EN 1993-1-5 allowed concluding that for some cases the estimation of the ultimate shear resistance is situated on the unsafe side and need to be revised.

Finally, in order to improve the accuracy in assessing the ultimate shear resistance of tapered steel plate girders, some modifications of existing formulae were proposed.

Paper no:	3;
Title:	Longitudinally stiffened tapered steel panels subjected to shear - Test and numerical research.
Authors:	A. Bedynek, E. Real, E. Mirambell;
Journal:	The Journal of Constructional Steel Research;
Impact factor:	1.327;
Status:	in revision;

Summary:

In this paper experimental and numerical results for tapered steel plate girders with one longitudinal stiffener under shear are presented. In the first part, devoted to the second experimental campaign, the results obtained from four small-scale tests are shown and discussed. Values measured during the tests were: strains, vertical and out-of-plane displacements. Due to the problem of the excessive initial geometrical imperfections, caused by fabrication process, only two girders could be examined up to their ultimate shear capacity and used in the comparison with the numerical model. All registered values were used in the verification of the numerical model and good concordance between experimental and numerical results allowed to its validation.

In the second part of the research, results from the numerical simulations conducted on the longitudinally stiffened tapered plates girders subjected to shear are presented. Moreover, research under the optimum rigidity of the longitudinal stiffener was done. Numerical studies were conducted for a wide range of geometric parameters such as: the aspect ratio, the web and flange slenderness and the slope of the inclined flange. Four different positions of the longitudinal stiffener were examined. In order to compare the numerical results with those obtained according to EN 1993-1-5, valid only for rectangular plates, extended interpretation of the design rules of EN 1993-1-5 had to be done. Finally, validation of the design code EN 1993-1-5 for tapered plate girders with longitudinal stiffener in various positions was done and discussed.

Paper no: 4;

Title: Design proposal for ultimate shear strength of tapered steel plate girders.

Authors: A. Bedynek, E. Real, E. Mirambell;

Journal: The Journal of Constructional Steel Research;

Impact factor: 1.327;

Status: in revision;

Summary:

In this document a new proposal for assessing the ultimate shear resistance of tapered steel plate girders V_u is proposed. Parametric studies conducted for a wide range of the geometric parameters allowed establishing four individual analytical expressions for each typology of tapered plate girders. Proposed formulae are based on existing rules included in EN 1993-1-5 which were adopted and extended for non-prismatic members. The main modification was done in calculating the contribution from the web for those typologies of tapered plate girders where the diagram of bending moments along the girder increases with the decrease of the structural depth (it means, the larger bending moment, the shorter cross-section) and, on the other hand, some minor changes for other usual typologies in design were done.

Unlike in rectangular plate girders, in tapered members, an additional factor influencing their ultimate shear resistance should be taken into account. It is well known the fact that in a case of non-rectangular girders an additional vertical component derived from the axial force existing in the inclined flange appears. This vertical force, called Resal effect, may have a positive or negative influence on the ultimate shear strength of such panels. In order to take it into account, a new mechanical model for assessment the Resal force was developed and included in the final proposal.

Numerical simulations were conducted for 85 numerical models and obtained results were used in verification of the new proposal. In general, a very good agreement between the numerical and the analytical values of the ultimate shear resistance V_u was achieved what confirmed a correctness of the new approach.

Moreover, the new proposal was checked for 12 tapered plate girders subjected to shear-bending interaction and belonging to four different typologies. Also here, a good agreement between both approaches was observed, however some additional studies in wider range of the geometric parameters would be recommended.

1.5. Development of the research

The fundamental issues presented in the PhD proposal were widely discussed in previously-mentioned publications. Three main topics studied extensively in this research should be pointed out:

- ✓ the critical shear load of simply-supported tapered plates;
- ✓ the ultimate shear resistance of tapered steel plate girders subjected to shear and shear-bending interaction;
- ✓ the ultimate shear resistance of tapered steel plate girders with longitudinal stiffener subjected to shear.

As it can be noticed, all papers are connected to the same topic, which is, tapered plate girders subjected to shear. Moreover, some additional studies conducted on the critical shear load of simply-supported non-prismatic plates were done. However, the results obtained from this part of the research states an integral part of the whole work and can be used separately.

Bibliographical research:

The very early stage of the research on the tapered plate girders subjected to shear was focused on the studying existing bibliography and various mechanical models developed at the turn of the last century. It was found out that the most of the publications are focused only on rectangular panels with significant simplifications in proposed models. Due to the scarcity of the research for non-rectangular panels, some attempts to develop a new numerical model for non-rectangular plates were done.

Development of the numerical model:

Further studies allowed developing advanced realistic numerical model and classifying tapered plate girders into four different typologies according to their geometry and stress-state inside the web-panel and flanges. This discovery stated an important point in whole investigation. Numerical model was useful in planning experimental tests. Before defining the final version of the numerical model some additional tasks had to be undertaken. To the most important belonged: benchmark tests of the finite element in a context of precision vs. time consumption and analysis of the influence of the structural imperfections (residual stresses) for the ultimate shear capacity of tapered plate girders.

Experimental campaigns:

In the period of the research work two large few-months lasting experimental campaign were carried out. The objective of the first one was the study of the structural behaviour of tapered steel plate girders subjected to shear and shear-bending interaction. Second experimental campaign was focused on the longitudinally stiffened tapered steel plate girders subjected to shear. Each of them was preceded by detailed and complex preparation. At the very early stage the numerical model was used to simulate the real behaviour and to define relevant points of the specimens where the measuring equipment were planned to be placed. Moreover, to be able to observe expected phenomena up to desirable level of the applied load, the characteristic parameters such as geometry of the specimens, properties of the material and design resistance had to be designed with use of the numerical model. It is important to point out that the properties of the tested girders were changed several times due to the fabrication problems (lack of the specific steel, problems with welding sheets with relevant differences of their thickness) or limitations of the measure equipments (maximum dimensions of girder, maximum ultimate shear resistance conditioned by carrying capacity of the press etc.)

Further preparation of the specimens included: placing strain gauges in the previously cleaned and polished surfaces and installation of the remaining measuring equipment such as: LVDT's (linear displacement transducers) and lasers and their connection to Data Acquisition System.

Additionally, some tensile coupon tests were conducted in order to verify properties of the steel used in the fabrication of the tested girders.

Analysis of the experimental results and numerical model validation:

Results obtained from detailed analysis of the experimental data: principal membrane strains, load-deflection curves and out-of-plane displacements of the web, allowed for verification of the numerical model and for establishing its final version.

Parametric studies:

To make shorter carrying out numerous high time-consuming simulations it was necessary to create an additional script which would allow for parameterisation of the numerical model. The parameterised model could be used for any combination of the geometric or material parameters. Moreover, results from large amount of simultaneous simulations in wide range of the changing parameters could be obtained automatically. To confirm the reliability of the numerical models used in the parametric studies always before their implementation, they were validated through the experimental tests.

Numerical results vs. EN 1993-1-5:

All numerical results published in particular articles always were related to current European design code for steel plate girders. In some situations due to the shortage of specific regulations for studied cases, new interpretations of design expressions were proposed and discussed. For those cases, for which such regulations did not exist, new approaches were proposed.

Conclusions and new proposals:

After detailed analysis of all results, in the end of each paper, some remarks and conclusions were done. For the most important issues discussed in this research the new interpretations of existing rules or the new proposals were presented. Moreover, in the final part of the thesis some recommendations with respect to the future work are pointed out.

2. *Shear buckling coefficient - Proposal for tapered steel plates*

2.1. Abstract

This paper presents a new proposal for estimation of critical load for non-prismatic, thin plates simply supported on four edges subjected to shear. The research included wide parametric studies using more than 500 samples. The parameters taken into account were the web thickness, the panel aspect ratio and the inclination angle. The influence of each was analysed separately and then some simplifications were made in order to find coherent expressions to describe the behaviour of the studied panels. The numerical results were then used to validate the solution proposed in EN 1993-1-5. As a result of this comparison, it is concluded that new design formulations are needed for tapered plates with a considerable slope. Based on previous research by the authors concerning four various geometrical typologies of tapered panels, four expressions for the shear buckling coefficient k_ϕ are proposed.

2.2. Notation

$\boldsymbol{A}$, $\boldsymbol{B}$, $\boldsymbol{C}$	constants in the searched functions
$\boldsymbol{a}$	length of panel
$\boldsymbol{b}_{\mathrm{f}}$	flange width
$\boldsymbol{E}$	Young's modulus
$\boldsymbol{f}_{\mathrm{y}}$	yield stress
$\boldsymbol{h}$	depth of rectangular panel
$\boldsymbol{h}_0$	smallest depth of tapered panel
$\boldsymbol{h}_1$	largest depth of tapered panel
$\boldsymbol{k}_{\tau}$	shear buckling coefficient (classic theory)
$\boldsymbol{k}_{\phi}$	shear buckling coefficient (tapered panel)
$\boldsymbol{k}_{\phi,\alpha}$	shear buckling coefficient (tapered panel with various aspect ratios)
$\boldsymbol{t}_{\mathrm{f}}$	flange thickness
$\boldsymbol{t}_{\mathrm{w}}$	web thickness
$\boldsymbol{V}_{\mathrm{cr}}$	critical load
$\boldsymbol{V}_{\mathrm{u}}$	ultimate shear strength
$\boldsymbol{\alpha}$	aspect ratio (a/h)
$\boldsymbol{\nu}$	Poisson's ratio
$\boldsymbol{\phi}$	angle of slope of inclined flange

2.3. Introduction

Slender plate girders are very often used as a part of long steel and composite bridges or portal frames where that are mostly subjected to shear and shear with bending. Significant post-buckling resistance of prismatic plate panels was first discovered and studied by Basler (1960). Further research carried out over the next few decades confirmed Basler's work and theoretical models were proposed. The most frequently quoted theories include those developed by Chern and Ostapenko (1969), Höglund (1971), Rockey and Škaloud (1972), Porter et al. (1975) and Davies and Mandal (1979). More recent approaches include those carried out by Mirambell and Zárate (2000) and Shanmugam and Min (2007).

Nowadays, and in the current European standard EN 1993-1-5 (2006), the post-critical carrying capacity of rectangular plates is taken into account. However, even though general understanding of the post-critical behaviour has improved, only a few models allow consideration of a plate with non-parallel flanges. To deal with this problem, a simplified method for tapered plate girders whose angle of the inclined flange is significant (greater than 10°) is proposed in EN 1993-1-5: the simplification consists of treating them as rectangular and substituting their varying depth with the greatest depth.

Recent studies ((Bedynek et al., 2011), (Real et al., 2010)) proved that the abovementioned approach successfully estimates the ultimate shear strength for some kinds of geometries of tapered panels. It was proved that tapered plate girders can be divided into four various typologies, depending on their geometry (**Fig. 2.1**), and the solution proposed in EN 1993-1-5 is safe only for two of them. With different behaviours observed, it seems necessary to study each case separately.

Tapered plate elements are also very often used as part of structures subjected to dynamic loads, such as highways or railway bridges. To fulfil safety requirements, additional conditions have to be checked. The higher slenderness of these panels can make them susceptible to a phenomenon called web breathing. This is caused by cyclic application of in-plane loading (the level of which rises above the critical load) and the large out-of-plane deformation of the web accompanying them. As a consequence, failure may be provoked by fatigue of weld connections between the flange-web-stiffener. This issue was studied by Günther and Kuhlmann (2004).

EN 1993-2 (2006) provides additional specification for very slender plate girders (which are especially susceptible to web breathing). Unfortunately, there are no rules for tapered elements and it could be concluded that they should be treated similarly as is proposed in EN 1993-1-5 (i.e. as rectangular). While the simplified method in static analysis of the ultimate shear resistance of tapered panels could give correct results, in the case of web breathing, precise estimation of the critical shear load may be crucial for an assessment of the structure in serviceability conditions.

Owing to this difficulty in estimating the beginning of web breathing for tapered plates, some effort has been made to modify existing classical formulae for simply supported rectangular panels and widen them to non-prismatic plates. This paper presents a numerical analysis of simply supported tapered plates subjected to shear. The influence on the critical shear load of parameters such as web thickness, aspect ratio and angle of the inclination was tested. As a result of the parametric studies, new expressions for the shear buckling coefficient k_{ϕ} for four different geometries of tapered plates are proposed.

2.4. Four typologies of tapered plate girders

These studies are based on the assumption of the existence of four different typologies of tapered plate girders. A brief description and general classification is shown in **Fig. 2.1**. A more detailed explanation and examples of application are given by Bedynek et al. (2011). The fundamental differences between the four types are the direction of the diagonal tension field (shorter or longer diagonal (see **Fig. 2.1**)) formed during the post-buckling stage and the stress state in the inclined flange (tension or compression).

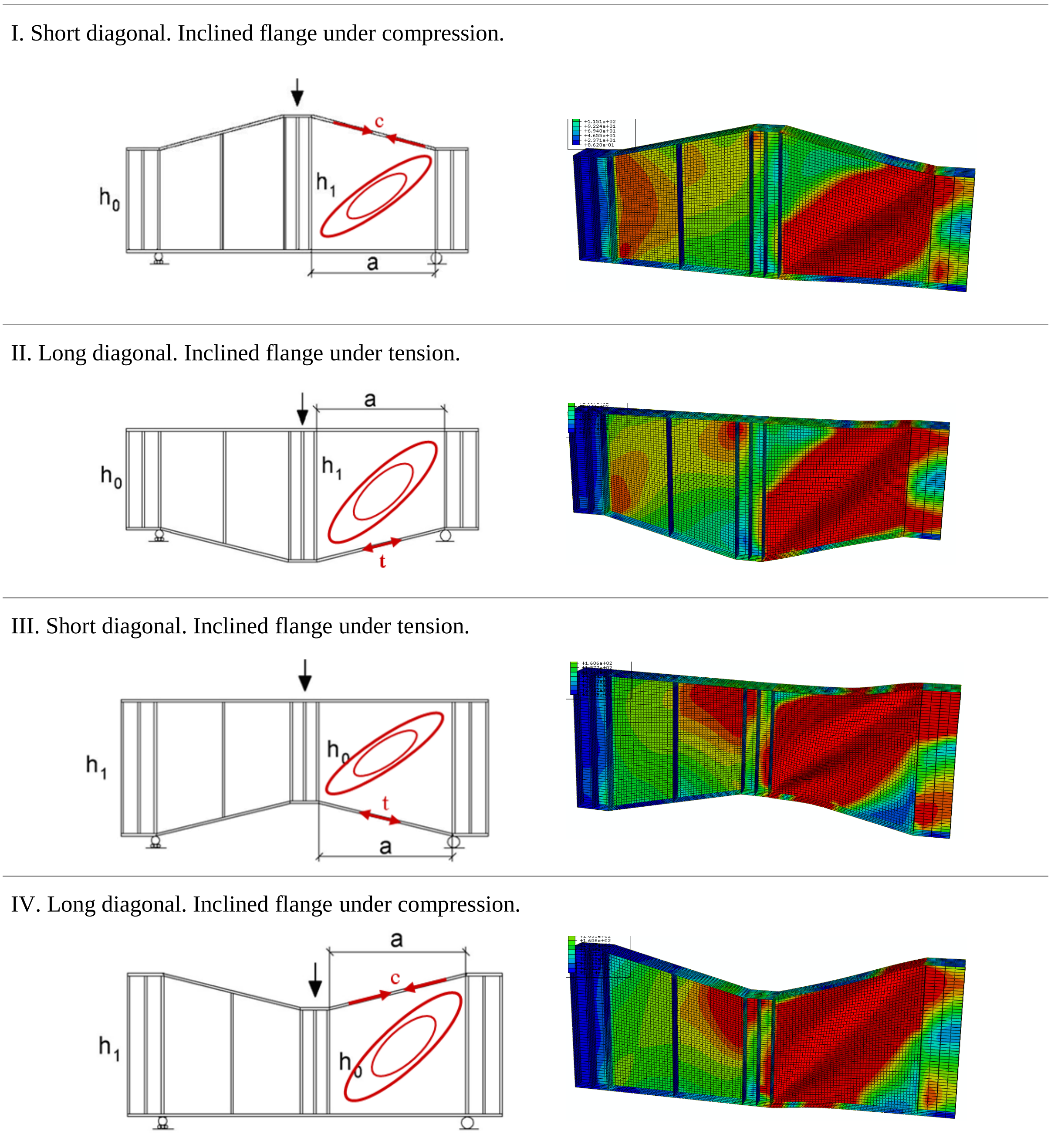

Fig. 2.1. Four typologies of tapered plate girders.

Not only qualitative differences can be observed. **Table 2.1** shows numerical results of critical load V_{cr} and ultimate shear strength V_u for four typologies of the same tapered plate girder (smallest depth h_0 =600 mm, largest depth h_1 =800 mm, length a =800 mm, web thickness t_w = 4 mm, flange width b_f =180 mm and flange thickness t_f =15 mm). The critical shear buckling load was obtained from a buckle analysis (eigenvalue mode) and the ultimate shear resistance from a non-linear analysis that concerned both material and geometric non-linearities.

Table 2.1. Numerical (FEM) results of critical load V_{cr} and ultimate shear strength V_u for four typologies of the same girder (h_0 =600 mm, h_1 =800 mm, a =800 mm, t_w =4 mm, b_f =180 mm, t_f =15 mm).

Typology	V_{cr} [kN]	V_u [kN]
I	238.0	366.9
II	217.3	351.3
III	188.0	274.9
IV	168.7	263.3

2.5. Numerical model

All numerical simulations were conducted using the Abaqus code (2010) based on the finite-element method (FEM). To create a numerical model of the simply supported tapered plate, a four-node shell element (S4R5) was used. An example of a finite-element single panel subjected to pure shear is presented in **Fig. 2.2**. Its boundary conditions are shown in **Table 2.2**. The material considered in all models was standard carbon steel S275 with yield stress f_y =275 MPa, Young's modulus E =210 GPa and Poisson's ratio ν = 0.3. In order to obtain the critical load, buckle analysis in the elastic range was performed.

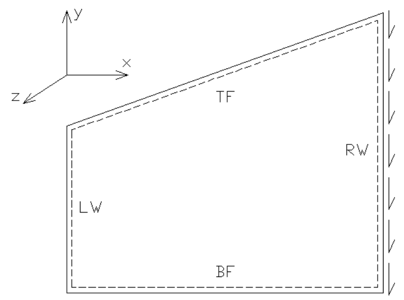

Fig. 2.2. Numerical model of tapered panel.

	u_x	u_y	u_z	θ_x	θ_y	θ_z
LW	0	1	1	1	0	0
RW	1	0	1	1	0	1
TF	1	0	1	0	1	1
BF	1	0	1	0	1	1

0 – free movement, 1 – restraint movement

Table 2.2. Boundary conditions for applied model.

2.5.1. Verification and comparison with Euler's solution for rectangular plates

Table 2.3 presents a comparison of the numerical and theoretical results for the shear buckling coefficient k_τ for rectangular plates simply supported on four edges. Theoretical values of k_τ were calculated according to the linear classic theory (**Eq. 2.1**) while the numerical values of k_τ (FEM) were obtained as a result of eigenvalue analysis. Only a few representative tested plates with random dimensions and aspect ratio $\alpha = a/h$ between 1 and 5 are presented. The last column of **Table 2.3** shows relative differences between numerical and analytical results. Overall, the differences are very small (-0.6 to 3.4%), proving that the numerical model with its assumption of specific boundary conditions was correctly defined and could be used in the further parametric studies of tapered panels.

Table 2.3. Critical shear buckling coefficient k_τ for rectangular simply-supported plate. FEM and Euler's solution.

Girder	h [mm]	a [mm]	t_w [mm]	α	k_τ Euler	k_τ FEM	Difference [%]
3000_3000_25	3000	3000	25	1.0	9.34	9.35	0.1
900_1350_8	900	1350	8	1.5	7.12	7.08	-0.6
2100_4200_25	2100	4200	25	2.0	6.34	6.56	3.4
1500_4500_15	1500	4500	15	3.0	5.78	5.85	1.2
2100_8400_8	2100	8400	8	4.0	5.59	5.64	0.9
1500_7500_20	1500	7500	20	5.0	5.50	5.54	0.7

The theoretical critical shear buckling stress is given by:

$$\tau_{cr} = k_\tau \frac{\pi^2 E}{12(1-\nu^2)}\left(\frac{t_w}{h}\right)^2 \tag{2.1a}$$

$$k_\tau = 5.34 + \frac{4}{\alpha^2} \tag{2.1b}$$

where k_τ is the shear buckling coefficient, E is Young's modulus, ν is Poisson ratio, t_w is the plate thickness and h is the web depth.

2.6. Parametric studies

2.6.1. Introduction

Parametric studies were carried out on the four tapered plate girder typologies. All were analysed separately and, within each typology, approximately 500 numerical models with different dimensions were tested. The proposal presented is valid for tapered, simply supported panels whose critical load is smaller than their ultimate shear resistance. All cases for which this requirement was not fulfilled were rejected from the analysis. The range of dimensions of the tested models is presented in **Table 2.4**.

Table 2.4. Range of dimensions of the tested models.

t_w	web thickness	[mm]	8,10,15,20,25
h_0	smaller depth	[mm]	900,1200,1500,1800,2100,2400,2700,3000
h_1	larger depth	[mm]	900,1200,1500,1800,2100,2400,2700,3000
a	panel length	[mm]	900,1200,1500,1800,2100,2400,2700,3000,3600,4200,4500, 4800, 6000,7200,7500,8400,9000,9600,10500,12000,15000
α	aspect ratio		1,2,3,4,5
$tan(\phi)$	flange slope		0.1 to 0.6
ϕ	slope angle	[°]	to 30.9

2.6.2. Analysis procedure

For all tested specimens, buckle analysis in the elastic range was conducted. The critical load was calculated based on the first positive eigenmode (corresponding to shear buckling). **Fig. 2.3** shows the procedure applied for the four typologies. All expressions were obtained in the same way, the only difference between them being the approximating functions: for typologies I and II, the final approximating functions depending on ***tan*(ϕ)** are linear while cases III and IV are described by more complex quadratic expressions.

All steps in searching the approximating functions for typologies I and II are the same. Therefore, a complete explanation of the applied procedure is presented only for typology I.

Cases III and IV were studied in a similar manner, however due to the more complex functions used in approximation, typology III is discussed additionally with all the necessary details. **Fig. 2.3** shows the applied procedure with differences between cases I and II and cases III and IV.

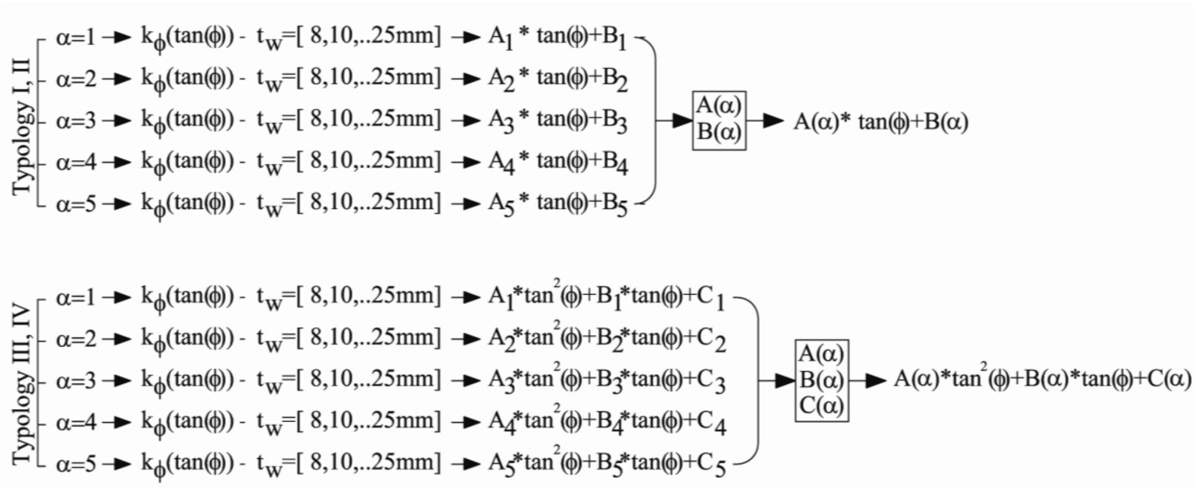

Fig. 2.3. Scheme of the analysis data procedure.

The first step of the analysis consisted of grouping all cases (numerical models) with respect to α. Then, for all models with the same α, the influence of the web thickness t_w for the shear buckling coefficient k_ϕ was analysed. Results of this step for α =1 are shown in **Fig. 2.4**.

Fig. 2.4 shows that, for different web thicknesses, all functions show a very similar trend line and can therefore be approximated by one linear function. The same procedure was repeated for aspect ratios α =2, 3, 4 and 5 and the same trends were observed.

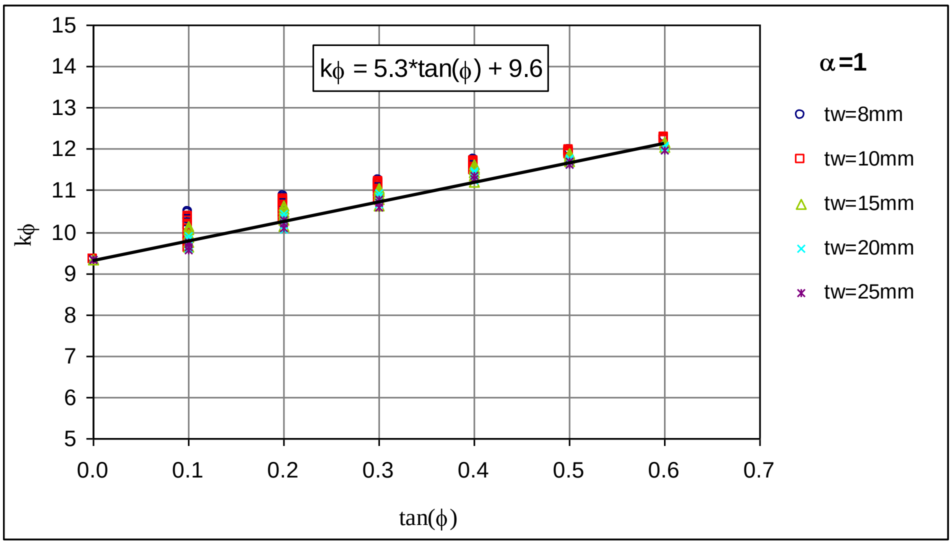

Fig. 2.4. Relationship k_ϕ - $tan(\phi)$ for α=1 and various t_w for typology I.

Therefore, the shear buckling coefficient k_ϕ is not strongly correlated with web thickness t_w and the searching function can thus be simplified to be independent of t_w. Consequently, the goal function could have the form:

$$k_\phi = A\tan(\phi) + B \quad \textbf{(2.2)}$$

where parameters A and B will be functions of α

$$k_{\phi,\alpha} = A(\alpha)\tan(\phi) + B(\phi) \quad \textbf{(2.3)}$$

The next step consists of searching for the functions $A(\alpha)$ and $B(\alpha)$. In order to find this relationship for each α_i the values of $A(\alpha_i)$ and $B(\alpha_i)$ were found in a way that approximating functions always give results of k_ϕ on the safe side (i.e. smaller than the k_ϕ obtained from numerical simulation). **Table 2.5** lists the constants A and B and, based on this data, two approximating functions $A(\alpha)$ and $B(\alpha)$ were found (**Fig. 2.5**).

Table 2.5. Constants *A* and *B* for various α for typology I.

α	1	2	3	4	5
A	5.3	10.5	14.5	17.4	20.5
B	9.6	6.6	5.9	5.6	5.5

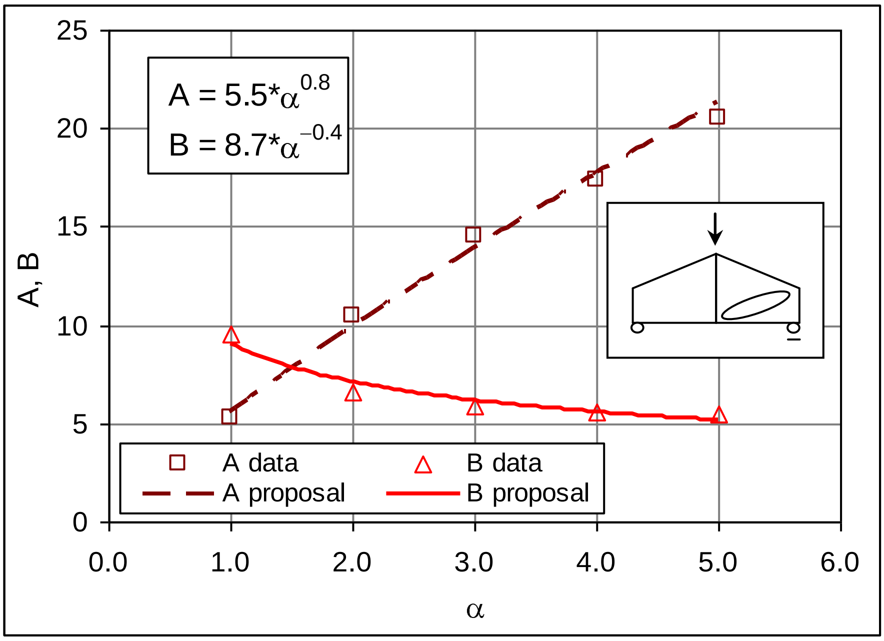

Fig. 2.5. Approximating functions for *A* and *B* for typology I.

The final form for the shear buckling coefficient $k_{\phi,\alpha}$ for simply supported tapered plates belonging to typology I is then:

$$k_{\phi,\alpha} = 5.5\alpha^{0.8}\tan(\phi) + 8.7\alpha^{-0.4} \quad \textbf{(2.4)}$$

The same procedure was repeated for typology II. **Table 2.6** shows the evaluated constants ***A*** and ***B*** and the approximating functions ***A*** and ***B*** are shown in **Fig. 2.6**.

Table 2.6. Constants *A* and *B* for various α for typology II.

α	1	2	3	4	5
A	10.5	16.0	18.8	22.0	23.8
B	8.6	5.9	5.3	4.9	4.8

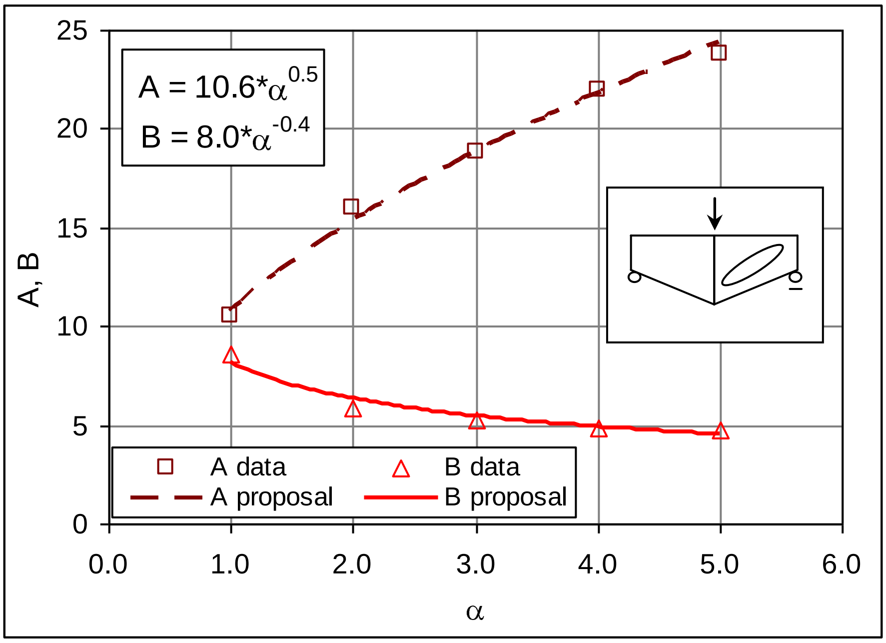

Fig. 2.6. Approximating functions for *A* and *B* for typology II.

The solution for typology II is then described by:

$$k_{\phi,\alpha} = 10.6\alpha^{0.5}\tan(\phi) + 8.0\alpha^{-0.4} \quad \textbf{(2.5)}$$

For typologies III and IV, the expressions are represented by more complex functions, although the procedure is the same as for typologies I and II. Typology III will be used as an example for both cases III and IV. Firstly, for each α =1, 2,..., 5 the influence of web thickness t_w on the shear buckling coefficient k_ϕ was analysed (**Fig. 2.7**).

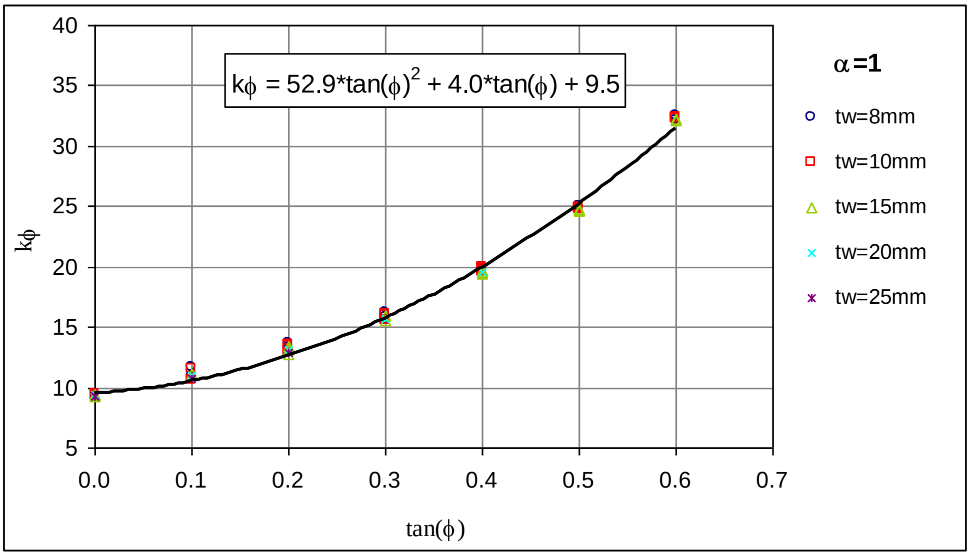

Fig. 2.7. Typology III: relationship between k_ϕ and *tan*(ϕ) for α=1 and various t_w.

As shown in **Fig. 2.7**, the shear buckling coefficient k_ϕ is not strongly correlated with t_w and the searching function can be simplified and independent of the web thickness parameter. After analysing all aspect ratios for tapered plate girders of typology III (the same for IV), it was concluded that the goal function will have the form:

$$k_\phi = A\tan^2(\phi) + B\tan(\phi) + C \tag{2.6}$$

where parameters A, B and C are functions of α:

$$k_{\phi,\alpha} = A(\alpha)\tan^2(\phi) + B(\alpha)\tan(\phi) + C(\alpha) \tag{2.7}$$

The next step consisted of searching for the functions $A(\alpha)$, $B(\alpha)$ and $C(\alpha)$. In order to find this relationship for each α_i the values of $A(\alpha_i)$, $B(\alpha_i)$ and $C(\alpha_i)$ were found in a way that approximating functions always give k_ϕ results on the safe side (i.e. smaller than the value obtained from numerical simulation). Constants A, B and C are presented in **Table 2.7** and the process of searching for functions A, B and C is illustrated in **Fig. 2.8**.

Table 2.7. Constants A, B and C for various α for typology III.

α	1	2	3	4	5
A	52.9	184.0	368.3	618.3	940.8
B	4.0	6.6	8.1	7.2	7.0
C	9.5	6.8	5.2	5.0	5.2

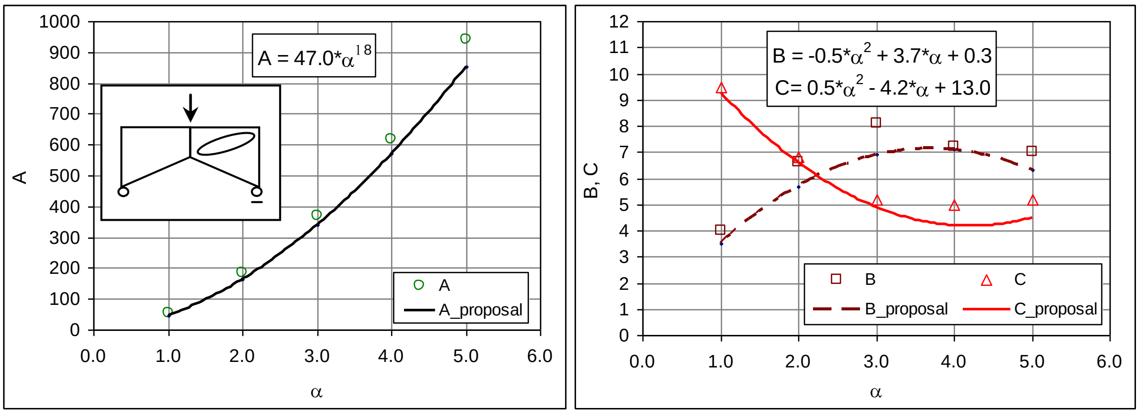

Fig. 2.8. Approximating functions for A, B and C for typology III.

Finally, the shear buckling coefficient for typology III is:

$$k_{\phi,\alpha} = 47.0\alpha^{1.8}\tan^2(\phi) + (0.3 + 3.7\alpha - 0.5\alpha^2)\tan(\phi) + (0.5\alpha^2 - 4.2\alpha + 13.0) \tag{2.8}$$

Similarly, for typology IV, ***A***, ***B*** and ***C*** are presented in **Table 2.8** and **Fig. 2.9** shows the required functions ***A***, ***B*** and ***C*** for typology IV.

Table 2.8. Constants *A*, *B* and *C* for various α for typology IV.

α	1	2	3	4	5
A	62.0	195.0	375.0	600.0	880.0
B	4.5	6.5	7.5	7.5	4.8
C	9.3	6.3	5.8	5.6	5.5

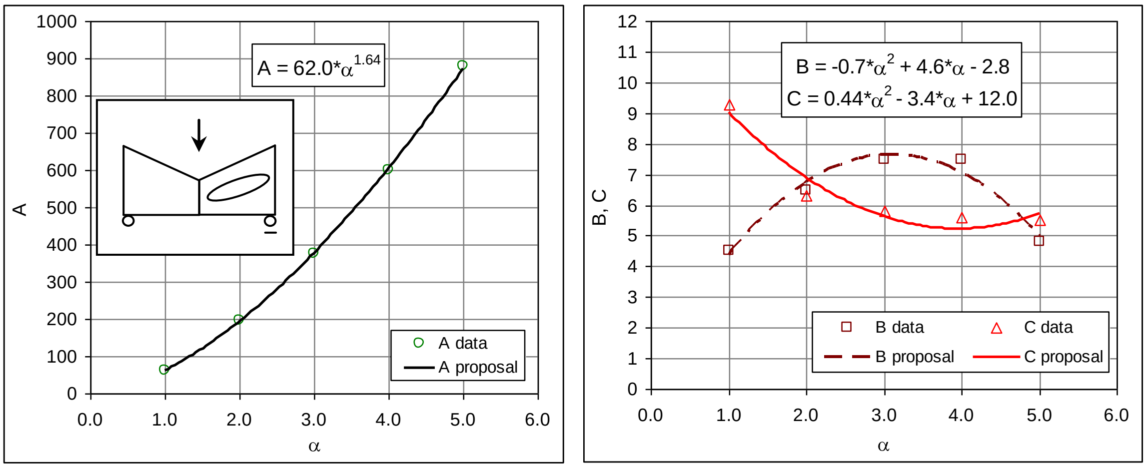

Fig. 2.9. Approximating functions for *A*, *B* and *C* for typology IV.

The shear buckling coefficient for typology IV is then described by:

$$k_{\phi,\alpha} = 62.0\alpha^{1.64}\tan^2(\phi) + (4.6\alpha - 0.7\alpha^2 - 2.8)\tan(\phi) + (0.44\alpha^2 - 3.4\alpha + 12.0) \qquad \textbf{(2.9)}$$

2.7. Comparison between present study and EN 1993-1-5

EN 1993-1-5 states that rules for plate buckling on uniform members may apply to non-rectangular panels provided the flange slope is not greater than 10°. If the slope exceeds 10°, a panel may be assessed assuming it to be a rectangular panel based on the larger depth of the panel. Shear buckling coefficients k_ϕ are calculated as for simply supported plates, as in **Eq. 2.1b** (EN 1993-1-5, Annex A.3).

2.7.1. Inclination greater than 2.5° (*tan*(ϕ) > 0.03)

As mentioned earlier, to obtain a solution for k_ϕ for tapered panels (according to EN 1993-1-5), it is necessary to simplify those cases to rectangular plates with the larger depth h_1. The theoretical results obtained in this way are compared with the numerical results.

Fig. 2.10a compares the results for shear buckling coefficient k_ϕ calculated according to the new proposal and EN 1993-1-5 for typology I. All values are correlated with the numerical solution, which is considered as exact, and then all points on the graph represent their relative values. From the comparison it is easy to conclude that both solutions remain on the safe side. Nevertheless, the differences between the results obtained according to EN 1993-1-5 and the numerical ones are considerable, varying between 7.1% and 41.0% (calculated as $100\%\cdot(k_{\mathrm{FEM}} - k_{\mathrm{EN}})/k_{\mathrm{FEM}}$), while the maximum difference in the case of the proposed expressions is reduced to 16.5% (calculated as $100\%\cdot(k_{\mathrm{FEM}} - k_{\mathrm{proposal}})/k_{\mathrm{FEM}}$). Thus, in situations where the critical shear load plays an important role, significant improvement can be achieved.

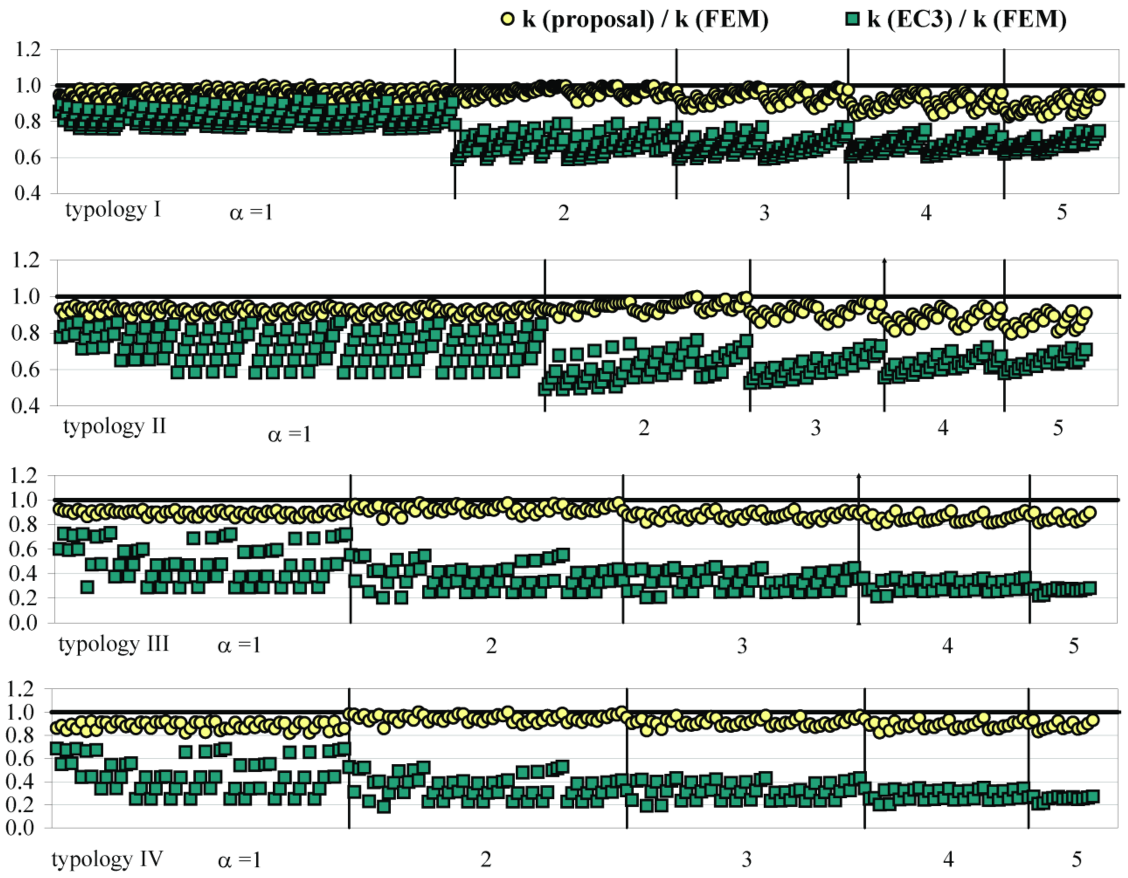

Fig. 2.10. Comparison of proposed equations with EN 1993-1-5:
a) typology I; **b)** typology II; **c)** typology III; **d)** typology IV.

Consequently, the same comparison for the other tapered plate typologies was carried out (**Figs. 2.10b–d**). The situation is similar for typology II, with a significant improvement in the estimation of k_ϕ. The differences between classical (EN 1993-1-5) and numerical solutions (even achieving 52.7%) using the new proposal could be reduced to 20.4% (**Fig. 2.10b**). For typology III, the differences were reduced from 79.9% to 19.6% (**Fig. 2.10c**) and for typology IV, an improvement from 81.6% to 18.1% was achieved (**Fig. 2.10d**).

Although EN 1993-1-5 gives an accurate estimation of the shear buckling coefficient k_ϕ for the most frequent typology I, there are other design situations where typologies II, III and IV can appear in real structures.

2.7.2. Inclination less than 2.5°

Since all the proposed functions (**Eqs. 2.4**, **2.5**, **2.8** and **2.9**) depend on $tan(\phi)$, the sensitivity of these expressions increases as the angle of the inclination approaches zero. Because of this, a limit angle of 2.5° was assumed, which is approximately equivalent to $tan(\phi)$ =0.04-0.05. Then, for tapered plates whose slope angle is in the range 0–2.5°, the approach proposed in EN 1993-1-5 is recommended. For these cases, the tapered panel can be calculated as a rectangular one substituting the depth h by h_1 (the largest depth).

To prove this, an additional study was conducted focused on tapered panels with a very small angle. The results of this study are presented in **Fig. 2.11** for each typology.

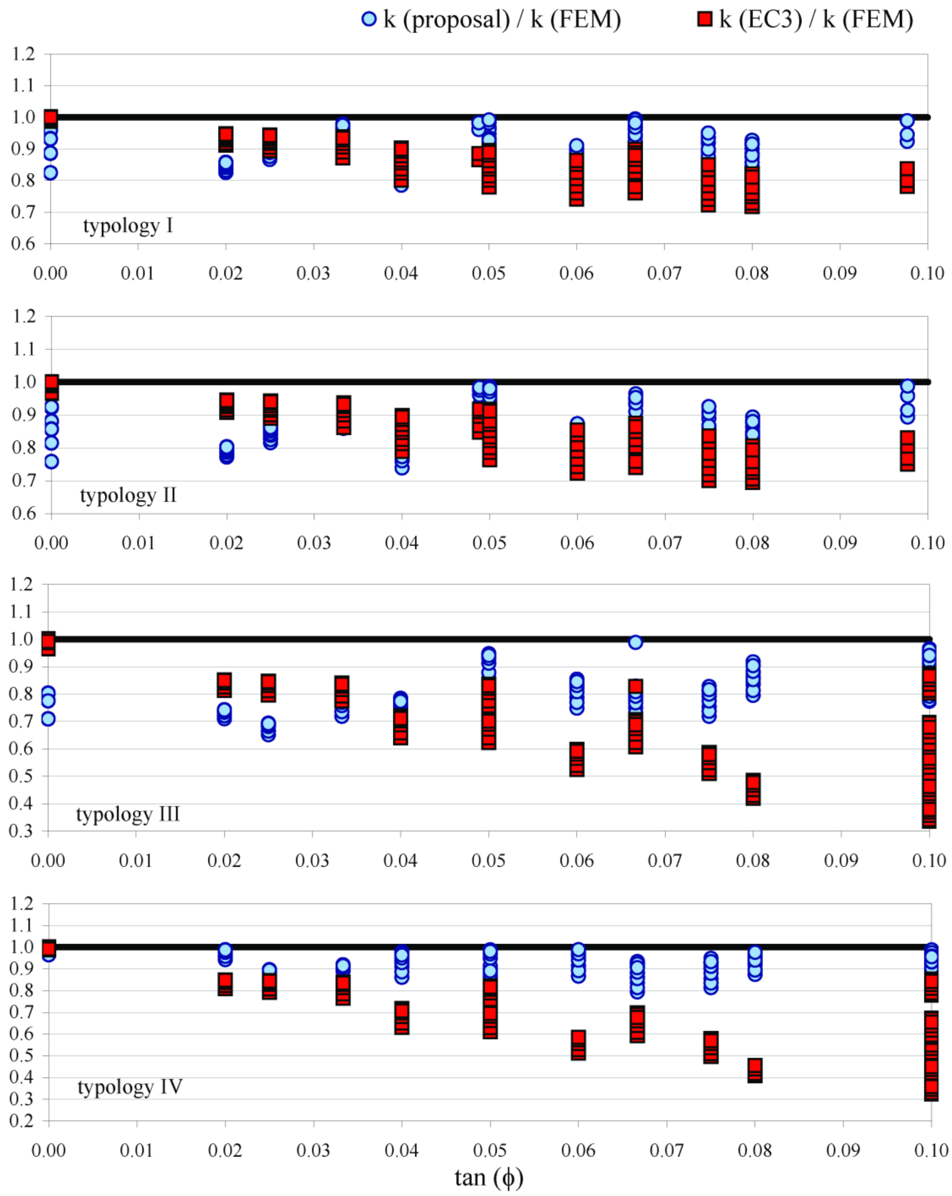

Fig. 2.11. Proposed methods compared with EN 1993-1-5 method for k_ϕ for tapered plates with a small slope: **a)** typology I; **b)** typology II; **c)** typology III; **d)** typology IV.

As is shown in the **Fig. 2.11**, the shear buckling coefficients k_ϕ calculated according to EN 1993-1-5 are better approximated by the expression for a rectangular plate if the slope does not exceed 2.5° ($tan(\phi) \approx 0.04$). In other cases, the expressions proposed in **Eqs. 2.4**, **2.5**, **2.8** and **2.9** are more accurate. For typology IV, the proposed expression (**Eq. 2.9**) can be used for any angle, even if it is less than 2.5° (**Fig. 2.11d**).

2.8. Conclusions

A comprehensive numerical study on the structural behaviour of web panels of tapered steel plate girders subjected to shear has been presented. The study considered over 500 cases with different geometries. The influence of various parameters (thickness of the web, aspect ratio and slope of the flange) on the critical shear buckling stress of tapered web panels has been analysed in depth. Previous studies developed by the authors have demonstrated the existence of four different types of tapered panels regarding their structural behaviour due to shear. These types are defined by the direction of the diagonal tension field and the stress state of the inclined flange (in compression or tension).

Results from the parametric studies confirmed that the influence of web thickness on the shear buckling coefficient is not significant, thus leading to simpler formulations. Different design expressions for the critical shear buckling coefficient in tapered steel panels, for the four types investigated, have been proposed. The outcomes of this work and the new design proposals are consistent with existing application rules for prismatic steel plate girders, while achieving significant improvement in the estimation of the critical shear buckling load for tapered steel plate girders. In addition, these new design expressions for the linear elastic shear buckling coefficient mean an improvement for checking web breathing in tapered web panels.

3. Tapered plate girders under shear: Tests and numerical research

3.1. Abstract

This paper presents an experimental and numerical research on tapered steel plate girders subjected to shear. Experimental tests included four small-scale tapered steel plate girders. Research was focused on both, critical shear load and ultimate shear resistance. Moreover, the post-buckling behaviour of tapered plates was studied.

Further, some parametric studies with various geometries of tapered panels were done in order to find the most favourable design situations. The analysed parameters were: the panel aspect ratio, the inclined flange angle, the web and the flange slenderness.

Numerical simulations allowed distinguishing four different typologies of tapered plate girders which should be considered separately in design because of their different behaviour. Verification of the simplified procedure for tapered plates proposed in Eurocode EN 1993-1-5 allowed concluding that for some cases the estimation of the ultimate shear resistance is situated on the unsafe side and need to be revised.

***Keywords*:** tapered plate girders; critical load; shear resistance; instability; FE model; imperfections; residual stress; Resal effect

3.2. Introduction

In building and civil engineering structures with large dimensions and subjected to high loads welded plate girders are currently designed. For efficient design it is usual to choose a relatively deep and non-prismatic girder. In these cases the web may be quite slender and so it may be prone to shear buckling. Although the shear buckling phenomenon has been widely studied for prismatic plates, there are very few theoretical and experimental investigations into the structural response of tapered steel plate girders under increasing shear load up to failure. Just as Galambos (1998) points out, more work is required to develop general design procedures for the ultimate strength of steel panels with variable depth. There are no rules in current steel codes for the design of tapered plate girders.

The current design code for plated structural elements, EN 1993-1-5 (2006) proposes to determine the ultimate shear resistance of tapered plate girders as prismatic ones. In order to evaluate this simplification, some experimental tests and a wide parametric study with different geometries of tapered plate girders were conducted.

This paper is divided into three principal parts. First of all the experimental tests on four tapered steel plate girders is presented. The experimental results were also used to validate a numerical FE model. Next part of this work is focused on the parametric study and research on the influence of geometric parameters and structural imperfections (residual stress) on the ultimate shear strength. A lot of numerical simulations with different geometric parameters, as the slope of the flange and the aspect ratio, were done. Finally, the outcome of these simulations was compared with the results obtained according to EN 1993-1-5 and discussed.

3.3. Shear models for tapered plate girders

3.3.1. State of art

The behaviour of the rectangular steel plates subjected to shear load was deeply studied during last century and different theories were developed in order to describe and analyse the mechanisms that take place during the post-buckling state and finally, to determine their ultimate shear capacity. Some of them are implemented in design codes: the Rotated Stress Field Model developed by Höglund (1971, 1997) and the Tension Field Model developed in Cardiff and Prague by Porter et al. (1975) and Rockey and Škaloud (1972).

However, these models are based on the assumption of simply supported rectangular plates and do not consider the boundary conditions existing in the flange–web junctions and in the stiffener–web junctions neither the geometry of the tapered steel plate girder. Some authors, among others Lee et al. (1996), Mirambell and Zárate (2000), Estrada et al. (2008) have demonstrated the importance of these effects.

The ultimate shear strength models for tapered plate girders proposed in literature are based on previous presented models for plate girders with constant depth. Several models for tapered girders have been developed by: Falby and Lee (1976), Davies and Mandal (1979), Takeda and Mikami (1987), Roberts and Newmark (1997), Zárate and Mirambell (2004) and Shanmugam and Min (2007). Recently, some other numerical studies have been published by Abu-Hamd and Abu-Hamd (2011).

3.3.2. Ultimate shear strength for tapered plate girders

It is well known that the structural behaviour of a prismatic steel plate girder subjected to an increasing shear load up to failure may be divided into three clearly different phases. Prior to buckling, equal tensile and compressive principal stresses are developed in the web panel. In the post-buckling stage, an inclined tensile membrane stress state is developed. The total stress state is obtained by adding the post-buckling to that induced at buckling. Once the web has yielded, failure of the steel plate girder occurs when plastic hinges are formed in the flanges. The failure load can be determined from the consideration of the mechanism developed in the last stage (upper bound solution) or by the consideration of the equilibrium of forces (lower bound solution (Porter et al., 1975)).

The behaviour of a tapered steel plate girder subjected to increasing shear load is practically identical to that exhibited in a prismatic steel girder. When the web buckles under the action of direct stresses, it does not exhaust the full capacity of the plate. After buckling, a significant increase in the strength of the steel plate girder can be observed. Experimental tests and numerical studies carried out on tapered steel plate girders reveal the existence of post-critical strength, by means of the development of the diagonal tension field anchored in the stiffeners and flanges.

Some models for the determination of the ultimate shear strength for tapered plate girders have been presented in the last years. All these studies are based on the tension field method, but one determines the ultimate shear load by the lower (equilibrium) bound method (Zárate and Mirambell, 2004); the other one by the upper (mechanism) bound method (Shanmugam and Min, 2007) and other one by both methods (Davies and Mandal, 1979).

It is important to explain here the limitation of the existing methods. The proposal of Zárate and Mirambell (2004) was thought only for these cases where the diagonal tension field develops in the short geometrical diagonal of the web panel. On the other hand, although the models proposed in (Shanmugam and Min, 2007) distinguish two different design situations, where inclined flange is in tension or in compression, there is no difference about the direction of the tension field.

In order to evaluate the methods abovementioned, a numerical study for rectangular and tapered plate girders was conducted. Research included various geometrical parameters and both situations, where the inclined flange is subjected to tension or compression, were analysed in (Real et al., 2010). The main conclusion of this study was that further ultimate shear models for tapered steel plate girders need to be developed in order to accurately evaluate the actual behaviour of tapered plate girders subjected to shear loads and their post-buckling resistance.

3.3.3. Shear resistance according to EN 1993-1-5

Despite being a very common type of beams, there are no specific rules for tapered plate girders in current codes. For calculating ultimate strength of tapered plate structures, EN 1993-1-5 suggests to use the expressions for prismatic plates without any changes if the angle of the inclined flange is not greater than 10°. In other cases is recommended to calculate a tapered plate as a rectangular plate with its larger depth. As it is shown in this paper, this approach cannot be used for some cases because overestimates the ultimate strength and thereby do not satisfy the safety requirements.

3.3.4. Four typologies – general behaviour

Previous numerical studies presented in (Real et al., 2010; Bedynek et al., 2011) demonstrated that both critical load and ultimate strength of tapered plate girder are strongly influenced by two factors: (1) inclination of the flange and whether the flange is under tension or compression and (2) the direction of the developed tension field, which may appear on the short or on the long web diagonal.

As a result it is possible to distinguish four different typologies of tapered plate girders (see **Fig. 3.1**):

I. inclined flange in compression and diagonal tension field developed in the short diagonal;
II. inclined flange in tension and diagonal tension field developed in the long diagonal;
III. inclined flange in tension and diagonal tension field developed in the short diagonal;
IV. inclined flange in compression and diagonal tension field developed in the long diagonal.

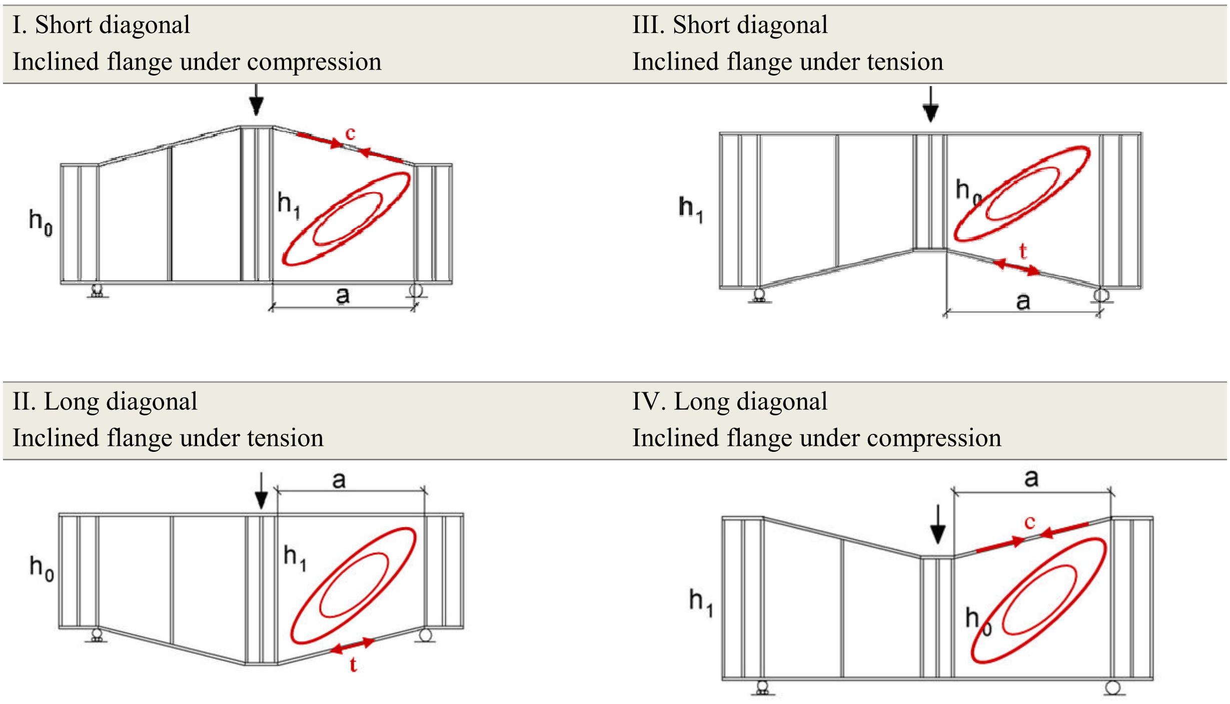

Fig. 3.1. Four typologies of tapered plate girders.

Fig. 3.2 shows examples of the application of each typology. Three of them can be met in various parts of a bridge span with non-prismatic cross-section, depending on the distribution of internal forces. The most common case is the first one, which appears frequently near to the intermediate supports of continuous bridges or in portal frames.

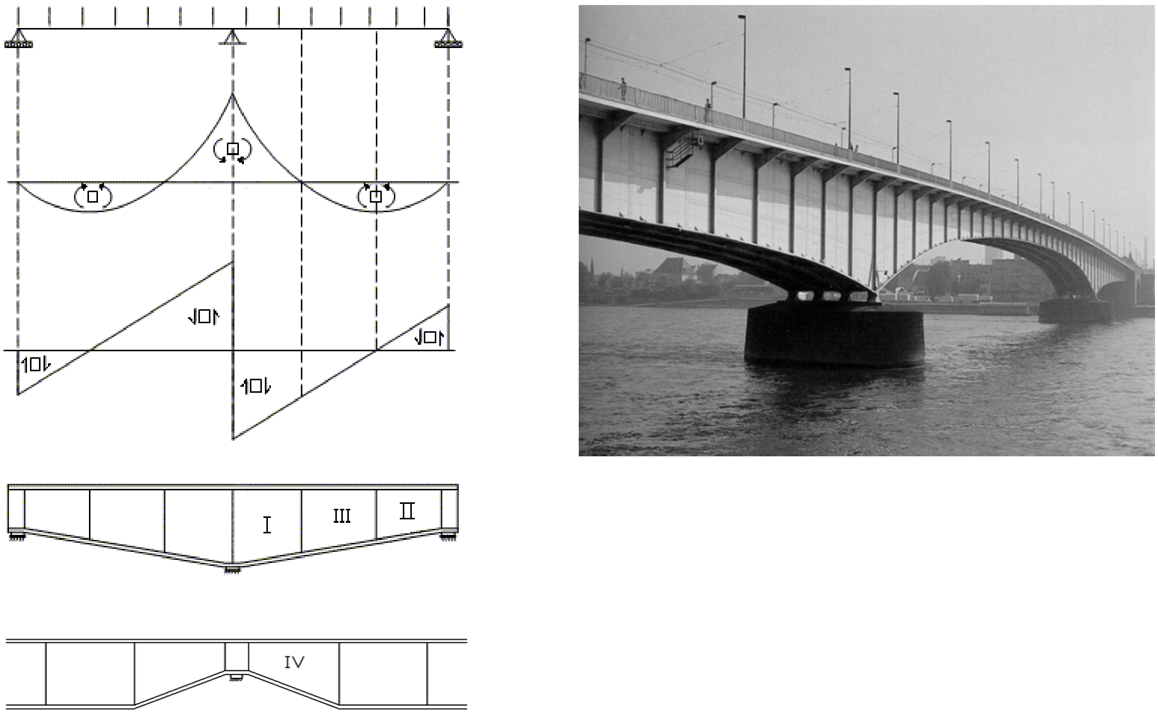

Fig. 3.2. Tapered plates in continuous steel bridges.

3.3.4.1. Resal effect

Different behaviour of each typology is provoked by appearance of an additional vertical component derived from the axial force in the inclined flange. This phenomenon is called Resal effect and can be favourable or not.

For these cases where the moment of inertia of the cross-section increases with the increase of internal forces (typology I and II), the vertical component acts against shear force and reduces it, thus the ultimate shear resistance is greater (positive influence). For typologies III and IV the opposite situation is observed. Graphical illustration of the Resal effect is presented in **Fig. 3.3**.

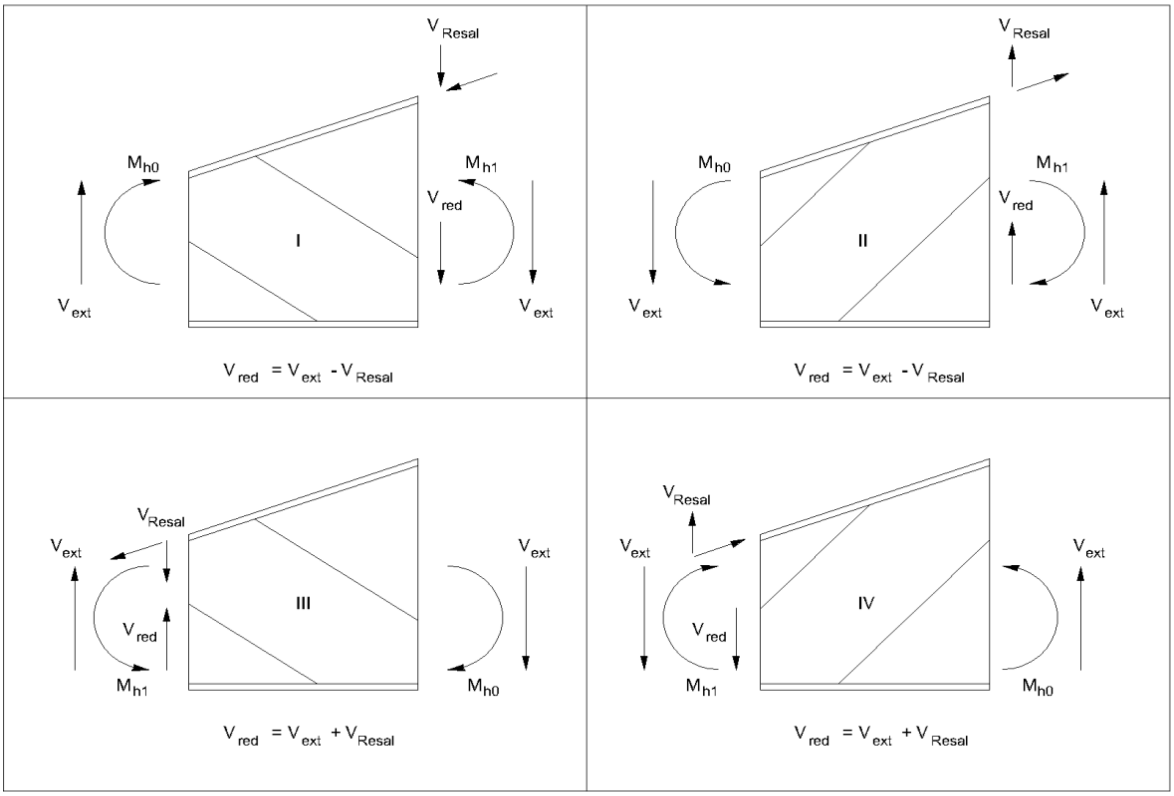

Fig. 3.3. Positive and negative influence of Resal effect on the ultimate shear resistance of tapered plate girders.

3.4. Experimental tests

Four small-scale experimental tests of tapered steel plate girders were carried out in the Laboratory of Structural Technology of the Polytechnic University of Catalonia to study the behaviour of tapered steel plate girders subjected to shear and shear-bending interaction. Experimental results were compared with those obtained by numerical simulation of the tests. All tested girders belonged to the same typology "I" which is considered as the most common case due to its geometry and the highest shear resistance (favourable Resal effect).

3.4.1. Geometry

The geometry of the tested girders with the symbols is presented in **Fig. 3.4**. All tested specimens had the same web thickness t_w and the same larger depth h_1. They differ in the aspect ratio $\alpha = a/h_1$ ($\alpha = 1$ and 1.5) and the slope of the inclined flange $tan(\phi)$ ($tan(\phi) = 0.25$ and 0.4). Dimensions of the analysed specimens are presented in **Table 3.1**. Terminology for girder's name is following: e.g. A_600_800_800_4_180_15 means: $h_0 = 600$ mm, $h_1 = 800$ mm, $a = 800$ mm, web thickness $t_w = 4$ mm, flange width $b_f = 180$ mm and flange thickness $t_f = 15$ mm (see **Fig. 3.4**)

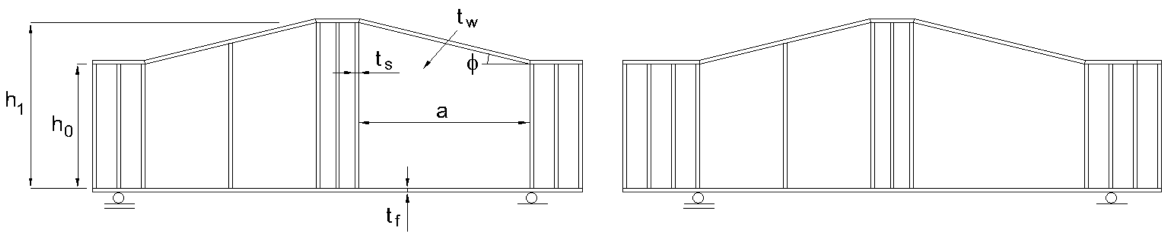

Fig. 3.4. Geometry of the tested specimens:
a) pure shear (girders A, B, C) **b)** shear-bending interaction (girder D).

Table 3.1. Dimensions of the tested girders.

Girder	h_0 [mm]	h_1 [mm]	a [mm]	t_w [mm]	b_f [mm]	t_f, t_s [mm]	α	$tan(\phi)$
A_600_800_800_4_180_15	600	800	800	4	180	15	1.0	0.25
B_500_800_1200_4_180_15	500	800	1200	4	180	15	1.5	0.25
C_480_800_800_4_180_15	480	800	800	4	180	15	1.0	0.40
D_600_800_800_4_180_15	600	800	800	4	180	15	1.0	0.25

Girders A, B and C (see **Fig. 3.4** and **Table 3.1**) were tested as simply-supported, rigid end posted, short beams with the load applied at the mid-span to consequently obtain a constant shear law. Girder D (see **Fig. 3.4** and **Table 3.1**) was tested in order to observe shear-bending interaction. Additional bending moment on the cross-section with the shorter depth h_0 was induced by increasing the distance between the right support and the cross-section where the load was applied (see **Fig. 3.4b**). In all girders, a single transverse stiffener was welded in the non-instrumented web panel in order to ensure that shear buckling started in the instrumented one.

3.4.2. Material properties

All analysed tapered plate girders were made of steel S275. Material properties were taken from the standard tensile coupon tests and they are represented by the average values obtained from five specimens, being Young's modulus $E = 211.3$ GPa, Poisson's ratio $\nu = 0.3$, yield strength $f_y = 320.6$ MPa and ultimate strength $f_u = 423.4$ MPa. Precise measurement of the tensile coupons cut out from the web showed that their actual thickness was $t_w = 3.9$ mm instead of the nominal value 4.0 mm. Therefore, for a better reproduction of the real conditions during the experimental tests, the actual web thickness was assumed in the numerical model for further comparisons.

3.4.3. Numerical simulations of the experimental tests

Several numerical analyses on tapered steel plate girders subjected to shear and shear-bending interaction were conducted with use of Abaqus code (2010). Both geometric and material non-linearities were taken into account. To reproduce the influence of large deformations that occur during the shear buckling phenomenon, 4-node shell element S4R5 was used. Due to the geometric and material non-linearities (post-buckling behaviour, softening and collapse) "modified Riks" method was applied. The stress–strain relationship was based on the simplified bi-linear diagram σ–ε with kinematic hardening and on the von Mises criterion for yielding stress assumed for ductile materials.

EN 1993-1-5 recommends both geometric and structural imperfections should be included in FE-model. Geometric imperfections may be based on the shape of the critical plate buckling modes. In this study, the deformed shape obtained from the 1st positive eigenvalue (responding to the shear buckling mode) was adopted for the geometric and material non-linear analysis with geometric imperfections to determine the ultimate shear strength V_u. The aforementioned imperfections were scaled in a way that their maximum value was 80% of the geometric fabrication tolerances according to EN 1993-1-5, Annex C.

Structural imperfections in terms of residual stress may be represented by a stress pattern from the fabrication process. In the literature, several proposals about taking into account the residual stress which appears during the manufacturing process of plate girders can be found. In order to consider the effects of welding and flame-cutting, the self-equilibrated stress distribution proposed in (Barth and White, 1998) was used in this work (see **Fig. 3.5**). In **Fig. 3.6** the distribution of the assumed residual stresses in the FE-model is shown. Comparison of the ultimate shear resistance without and with structural imperfections is presented in **Table 3.2**. The maximum difference achieves 1.7% and may be concluded that the influence of the residual stresses for slender tapered plate panels is relatively small and can be neglected in the further numerical analysis.

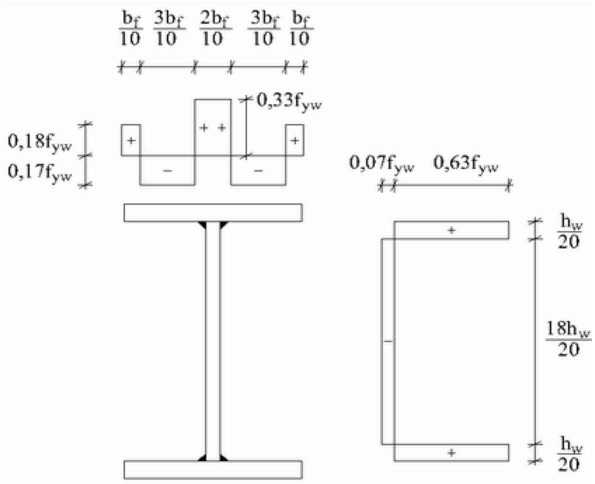

Fig. 3.5. Simplified residual stress pattern used (compression, negative).

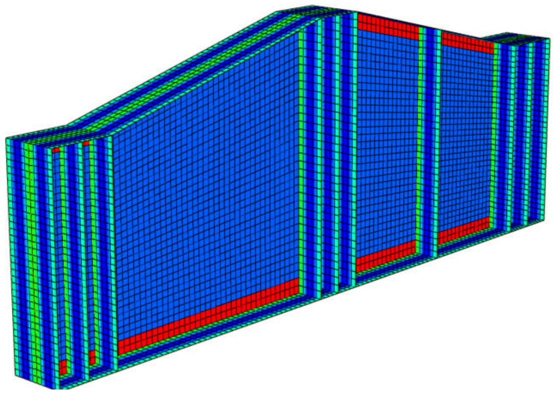

Fig. 3.6. Residual stresses included in the numerical model.

Table 3.2. Influence of the residual stresses on the ultimate shear strength (numerical model).

Girder	$V_{u\,(FEM)}$ [kN]		Diff [%]
	Residual Stresses - NO	Residual Stresses - YES	
A_600_800_800_3.9_180_15	410.8	408.5	0.6
B_500_800_1200_3.9_180_15	346.5	340.6	1.7
C_480_800_800_3.9_180_15	408.7	403.8	1.2
D_600_800_800_3.9_180_15	424.3	421.3	0.7

3.4.4. Results and numerical model validation

Below qualitative and quantitative comparison of the numerical and the experimental results is presented. **Fig. 3.7** shows the deformed shape of one of the tested tapered steel plate girders in the post-buckling range, near to failure. Yielded zones on the short diagonal are represented by darker grey colour (**Fig. 3.7a**). Total exhaustion of the shear capacity was achieved as a result of the web yielding, appearing two plastic hinges in both flanges (failure mechanism).

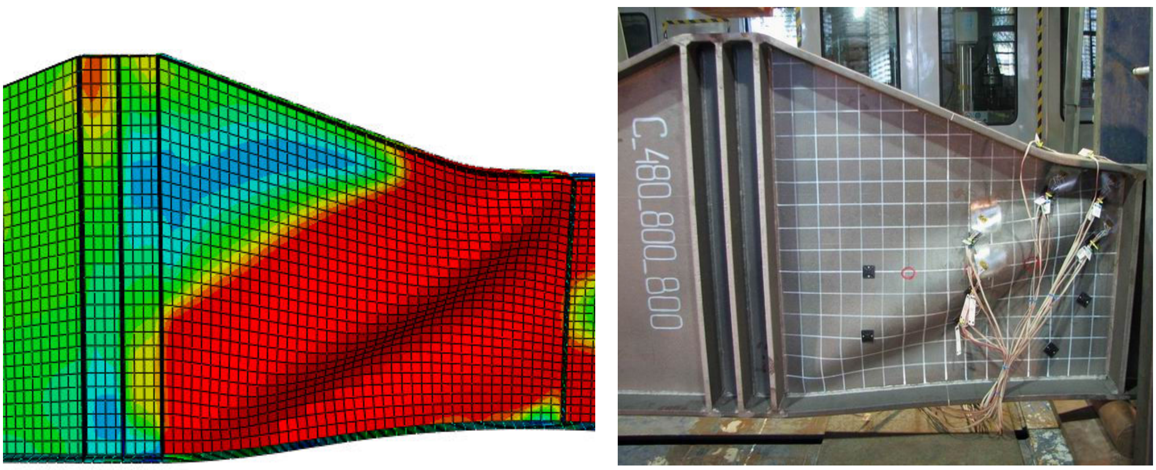

Fig. 3.7. Qualitative comparison of the deformed shape of the girder C_480_800_800_3.9_180_15:
a) numerical model **b)** experimental test.

Table 3.3 compares the critical and the ultimate shear forces obtained from the numerical analyses (FEM), from the experimental tests, and those calculated according to EN 1993-1-5, respectively. In this table, the critical shear buckling loads were obtained numerically as a result of eigenvalue analysis. The experimental critical shear buckling loads were obtained from the load–deflection relationships for each girder (**Fig. 3.8**), in the point where the curves lose their linearity.

Table 3.3. Numerical and experimental results of critical shear buckling load and ultimate shear force.

Girder	FEM (with residual stresses)		Tests		EN 1993-1-5	
	V_{cr} [kN]	V_u [kN]	V_{cr} [kN]	V_u [kN]	V_{cr} [kN]	V_u [kN]
A_600_800_800_3.9_180_15	223.9	408.5	225.0	392.0	132.3	341.7
B_500_800_1200_3.9_180_15	212.0	340.6	220.0	320.5	100.8	294.1
C_480_800_800_3.9_180_15	269.1	403.8	265.0	388.2	132.3	341.7
D_600_800_800_3.9_180_15	236.6	421.3	225.0	425.3	132.3	331.7

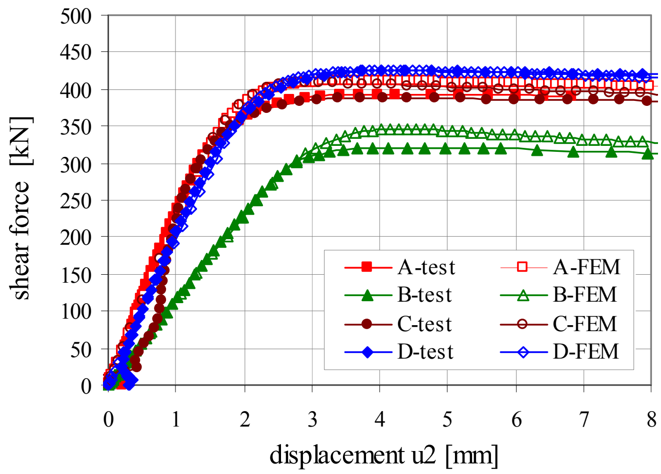

Fig. 3.8. Shear force vs. vertical displacement for all tested girders (experimental/FEM).

For all tested tapered plate girders the critical loads were smaller than the ultimate shear loads, which leads to the conclusion that the loss of linearity in the load–displacement curve was caused rather by geometric non-linear effects (buckling) than by material non-linearity (yielding).

Fig. 3.8 shows experimental and numerical curves of shear force vs. vertical displacement. For each tested girder, there is a good agreement between the numerical and the experimental results. Despite that the ultimate shear loads obtained from the FE analysis are slightly greater than those obtained experimentally, the maximum absolute difference between them does not exceed 6.3%. A proper validation of the numerical model is confirmed (see **Table 3.4**).

Table 3.4. FE-model validation.

Girder (t_w=3.9mm)	V_u (FEM) [kN]	V_u (test) [kN]	Diff. [%]
A_600_800_800_3.9_180_15	408.5	392.0	4.2
B_500_800_1200_3.9_180_15	340.6	320.5	6.3
C_480_800_800_3.9_180_15	403.8	388.2	4.0
D_480_800_800_3.9_180_15	421.3	425.3	-0.9

Fig. 3.9 shows the numerical and the experimental evolution of the membrane principal strains at the centre of the web panel of the girder A. Good agreement between both numerical and experimental curves is also observed. Detailed analyses carried out for the four tested girders confirmed good accuracy of the FE-model.

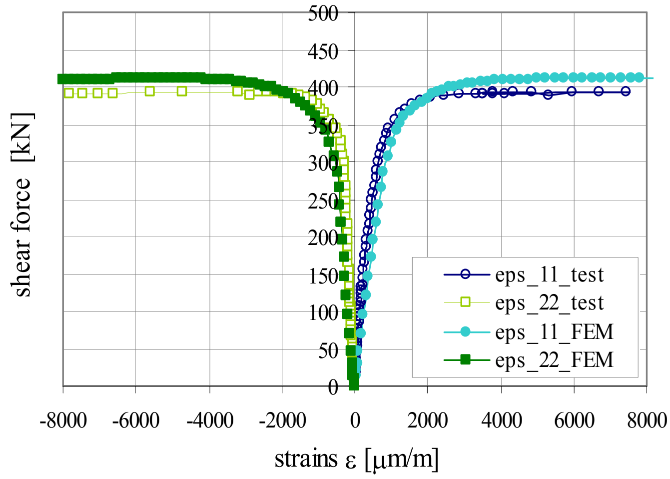

Fig. 3.9. Principal strains at the centre of the web panel (girder A_600_800_800_3.9_180_15).

It is important to point out that, the critical shear force should be calculated for simply supported conditions when the design procedure from EN 1993-1-5 is used. However, there is no influence on the ultimate shear resistance, because the corresponding reduction factor for the web contribution was calibrated using such elastic critical resistance.

Moreover, to be able to compare numerical ultimate shear resistance with ultimate shear resistance obtained according to EN 1993-1-5, the last one should be calculated without the resistance partial factor.

3.4.5. Experimental results vs. EN 1993-1-5

Table 5 presents a comparison of the experimental and analytical results for the critical shear buckling load V_{cr} and the ultimate shear resistance V_u. As it has been explained before, EN 1993-1-5 adopts the assumption that the critical shear load should be calculated as for a simply supported plate. Due to this fact, it is not compulsorily essential to achieve an agreement between experimental and theoretical critical shear buckling load.

Comparing the ultimate shear forces the accuracy seems to be better and does not exceed 17.6% (on the safe side) for the tapered girder D.

Table 3.5. Experimental results vs. analytical results according to EN 1993-1-5.

Girder	test	EN 1993-1-5	Diff. [%]	test	EN 1993-1-5	Diff. [%]
	V_{cr} [kN]			V_u [kN]		
A_600_800_800_3.9_180_15	225.0	132.3	41.2	392.0	341.8	12.8
B_500_800_1200_3.9_180_15	220.0	100.8	54.2	320.5	294.1	8.2
C_480_800_800_3.9_180_15	265.0	132.3	50.1	388.2	341.8	12.0
D_600_800_800_3.9_180_15	225.0	132.3	41.2	402.6	331.7	17.6

3.5. Parametric studies

In order to verify the applicability of the expressions proposed in EN 1993-1-5 for non-rectangular plates with a slope of the flange greater than 10°, a parametric study covering the four different typologies presented before was conducted. Influence of various geometric parameters, such as the aspect ratio, the angle of the inclined flange and the web slenderness, on the critical and the ultimate shear load was investigated.

For each typology of tapered panels two different aspect ratios $\alpha = 1$ or 2 (named AA and BB respectively) and various slopes of the inclined flange (up to 26.6°) were considered. Web thickness of 4 mm was adopted for all tested girders. Moreover, the results for the equivalent prismatic panels ($\tan(\phi) = 0$) for both aspect ratios ($\alpha = 1$ (AA^*) and 2 (BB^*)) are presented and used as a reference for other tapered panels. All detailed dimensions of the tested models are included in **Table 3.6**. It is important to point out that plate girders AA and BB are not comparable as they have different flange slenderness.

All analysed tapered plate girders were assumed of steel S275 ($f_y = 275$ MPa, $E = 210$ GPa, $\nu = 0.3$). The stress–strain relationship was adopted as a bilinear diagram with kinematic hardening. As it was demonstrated before, structural imperfections (residual stresses) have very small influence on the ultimate shear strength, thus they were not considered in this analysis.

In **Table 3.6**, the numerical and theoretical values of the ultimate shear resistance are presented. It is necessary to emphasize that to determine the ultimate shear resistance $V_{u\,(EN)}$ according to EN 1993-1-5, the critical shear buckling load for a simply supported rectangular plate was used. For prismatic girders AA^* and BB^* the critical shear buckling loads (simply supported plates, determined according to EN 1993-1-5) were $V_{cr} = 141.8$ kN and $V_{cr} = 64.2$ kN, respectively.

Table 3.6. Critical shear buckling loads and ultimate shear resistances for the prototypes analysed. Numerical results (FEM) and theoretical results (EN 1993-1-5).

Typology		Girder	α	ϕ [º]	$tan(\phi)$	FEM		EN 1993-1-5		Diff.	Diff.
						V_{cr} [kN]	V_u [kN]	$V_{u(1)}$ [kN]	$V_{u(2)}$ [kN]	(1) [%]	(2) [%]
rect. AA*		800_800_800_4_180_15	1.0	0.0	0.00	190.5	360.1	318.3	-	11.6	-
rect. BB*		1200_1200_2400_4_250_25	2.0	0.0	0.00	69.0	354.0	312.1	-	11.8	-
typology I	AA	680_800_800_4_180_15	1.0	8.5	0.15	215.8	365.6	318.3	-	12.9	-
		600_800_800_4_180_15	1.0	14.0	0.25	238.0	366.9	318.3	-	13.2	-
		480_800_800_4_180_15	1.0	21.8	0.40	285.0	364.8	318.3	-	12.7	-
		400_800_800_4_180_15	1.0	26.6	0.50	331.8	356.8	318.3	-	10.8	-
	BB	850_1200_2400_4_250_25	2.0	8.3	0.15	130.3	367.9	312.1	-	15.2	-
		600_1200_2400_4_250_25	2.0	14.0	0.25	177.9	368.4	312.1	-	15.3	-
		250_1200_2400_4_250_25	2.0	21.6	0.40	332.0	342.0	312.1	-	8.7	-
typology II	AA	680_800_800_4_180_15	1.0	8.5	0.15	202.5	354.8	318.3	-	10.3	-
		600_800_800_4_180_15	1.0	14.0	0.25	217.3	351.3	318.3	-	9.4	-
		480_800_800_4_180_15	1.0	21.8	0.40	256.3	335.4	318.3	-	5.1	-
		400_800_800_4_180_15	1.0	26.6	0.50	300.7	318.4	318.3	-	0.0	-
	BB	850_1200_2400_4_250_25	2.0	8.3	0.15	130.5	361.7	312.1	-	13.7	-
		600_1200_2400_4_250_25	2.0	14.0	0.25	180.0	355.2	312.1	-	12.1	-
		250_1200_2400_4_250_25	2.0	21.6	0.40	358.4	327.1	312.1	-	4.6	-
typology III	AA	800_680_800_4_180_15	1.0	8.5	0.15	189.3	310.4	318.3	**270.6**	-2.5	**12.8**
		800_600_800_4_180_15	1.0	14.0	0.25	188.0	274.9	318.3	**238.7**	-15.8	**13.2**
		800_480_800_4_180_15	1.0	21.8	0.40	186.6	221.0	318.3	**191.0**	-44.0	**13.4**
		800_400_800_4_180_15	1.0	26.6	0.50	185.8	182.4	318.3	**159.2**	-74.5	**12.7**
	BB	1200_850_2400_4_250_25	2.0	8.3	0.15	95.5	263.5	312.1	**221.1**	-18.4	**16.1**
		1200_600_2400_4_250_25	2.0	14.0	0.25	95.4	186.9	312.1	**156.1**	-67.0	**16.5**
		1200_250_2400_4_250_25	2.0	21.6	0.40	95.8	76.2	312.1	**65.0**	-309.6	**14.7**
typology IV	AA	800_680_800_4_180_15	1.0	8.5	0.15	176.4	300.5	318.3	**270.6**	-5.9	**10.0**
		800_600_800_4_180_15	1.0	14.0	0.25	168.7	263.3	318.3	**238.7**	-20.9	**9.3**
		800_480_800_4_180_15	1.0	21.8	0.40	161.6	202.7	318.3	**191.0**	-57.0	**5.8**
		800_400_800_4_180_15	1.0	26.6	0.50	160.1	161.4	318.3	**159.2**	-97.2	**1.4**
	BB	1200_850_2400_4_250_25	2.0	8.3	0.15	95.1	259.0	312.1	**221.1**	-20.5	**14.6**
		1200_600_2400_4_250_25	2.0	14.0	0.25	94.6	182.1	312.1	**156.1**	-71.4	**14.3**
		1200_250_2400_4_250_25	2.0	21.6	0.40	94.9	71.2	312.1	**65.0**	-338.3	**8.7**

Comparing numerical results of any plate girder may be concluded that both V_{cr} and V_u change among the typologies. This effect is observed for all analysed cases and confirms different behaviour within each typology.

It can also be observed easily, that the values of $V_{u(1)}$ for typology III and IV obtained according to EN 1993-1-5 are on the unsafe side.

The critical shear buckling loads, obtained numerically as a result of eigenvalue analysis, are presented in **Fig. 3.10**. It is shown that an increase of the slope of the inclined flange leads to higher critical loads for typologies I and II (continuous lines), while for cases III and IV (dashed lines) the critical shear load does not depend on the flange inclination. In addition, the critical shear buckling loads are higher for typologies I and II than for typologies III and IV. Also is observed that, within each typology, girders with various aspect ratios (A and B) maintain the same tendency.

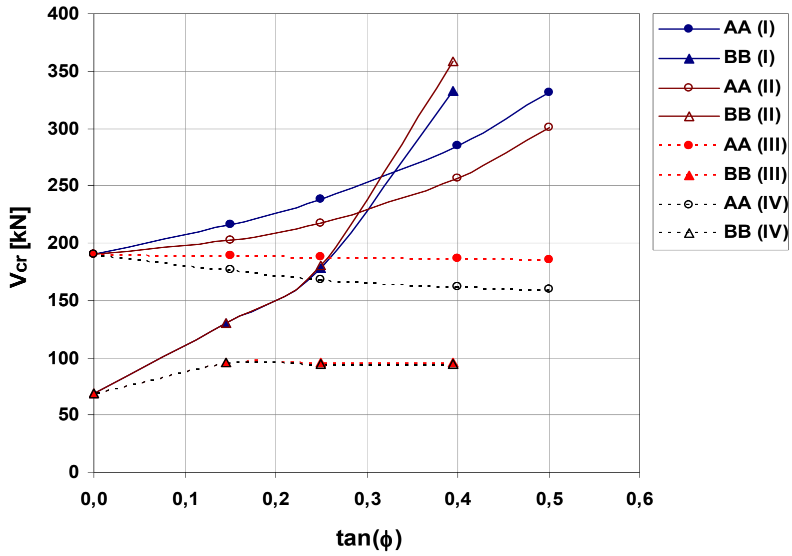

Fig. 3.10. Critical shear buckling load vs. flange inclination (*tan*(ϕ)) for all typologies.

As it was mentioned before, the critical shear buckling load calculated according to EN 1993-1-5 for tapered panels (reduced to the case of a rectangular simply supported plate) does not consider the actual boundary conditions of the web panel. However, there is no influence on the ultimate shear resistance, because the corresponding reduction factor for the web contribution was calibrated using such elastic critical resistance. More realistic critical resistance (taking account of clamping effects at the edges) would result in too optimistic shear resistance. To use more realistic critical forces the corresponding factor for the web contribution for the ultimate shear resistance calculations should be recalibrated. This limitation applies also to the web breathing check in EN 1993-2 (for the similar reason) but not for fatigue verifications, if the secondary stresses from local buckling are calculated explicitly (not very usual).

Fig. 3.11 presents numerical ultimate shear resistance $V_{u\,(FEM)}$ related to the $V_{u\,(EN)}$ obtained according to EN 1993-1-5. The curves for typologies I and II have similar trend with small differences between them. The same applies to the curves for typologies III and IV.

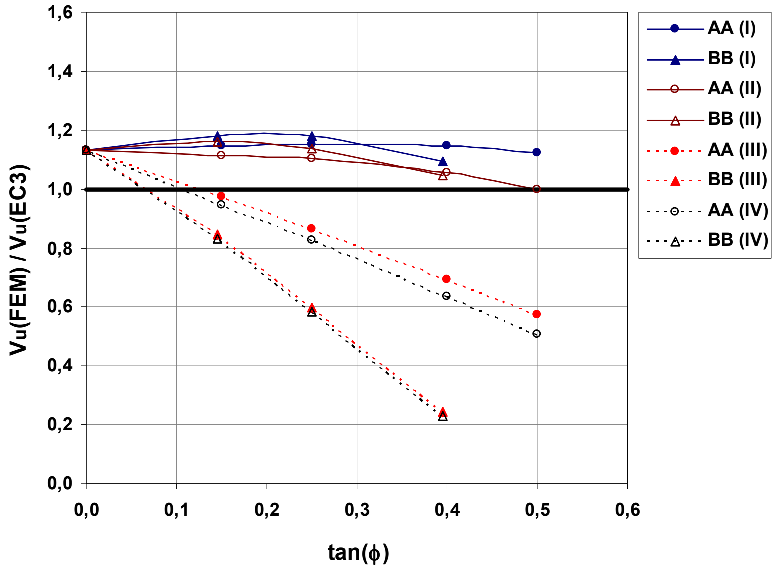

Fig. 3.11. Ultimate shear resistance vs. flange inclination (*tan*(ϕ)) for all typologies.

For typologies I and II there is no significant influence of the angle of inclined flange in the ultimate shear resistance, while for typologies III and IV there is a great decrease of the shear capacity with the increase of the angle of the inclined flange.

The highest shear capacity is observed for typologies I and II. In these cases, the diagram of bending moments along the beam increases with the increase of the beam rigidity (it means, the larger bending moment, the larger cross-section). The opposite situation takes place for the typologies III and IV.

For types I and II, in which the bending moment law varies in the same sense in which it makes the inertia of the cross section along the beam, the shear strengths obtained in this study are slightly higher than those obtained adopting an equivalent rectangular panel. It may therefore be of interest to consider this effect to achieve more economical designs with lower consumption of steel. In any case, as already stated above, types I and II can be designed in accordance with EN 1993-1-5, with sufficient accuracy.

However, for types III and IV, the ultimate shear strengths obtained numerically are clearly lower than those obtained by adopting a rectangular equivalent panel with its larger depth. Therefore, these types should not be designed according to EN 1993-1-5 rules, because the value of the shear strength of the tapered web panels is overestimated.

Despite the cases III and IV being not very usual in design, an improvement for the simplified method proposed in EN 1993-1-5 would be necessary. In these cases an additional step should be performed by calculating the web reduction factor for the largest depth as proposed in EN 1993-1-5 but the web resistance should be calculated for the smallest depth. As the flange contribution in these cases is not very high, an approximation value can be obtained by reducing the ultimate shear resistance by the ratio h_0/h_1.

Second values of $V_{u(2)}$ (bold) from **Table 3.6**, respond to the final resistance reduced by abovementioned factor. It is easy to find out an enormous improvement of all results and observe that now all of them stay on the safe side. The differences between numerical and theoretical values do not exceed 16.5% which can be considered as a satisfactory solution.

3.6. Discussion and conclusions

The study of the behaviour of tapered steel plate girders subjected to shear load revealed the existence of four different structural responses depending on the stress state of the inclined flange and the direction of the tension field. These differences are also influenced by the Resal effect, were the vertical component of the axial force in the inclined flange may increase or decrease the shear capacity of the tapered panel.

For typologies I and II where the diagram of bending moments along the beam increases with the increase of the beam rigidity, the ultimate shear resistance is very similar as the one for the equivalent rectangular panel. Therefore, there are some good reasons to design the panels as tapered such as good appearance, higher slenderness and an important reduction of material with similar ultimate shear resistance.

Moreover, the critical shear load is higher for typologies I and II than for typologies III and IV. For typologies I and II the critical shear buckling load increases with the increase of the flange inclination, while for typologies III and IV this situation does not occur.

For typologies I and II the ultimate shear resistance seems not to depend on the flange inclination but for cases III and IV sudden decrease of the ultimate shear resistance is observed as the inclination increases. The same trends are also observed for girders with different aspect ratios.

Concerning the design model proposed in EN 1993-1-5 following conclusions could be done:

The ultimate shear resistance calculated according to EN 1993-1-5 is on the safe side only for prototypes I and II, because these typologies behave similarly to the equivalent rectangular plates. Nevertheless, the ultimate shear resistance calculated according to design code seems to be too conservative for some cases (for the cases analysed in this paper the differences achieve 15.3%).

On the other hand, for typologies III and IV, EN 1993-1-5 rules overestimate the ultimate shear resistance. This fact could lead the tapered structure to be on the unsafe side. For some cases, especially when the angle of the inclined flange is considerable, the results do not match at all, achieving even up to -338.3%.

Then, the expressions proposed in EN 1993-1-5 for the typologies III and IV of tapered plate girders cannot be treated as a reliable design tool. For these cases it is possible to obtain much more accurate results reducing the ultimate shear resistance by a factor h_0/h_1.

The studies presented in this work pointed out a necessity to make additional research of the Resal effect and its influence on the ultimate shear strength for tapered panels, especially for the typologies III and IV.

4. Longitudinally stiffened tapered steel panels subjected to shear - Test and numerical research

4.1. Abstract

Tapered steel plate girders often can be found in long-span bridges or industrial buildings. In order to maintain the slenderness of the web plate and to reduce the consumption of steel, longitudinal stiffeners are often required. Additional stiffening should be rigid enough to avoid global buckling and thereby reduce the problem to local buckling of the individual sub-panels. Insufficient knowledge about the behaviour of the longitudinally stiffened tapered panels and the lack of analytical expressions for calculating their ultimate shear resistance, determined the main goals of this study.

The presented research can be divided into two parts, the experimental and the numerical one. Laboratory tests were performed on four small-scale steel girders, where the tested panels varied by the aspect ratio and the position of the longitudinal stiffener. Since the stiffeners were designed as rigid ones, a development of the individual tension field within each sub-panel was observed. The experimental results are compared with the results derived from a numerical model and used to its validation. The numerical part of this work is focused on the optimal design of the longitudinal stiffeners: influence of their rigidity and position on the behaviour of the tapered members.

Finally, the rules proposed in EN 1993-1-5 (2006) for rectangular plates with longitudinal stiffeners are revised and an attempt of their interpretation and extension for non-prismatic members is discussed.

***Keywords*:** tapered plate girders; shear resistance; longitudinal stiffening; optimal stiffness; FE model; imperfections; panel slenderness; experimental tests;

4.2. Introduction

In many modern structures, such as long-span steel bridges or industrial warehouses, steel plate girders with varying depth are used. There are numerous advantages of their trapezoidal shape and the most important are: more slender appearance and economic aspects which are a consequence of better adjustment between the changing cross-section and the non-uniform distribution of existing internal forces. Numerical and experimental studies on the structural behavior of tapered steel plate girders without longitudinal stiffeners, under shear, have already been previously conducted ((Zárate and Mirambell, 2004), (Shanmugam and Min, 2007), (Bedynek et al., 2013)).

Tapered panels are often used in large-scale structures susceptible to instability problems. The most common solution to avoid global buckling and to reduce the slenderness of the webs is to weld additional profiles such as longitudinal stiffeners. Depending on the panel slenderness and on the stress distribution, these extra profiles usually have a closed cross-section because of the higher flexural and torsional rigidity of the whole panel (Pavlovčič et al., 2007a). In some structural cases, the application of multiple longitudinal stiffeners within the same panel may be justified, which are usually welded on the same side of the web.

Another issue studied in this research is the optimal position of the longitudinal stiffener which depends on the stress distribution. Thus, for girders subjected mainly to shear, when the compressive stresses caused by bending moment can be neglected, the optimal position for one longitudinal stiffener would be at the mid-depth of the web, dividing the whole panel into two sub-panels with similar slenderness.

On the other hand, in design situations where the tapered panel is subjected to shear-bending interaction and the bending moment reaches significant values, the longitudinal stiffener may be more desirable in those parts of the structure which are under compression. In such situations, the limitation of the slenderness of the compressed sub-panel may be sufficient to improve its ultimate shear resistance significantly. Then, if the longitudinal stiffener has enough rigidity and the web panel is divided into two independent sub-panels, the problem of global buckling of the whole web may be simplified to the phenomenon of local buckling of each sub-panel, which is more favourable.

During the last century, several mechanical models assessing the ultimate shear resistance of longitudinally stiffened panels were developed ((Cooper, 1967), (Ostapenko and Chern, 1971), (Rockey et al., 1974), (Evans, 1983), (Höglund (1995, 1997)). The model developed by Cooper considered a failure of the web as a result of the development of two independent diagonal tension fields. In this method, the only advantage of applying longitudinal stiffeners was an increase of the critical shear load as a result of the reduction of the slenderness of the web. In 1971 Ostapenko and Chern made a comparison of four existing models with 40 experimental tests. Based on the obtained results and on new experimental tests conducted in

Cardiff ((Evans, 1983), (Evans and Tang, 1984, 1986)), a good accuracy of the tension field model, initially proposed by Rockey et al. (1974), was confirmed. Further design codes used the Rockey's method with assumption that longitudinal stiffeners may cause merely an increase of the critical shear load. Once the web panel buckles, the tension field develops over the whole web panel without considering the existence of the longitudinal stiffeners.

The mechanical model developed by Höglund (1995, 1997), called rotated stress field method, was included in the current design code EN 1993-1-5 (2006). The model exhibits a good agreement between numerical and experimental test and its undisputed advantage is its ease of application. Moreover, Höglund's model takes into account the existence of the longitudinal stiffeners in the post-critical phase.

4.3. Experimental tests

4.3.1. Objective

Four small-scale experimental tests of tapered steel plate girders with longitudinal stiffeners were carried out in the Laboratory of Structural Technology of the Universitat Politècnica de Catalunya. The experimental campaign was carried out in order to observe the behaviour of tapered steel plate girders with a single longitudinal stiffener and their nonlinear structural response under shear load. Two geometric parameters were studied: the aspect ratio of the girder and the position of the longitudinal stiffener. Finally, the experimental results were compared with the numerical ones in order to verify the numerical model.

4.3.2. Geometry and material properties of the tested girders

According to the geometry of the tested girders, they can be grouped into two types A and B. Specimens of type A (A1 and A2) had the same dimensions and the same aspect ratio $\alpha = a/h_1 = 1.0$ but different position of the longitudinal stiffener (see **Fig. 4.1**). Both specimens of type B (B1 and B2) had also the same dimensions, the same aspect ratio $\alpha = 1.5$ and the longitudinal stiffener placed in two positions. In girders A1 and B1, the longitudinal stiffener was placed horizontally at the middle of their shorter depth $0.5\,h_0$ (**Fig. 4.1a**) and in girders A2 and B2, the stiffener was inclined in such a way that two points at the middle of the largest $0.5\,h_1$ and the shortest depth $0.5\,h_0$ were connected (**Fig. 4.1b**). All dimensions and corresponding notation are presented in **Table 4.1** and **Fig. 4.1**. Moreover, denotation of girders has to be explained. For example symbol: A1_600_800_800_3_180_15 means a girder with the following dimensions: the shortest depth $h_0 = 600$ mm, the largest depth $h_1 = 800$ mm, the panel length $a = 800$ mm, the web thickness $t_w = 3$ mm, the flange width $b_f = 180$ mm and the flange and stiffener thickness $t_f = t_s = 15$ mm (see **Table 4.1**).

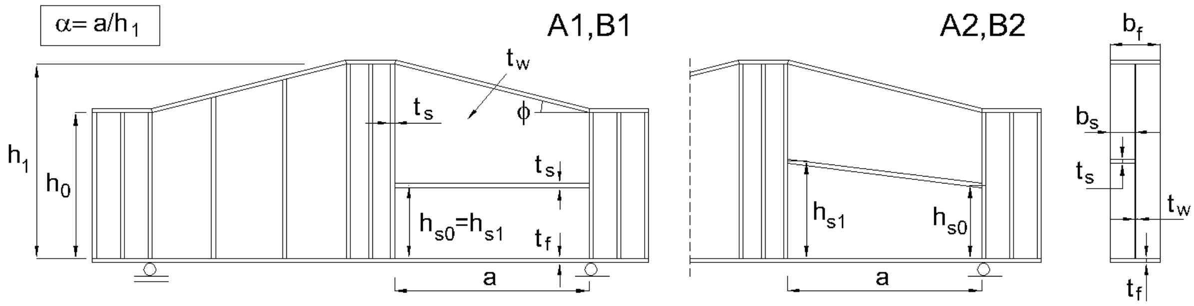

Fig. 4.1. Geometry and notation of the tested specimens: **a)** girders A1, B1; **b)** girders A2, B2.

Table 4.1. Dimensions of the tested girders.

Girder	h_0 [mm]	h_1 [mm]	a [mm]	t_w [mm]	b_f [mm]	t_f , t_s [mm]	h_{s0} [mm]	h_{s1} [mm]	α	$tan(\phi)$ slope
A1_600_800_800_3_180_15	600	800	800	3	180	15	300	300	1.0	0.25
A2_600_800_800_3_180_15	600	800	800	3	180	15	300	400	1.0	0.25
B1_500_800_1200_3_180_15	500	800	1200	3	180	15	250	250	1.5	0.25
B2_500_800_1200_3_180_15	500	800	1200	3	180	15	250	400	1.5	0.25

All tested girders were simply supported, with rigid end-posts. The load was applied at the mid-span, on the upper flange, obtaining a constant value of the shear force (**Fig. 4.2**).

The longitudinal stiffener was welded in an asymmetric way – on one side of the instrumented web-panel. Its geometry was designed in order to avoid its buckling and keep it undeformed up to the ultimate shear resistance of the girder. In order to ensure that shear buckling starts in the instrumented panel, two extra transverse stiffeners were welded on both sides of the non instrumented web panel (**Fig. 4.3**).

Since the critical shear load lower than the ultimate shear strength was desired, all examined web panels were designed with high slenderness to fulfill this requirement. It allowed observing two typical phases: the pure shear stress state, where the principal compressive and tensile stresses increase simultaneously and the post-critical resistance observed as a development of two separated diagonal tension fields in each sub-panel.

All tested girders were made of steel S235. In order to be able to compare the experimental and numerical results it was necessary to carry out the standard tensile coupon tests to determine actual properties of the steel. As a result of those tests conducted on six specimens, an average value of the yield stress of 300 MPa (all values between 290-322 MPa) was found. Nominal values of modulus of elasticity E and Poisson's ratio ν were assumed ($E = 210$ GPa and $\nu = 0.3$).

4.3.3. Measuring equipment

Four simply supported steel plate girders were instrumented the same way. Measuring equipment consisted of six triaxial strain gauges, placed symmetrically on each surface of the web, and three uniaxial strain gauges, placed on the inclined flange, in the points where the plastic hinges were expected to appear, and on the transversal and longitudinal stiffeners. Moreover, four displacement transducers were used. Three of them were placed on the web panel to measure the out-of-plane displacements, and the other one on the bottom flange, at the mid-span cross-section, in order to control the maximum vertical displacement (deflection) of the girder. Detailed distribution of the measuring equipment is presented in **Figs. 4.2** and **4.3**.

Fig. 4.2. Tested girders with the measuring equipment.

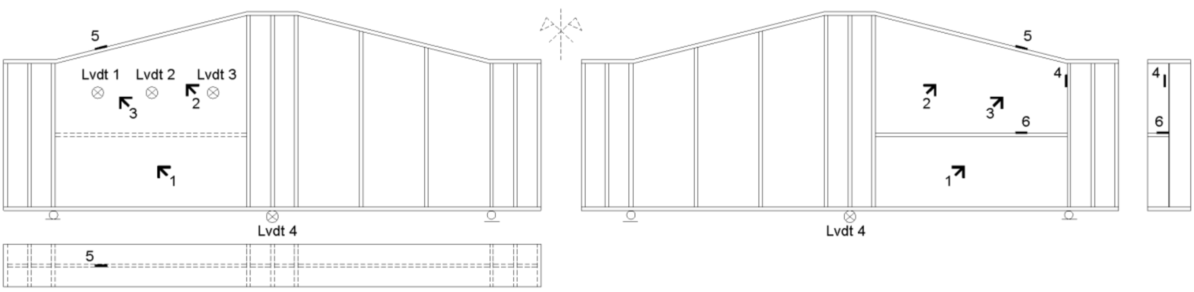

Fig. 4.3. Measuring equipment:
1-3 – triaxial strain gauges; 4-6 – uniaxial strain gauges; LVDT 1-4 – transducers.

The load was applied as uniformly distributed pressure, acting on the horizontal surface of the upper flange. Pressure was transmitted by the hydraulic piston through the rectangular contact area with dimensions 160x180mm and displacement control was used. The carrying capacity of the press could not exceed 1000 kN thus both the material properties and geometry of tested specimens had to be designed taking into account above-mentioned restrictions and preliminary numerical simulation had to be done.

4.3.4. Imperfections

The web thickness of all tested girders was $t_f = 3.0$ mm and the flanges and stiffeners thickness was $t_f = t_s = 15.0$ mm. This difference in rigidity of the connected plates and overall production process caused not only structural imperfections (flame cutting) but also considerably and visible geometrical imperfections (welding) observed as initial deformed shape of the webs. This problem was observed especially for girders type B (B1 and B2) due to their larger aspect ratio ($\alpha = 1.5$) and their lower general rigidity compared to the girders of type A. Although previous studies conducted by Bedynek et al. (2013) proved insignificant influence of the initial deformed shape on the ultimate shear resistance of tapered steel plate girders (differences approx. up to 2%), this statement is only valid if the imperfections are within the manufacturer's tolerances. For cases where such tolerance limits are exceeded, what took place for girders B1 and B2, the influence of the initial geometric imperfections may be much more significant.

4.4. Test results and numerical model validation

4.4.1. Introduction

In order to carry out a continued control of the structural response of the steel girder during the test, the measuring equipment was distributed in 13 check points. In this section, the most important experimental results are presented and discussed.

First of all, it is necessary to mention that the experimental results for girders B1 and B2 were registered only for the lower values of the applied load and had to be stopped. It happened due to the significant geometric imperfections detected in both girders, which made impossible to continue the tests over a certain value of applied load. At approximately halfway of the ultimate shear strength, both tests had to be stopped. As a result of the mentioned initial deformed shapes, an additional horizontal force at the point of the applied load occurred and started to push the tested girders out of their plane.

4.4.2. Numerical model

Numerical model used in the simulations is shown in **Fig. 4.4**. It is represented by the full 3D-girder with the actual boundary conditions (flanges and stiffeners) - simply supported along the roller-supports below the first inner transversal stiffeners of the girder. Detailed data for the boundary conditions for both supports are resumed in **Table 4.2**.

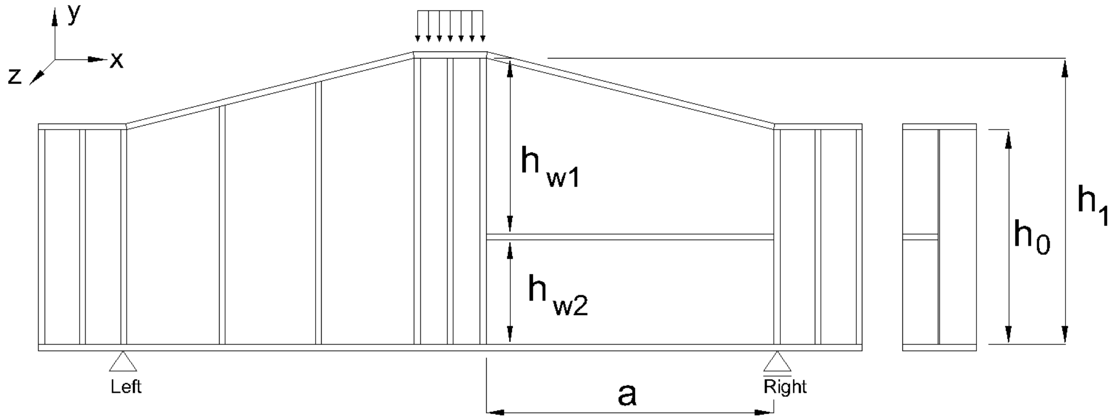

Fig. 4.4. Numerical model.

Table 4.2. Boundary conditions.

	u_x	u_y	u_z	θ_x	θ_y	θ_z
Left	0	1	1	1	1	0
Right	1	1	1	1	1	0

* 0 – free movement; 1 – restraint

The load was applied in the same way as in the experimental tests, as a pressure distributed on the horizontal surface of the upper flange with dimensions 160x180 mm or 160x220 mm depending on the width of the flange.

The parametric studies on tapered steel plate girders with one longitudinal stiffener subjected to shear are conducted with the use of ABAQUS (2010). To reproduce the influence of large deformations that occur during the shear buckling phenomenon, the 4-node shell element S4R5 is used. Due to the geometric nonlinearities (post-buckling behaviour) the "modified Riks" method is applied. The stress-strain relationship is based on the simplified bi-linear diagram σ-ε with kinematic hardening and on the von Mises criterion for yielding stress assumed for ductile materials. In the parametric studies a steel S275, with yield stress of 275 MPa, Young's modulus E = 210 GPa and Poisson's ratio ν = 0.3 is used.

4.4.2.1. Imperfections

EN 1993-1-5 recommends both geometric and structural imperfections should be included in FE-model. Geometric imperfections may be based on the shape of the critical plate buckling modes. In this study, the deformed shape obtained from the 1st positive eigenvalue (responding to the shear buckling mode – **Fig. 4.5**) was adopted for the geometric and material non-linear analysis with geometric imperfections to determine the ultimate shear strength V_u. The aforementioned imperfections were scaled in a way that their maximum value was 80% of the geometric fabrication tolerances according to EN 1993-1-5, Annex C.

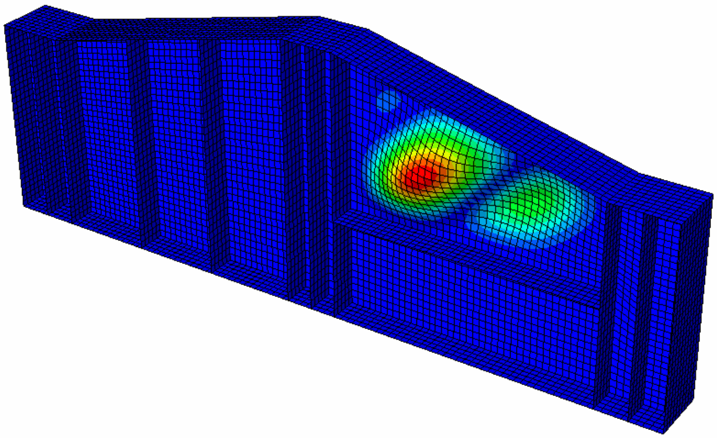

Fig. 4.5. Example of a shape of the initial geometric imperfections based on the buckling mode.

Previous studies presented by Bedynek et al. (2013) for tapered plate girders with transversal stiffeners and Pavlovčič et al. (2007a) for rectangular plate girders with longitudinal stiffeners allowed concluding that the plate girders are not very susceptible to the structural imperfections such as residual stresses, thus in this research only geometrical imperfections are considered.

4.4.3. Comparison of the results

4.4.3.1. Shear force-deflection curves (girders A1, A2, B1, B2)

A comparison of the shear force-deflection curves obtained from the numerical simulations and the experimental tests is shown in **Figs. 4.6** and **4.7**. The maximum vertical displacement was measured at the mid-span of the girder (LVDT no. 4). For girders A1 and A2, a good agreement between each pair of the numerical and experimental curves is observed. Differences between the experimental and numerical force-deflection curves (near to the maximum shear forces) may be caused by combination of the geometric and structural imperfections existing in the tested girders.

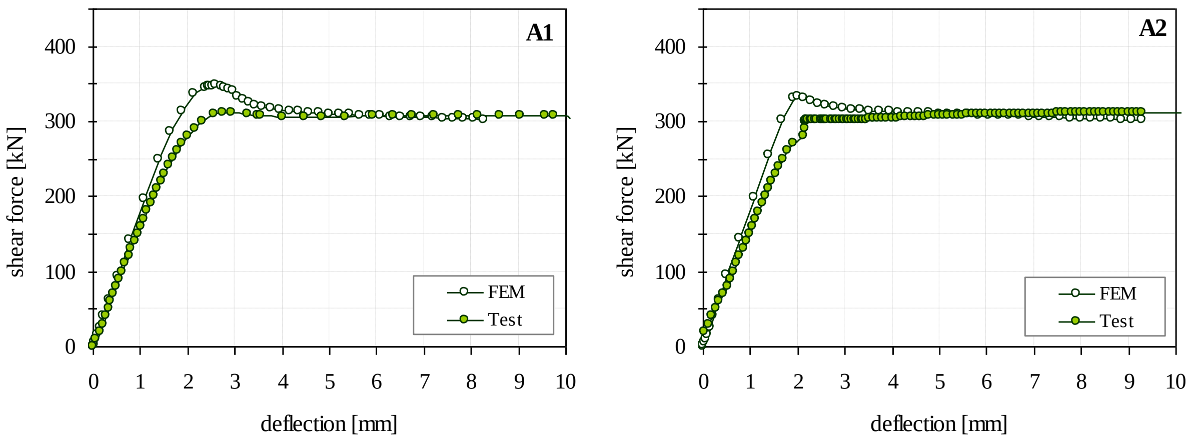

Fig. 4.6. Shear force-deflection curves. Numerical and experimental curves for girders A1 and A2.

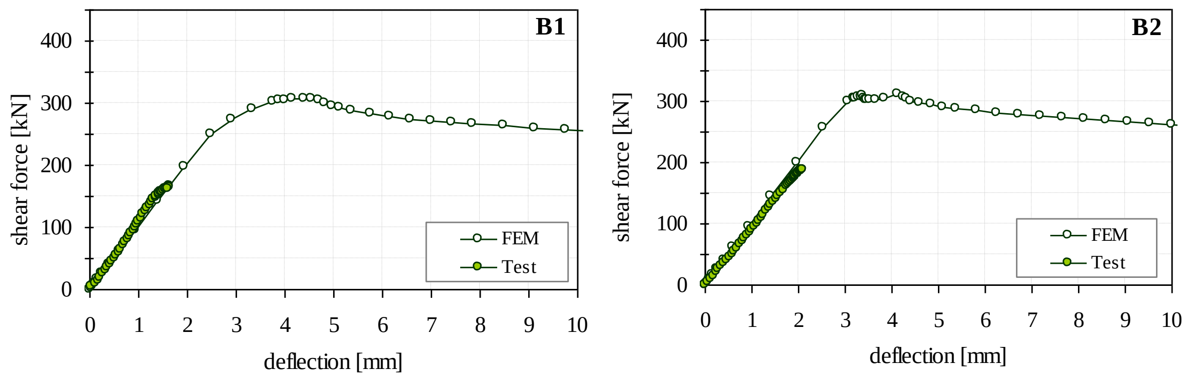

Fig. 4.7. Shear force-deflection curves. Numerical and experimental curves for girders B1 and B2.

4.4.3.2. Strain gauges

A pair of rosettes was put symmetrically in both sides of the web (see **Fig. 4.3**) in such way that from the average value of each corresponding pair of uniaxial gauges (having the same direction) it was possible to calculate the membrane strains. Knowing the membrane strains in these three directions and transforming the coordinate system the principal membrane strains can be obtained.

A comparison of the numerical and experimental principal membrane strains is presented in this section. For all tested girders, the upper trapezoidal sub-panel buckled first.

Figs. 4.8 and **4.9** illustrate the principal membrane strain-shear force relationships registered in the strain gauges no. 3, where for all tested girders theoretically the buckling should start. A very good agreement is observed between the numerical and experimental curves and possible differences observed for girders type A can be caused by the geometric imperfections (initial deformed shape of the web) or/and the structural imperfections (residual stresses introduced in the fabrication process, flame cutting, welding). These factors also explain the lower experimental resistance of girders A1 and A2.

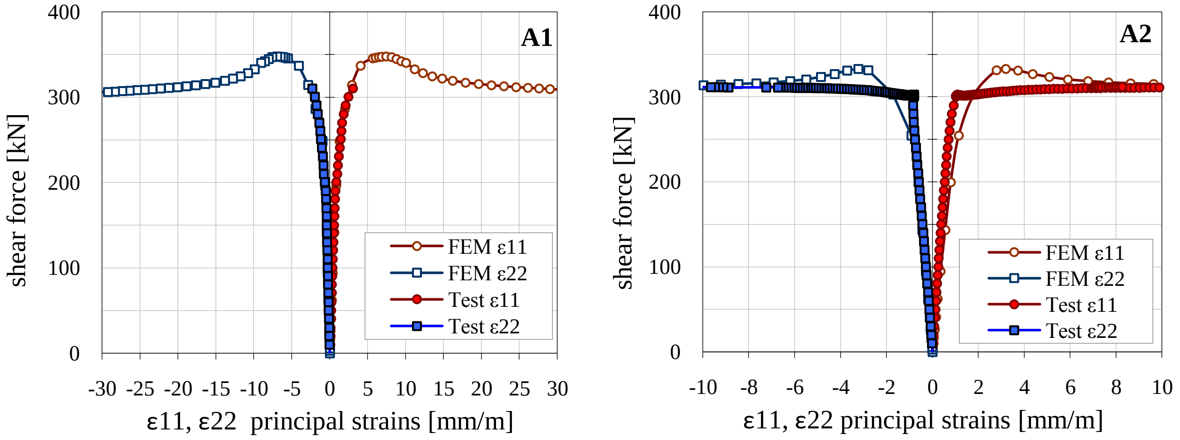

Fig. 4.8. Principal membrane strains (central strain gauge – no.3).
Numerical and experimental curves for girders A1 and A2.

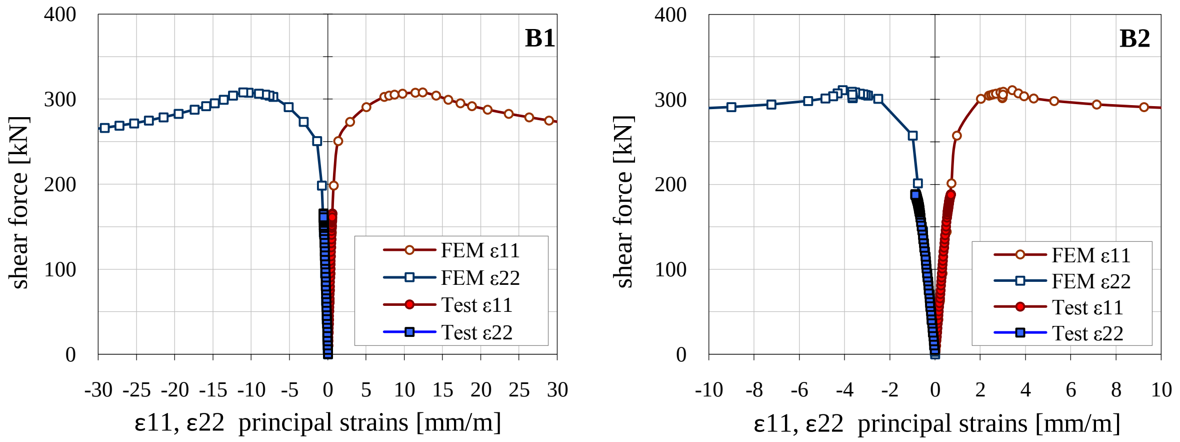

Fig. 4.9. Principal membrane strains (central strain gauge – no.3).
Numerical and experimental curves for girders B1 and B2.

4.4.3.3. Deformed shape

Fig. 4.10 shows an example of a qualitative comparison between the experimental and numerical deformed shape of girder A1. Also here, a very good agreement between the experimental and numerical buckling "waves" is observed. In the case of the girder A1, the upper trapezoidal sub-panel buckles before the lower rectangular one. Next, two diagonal tension fields are created independently according to the slenderness of the sub-panels. The development of two independent tension fields in each sub-panel, ensures that the longitudinal stiffener used in the tests posses enough rigidity to avoid out-of-plane displacements of the whole web panel along its length.

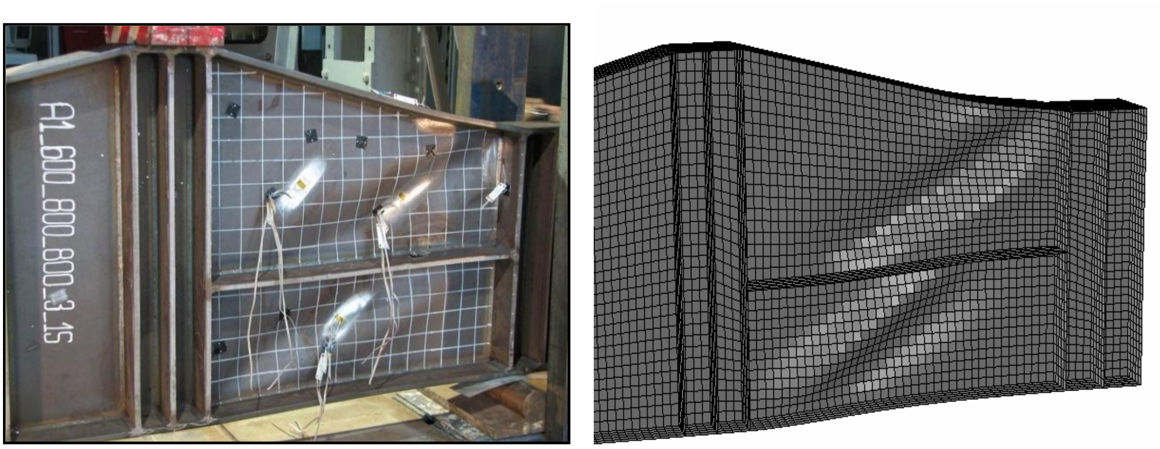

Fig. 4.10. Comparison of deformed shape for girder A1: **a)** experimental test **b)** numerical model.

Fig. 4.11b shows the out-of-plane displacements measured in three points of the web (LVDT 1, 2 and 3). The transducers were placed, respectively, at 140 mm, 378 mm and 656 mm from the outer support. For all tested girders their location was very similar. Three displacement transducers were placed on the upper sub-panel in order to know, as far as possible, the deformed shape of the web along its length. As an example, **Fig. 4.11** shows the out-of-plane displacements obtained experimentally and numerically for the similar values of the applied loads.

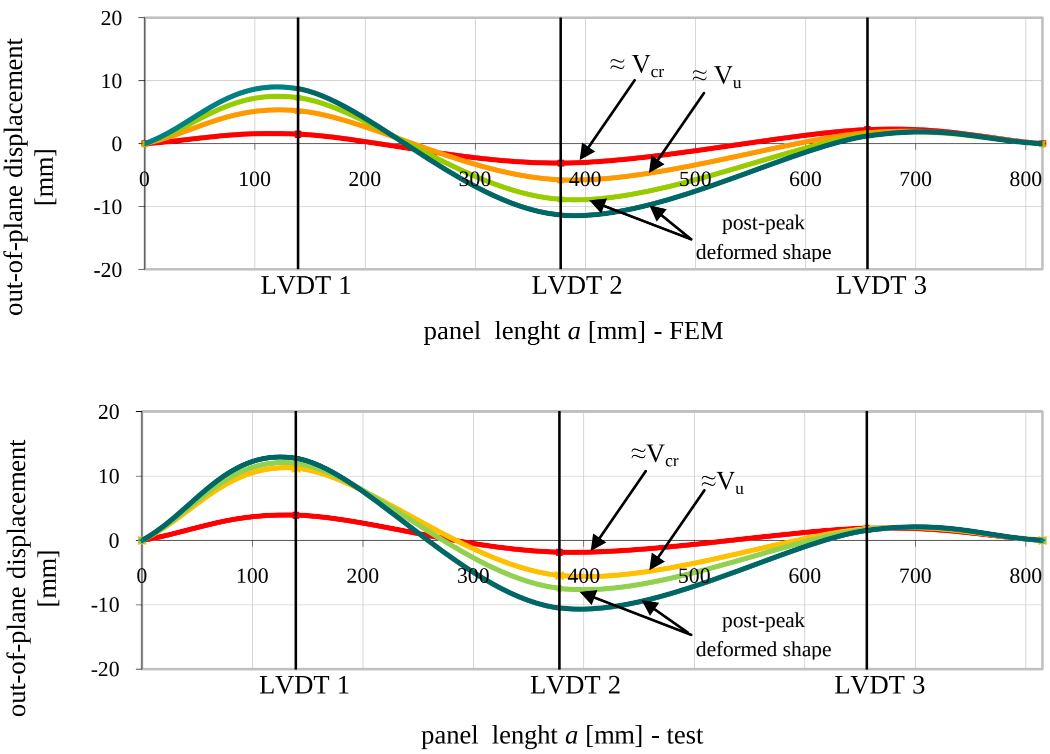

Fig. 4.11. Deformed shape of girder A1: **a)** numerical model; **b)** experimental test.

4.4.4. Numerical model validation

In **Table 4.3**, the numerical values of the critical shear loads $\boldsymbol{V}_{\mathbf{cr}}$ and the comparison of the experimental and numerical values of the ultimate shear strength $\boldsymbol{V}_{\mathbf{u}}$ are presented. As it can be seen, the differences between the ultimate shear strength $\boldsymbol{V}_{\mathbf{u}}$ obtained for both girders A1 and A2 show a good agreement and do not exceed -11.3 %. The lower values of the experimental ultimate shear strengths $\boldsymbol{V}_{\mathbf{u}}$ comparing to the numerical ones could be caused by excessive initial imperfections observed in all girders.

Table 4.3. Numerical model validation.

Girder	V_{cr} (FEM NLG) [kN]	V_u (test) [kN]	V_u (FEM) [kN]	Diff. [%]
A1_600_800_800_3_180_15	196.6	312.5	347.8	-11.3
A2_600_800_800_3_180_15	250.0	311.9	333.1	-6.8
B1_500_800_1200_3_180_15	198.3	-	307.9	-
B2_500_800_1200_3_180_15	257.5	-	310.8	-

As it was mentioned before, the initial deformed shapes of girders B1 and B2 made impossible to continue both tests with loads exceeding their critical shear level. For this reason, the validation of the numerical model is based only on two specimens A1 and A2.

Recapitulating and taking into account a very good agreement between the experimental and the numerical force-deflection curves, the deformed shape and strain-state measured in the characteristic points, it can be concluded that the numerical model is validated successfully and can be used in the further research.

4.5. Shear resistance according to EN 1993-1-5

4.5.1. Rectangular longitudinally stiffened panels

The rotated stress field method proposed by Höglund (1995, 1997) turned out to be an efficient design tool for steel and aluminium alloy plate girders subjected to shear for unstiffened, transversally and longitudinally stiffened panels. Also, the rotated stress field method has been used in the case of stainless steel girders under shear (Estrada et al., 2007a, 2007b).

Due to the good agreement with experimental tests and its robustness and simplicity, Höglund’s method has been adopted in EN 1993-1-5. Unlike other mechanical models, the current method included in EN 1993-1-5 takes into account a bending stiffness of the longitudinal stiffeners what gives more realistic results of the ultimate shear resistance. Nevertheless, EN 1993-1-5 does not provide specific rules for tapered plates with longitudinal stiffeners.

The procedure of obtaining the ultimate shear resistance $V_{b,Rd}$ (**Eq. 4.1**) of unstiffened or longitudinally stiffened prismatic plate girders is very similar but some additional circumstances must be taken into account. For both cases, the ultimate shear strength is calculated as a sum of the contribution from the web $V_{bw,Rd}$ (**Eq. 4.2**) and flanges $V_{bf,Rd}$ (**Eq. 4.3**).

$$V_{b,Rd} = V_{bw,Rd} + V_{bf,Rd} \tag{4.1}$$

$$V_{bw,Rd} = \frac{\chi_w f_{yw} h_w t_w}{\sqrt{3}\,\gamma_{M1}} \tag{4.2}$$

$$V_{bf,Rd} = \frac{b_f t_f{}^2 f_{yf}}{c\,\gamma_{M1}}\left(1-\left(\frac{M_{Ed}}{M_{f,Rd}}\right)^2\right) \tag{4.3}$$

Unlike unstiffened plates, the ultimate shear strength $V_{b,Rd}$ of longitudinally stiffened members not only should be calculated with consideration of the capacity of the whole web panel but also the resistance of each sub-panel has to be checked. The main difference between unstiffened and longitudinally stiffened panels can be observed in the calculation of the contribution from the web $V_{bw,Rd}$. In that last case, the slenderness of the whole panel as well as the slenderness of all sub-panels has to be known, and the largest one should be used in the expression for the reduction factor χ_w (EN 1993-1-5, point 5.3, Table 5.1).

The slenderness of the whole web should be assessed with the consideration of the effective section of the longitudinal stiffener and the contributing part of the web (**Fig. 4.12**).

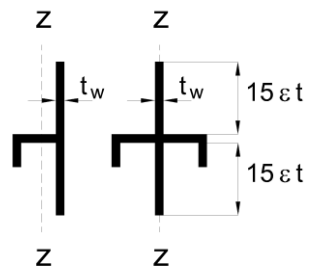

Fig. 4.12. Second moment of the area of a longitudinal stiffener I_{sl} about z-z axis.

Due to the lower post-buckling strength of stiffened plates, compared to unstiffened ones, in order to calculate k_τ, EN 1993 1-5 recommends a reduction of the second moment of the area of the longitudinal stiffener I_{sl} to 1/3 of its actual value (Johansson et al., 2007). The following formulae for k_τ taking into account this reduction may be used (EN 1993 1-5, Annex A.3). For plates with one or two longitudinal stiffeners and the aspect ratio $\alpha = a/h_w < 3$, the shear buckling coefficient k_τ should be taken from (**Eq. 4.4**):

$$k_\tau = 4.1 + \frac{6.3 + 0.18\,\frac{I_{sl}}{t_w{}^3\,h_w}}{\alpha^2} + 2.2\,\sqrt[3]{\frac{I_{sl}}{t_w{}^3\,h_w}} \tag{4.4}$$

If the aspect ratio $\alpha \geq 3$ (**Eqs. 4.5a-b**):

$$k_\tau = 5.34 + 4.00\left(\frac{h_w}{a}\right)^2 + k_{\tau sl} \qquad \text{when } a/h_w \geq 1 \tag{4.5a}$$

$$k_\tau = 4.00 + 5340\left(\frac{h_w}{a}\right)^2 + k_{\tau sl} \qquad \text{when } a/h_w < 1 \tag{4.55b}$$

where $$k_{\tau sl} = 9\left(\frac{h_w}{a}\right)^2 \sqrt[4]{\left(\frac{I_{sl}}{t_w{}^3\,h_w}\right)^3} \qquad \text{but not less than} \qquad \frac{2.1}{t_w}\sqrt[3]{\frac{I_{sl}}{h_w}}$$

To calculate the shear buckling coefficient k_τ of each sub-panel, the depth h_w should be substituted by the corresponding depth of the given sub-panel h_{wi}.

Next, using the obtained coefficients $k_{\tau i}$, the slenderness parameters of the whole web panel and the sub-panels should be calculated according to expression (**Eq. 4.6**):

$$\bar{\lambda}_{wi} = \frac{h_{wi}}{37.4\, t_w\, \varepsilon \sqrt{k_{\tau i}}} \tag{4.6}$$

The contribution from the web χ_w should be obtained considering the largest relative slenderness.

4.5.2. Interpretation of EN 1993-1-5 for tapered panels with longitudinal stiffening

Specifications provided by EN 1993-1-5, and commented by Johansson et al. (2001), concern only prismatic plates with various configurations of longitudinal stiffeners.

EN 1993-1-5 rules may apply to non-rectangular panels provided the angle of the inclined flange with the horizontal axis is not greater than 10˚. If this angle exceeds 10˚, panels may be assessed assuming it to be a rectangular panel based on the largest depth h_1.
The same assumption may be done for tapered panels with one longitudinal stiffener. In this case it is necessary to take into account the following situations: shear buckling of the whole

web-panel and shear buckling of each sub-panel. The upper non-rectangular sub-panel may be assessed assuming it to be a rectangular one based on the largest depth of the panel (h_{w1}) according to the general rule for tapered plates without longitudinal stiffeners. **Fig. 4.13** illustrates this situation.

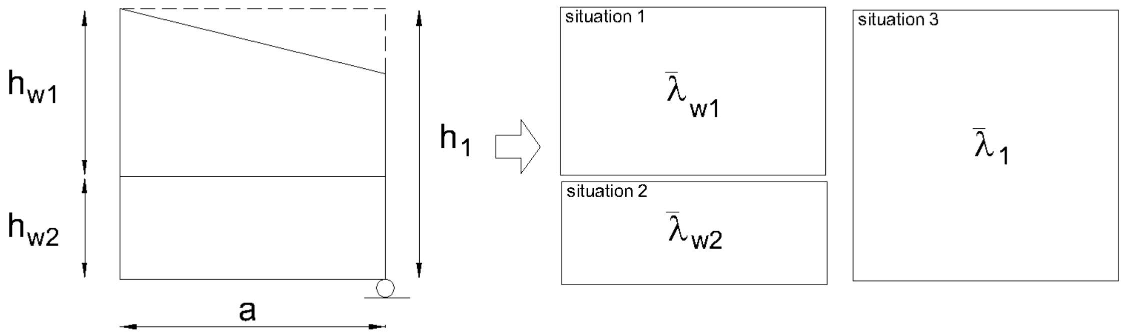

Fig. 4.13. Tapered panel and its division into sub-panels.

EN 1993-1-5 (point 5.3 (5)) states that for webs with longitudinal stiffeners the slenderness $\bar{\lambda}_w$ should not be taken as less than the expression given in **Eq. 4.6**, where h_{wi} and $k_{\tau i}$ refer to the sub-panel with the largest slenderness of all sub-panels within the web panel under consideration.

The presence of the longitudinal stiffening affects the failure mode of the girder and consequently has an influence on its ultimate shear resistance. The main parameter which defines the stiffness of the longitudinal stiffeners is called "relative flexural rigidity γ". There is a theoretical minimum value for this parameter γ^*, known as "critical limit stiffness" or "optimum rigidity ", which theoretically prevents global buckling of the panel up to the moment when the critical load is reached and allows calculating the critical shear load of the sub-panels according to the classic theory of elastic stability for simply supported plates.

The non-dimensional parameter γ is given by the following expression:

$$\gamma = \frac{12\,(1-\nu^2)\,I_{sl}}{h_w\,t_w{}^3} = 10.92\,\frac{I_{sl}}{h_w\,t_w{}^3} \qquad \textbf{(4.7)}$$

The parameter γ^* is defined as a function of the loading case and the position of the longitudinal stiffener (Skaloud, 1983). Thus, for example, for girders subjected to shear with one longitudinal stiffener placed at the mid-depth, the equation for γ^* is determined by:

$$\gamma^* = 5.4\,\alpha^2\,(2\alpha + 2.5\alpha^2 - \alpha^3 - 1) \qquad \text{for } 0.5 \le \alpha \le 2.0 \qquad \textbf{(4.8)}$$

where $\alpha = a/h_w$ is the aspect ratio of the plate.

In **Table 4.4** the experimental values of the ultimate shear resistance V_u (for two girders A1 and A2) are compared with their equivalent values obtained according to EN 1993-1-5. Additionally, the parameter γ/γ^* is calculated for those cases where the longitudinal stiffener is placed at the middle of the largest depth h_1 (girders A2 and B2). As it is mentioned before, only for these cases, an analytical expression exists for γ^* assuming that both sub-panels have a rectangular shape.

Table 4.4. Numerical and experimental results of the ultimate shear force.

Girder	V_u (test) [kN]	V_u (FEM) [kN]	V_u (EN) [kN]	Diff. V_u (test - EN) [%]	Diff. V_u (test - FEM) [%]	γ	γ^*	γ/γ^*
A1_600_800_800_3_180_15	312.5	347.8	262.6	15.7	-11.3	-	13.5	-
A2_600_800_800_3_180_15	311.9	333.1	294.3	5.6	-6.8	228.6	13.5	16.93
B1_500_800_1200_3_180_15	-	307.9	224.3	-	-	-	51.6	-
B2_500_800_1200_3_180_15	-	310.8	258.2	-	-	228.6	51.6	4.43

From the comparison of girders A, it can be observed that for the two examined cases, the assessment of V_u given by EN 1993-1-5 is on the safe-side, however somehow conservative (up to 15.7 %). Moreover, from the comparison of the numerical results, it can be observed that the ultimate shear resistances $V_{u(FEM)}$ within each pair of girders A (A1 and A2) and B (B1 and B2) have similar values. This fact allows concluding that for the examined geometries of tapered panels, the position of the longitudinal stiffener does not play an important role.

4.6. Parametric studies

4.6.1. Introduction

The parametric studies are focused on a few relevant issues. The main objective of the numerical studies is the validation of the approach given in EN 1993-1-5 for rectangular plates with one longitudinal stiffener and research on the possibility of its application and extension for non-prismatic members. For this reason, 36 numerical simulations for tapered girders with different geometry and three different positions of the longitudinal stiffener were done. In order to assure a minimum rigidity of the applied stiffeners, some additional studies had to be carried out. Apart from the principal goal, the optimal position of the longitudinal stiffener is also studied.

4.6.2. Optimum rigidity of the longitudinal stiffener

First of all, it is necessary to recall some terms which are used in the further part of this research. There are two parameters: γ - called relative flexural stiffness (**Eq. 4.7**) and γ^* - the minimum rigidity of the longitudinal stiffener, which theoretically should avoid the global buckling of the web up to the critical shear load. Even though, EN 1993-1-5 does not provide any requirements for the minimum rigidity of the longitudinal stiffeners, there are some experimental and numerical studies focused on its influence on the post-critical shear resistance. Results of these studies can be found in the research works conducted by Pavlovčič et al. (2007b) and Estrada et al. (2008).

This research is based on the assumption of the minimum rigidity of the longitudinal stiffening what assures that such element becomes undeformed at least up to the critical shear load. Due to the fact that there is no exact limit of the value γ^* for non-prismatic girders, an additional study in order to find this value has to be done. In calculating both parameters γ and γ^*, it is assumed that the non-rectangular panels and sub-panels are substituted by equivalent rectangular plates with their largest depths.

Below, based on the two girders A_600_1000_1000_3_180_15 and B_800_1500_3000_4_220_25 which are used as example, it is explained how the minimum rigidity of the longitudinal stiffener γ/γ^* is checked. The girders in **Table 4.5** have the same geometry, the web thickness $t_w = 3$ mm, the flange thickness $t_f = 15$ mm and the longitudinal stiffener thickness $t_s = 15$ and 25 mm. Similarly, the girders in **Table 4.6** have the same web thickness $t_w = 4$ mm, the flange thickness $t_f = 25$ mm and the longitudinal stiffeners $t_s = 25$ and 40 mm. The width (b_s) of the longitudinal stiffeners is variable.

According to the recommendation included in EN 1993-1-5, when calculating the relative flexural rigidity γ, the second moment of area of the longitudinal stiffener I_{sl} should be reduced to the 1/3 of its value.

In **Tables 4.5** and **4.6** the geometry of the analysed stiffeners with their characteristic parameters are presented. Moreover, in the last two columns corresponding values of the critical shear load V_{cr} and ultimate shear strength V_u for each studied case are shown. The critical loads were established from buckle analysis and the ultimate shear strengths as a result of the nonlinear analysis.

For all cases studied in **Table 4.5** and **Table 4.6**, the stiffener is placed horizontally at the mid-depth of the largest depth h_1.

Table 4.5. Numerical results for the girder A_600_1000_1000_3_180_15.

b_s [mm]	t_s [mm]	γ	γ^*	γ/γ^*	$\bar{\lambda}_{panel}$	$\bar{\lambda}_{sub-panel}$	Buckling mode	$V_{cr\,(FEM)}$ [kN]	$V_{u\,(FEM)}$ [kN]
0	0	0.0	13.5	0.0	3.16	-	panel	98.1	294.3
20	15	2.7	13.5	0.2	2.72	1.92	panel	168.8	317.2
25	15	5.1	13.5	0.4	2.66	1.92	panel	174.5	319.6
30	15	8.5	13.5	0.6	2.60	1.92	panel	180.2	322.4
40	15	18.9	13.5	1.4	2.48	1.92	sub-panel	181.4	326.7
60	15	57.8	13.5	4.3	2.22	1.92	sub-panel	183.4	330.6
80	15	127.6	13.5	9.5	1.97	1.92	sub-panel	184.1	334.0
90	15	184.9	13.5	13.7	1.83	1.92	sub-panel	184.5	335.5
90	25	274.6	13.5	20.3	1.67	1.92	sub-panel	185.6	348.5

Table 4.6. Numerical results for the girder B_800_1500_3000_4_220_25.

b_s [mm]	t_s [mm]	γ	γ^*	γ/γ^*	$\bar{\lambda}_{panel}$	$\bar{\lambda}_{sub-panel}$	Buckling mode	$V_{cr\,(FEM)}$ [kN]	$V_{u\,(FEM)}$ [kN]
0	0	0.0	108.0	0.00	4.31	-	panel	131.0	392.0
95	25	97.1	108.0	0.90	2.96	2.29	panel	229.3	475.7
110	25	145.9	108.0	1.35	2.78	2.29	sub-panel	229.9	476.0
110	40	211.2	108.0	1.96	2.65	2.29	sub-panel	231.5	516.9

As it can be observed in **Tables 4.5** and **4.6**, for both tested girders the limit value of the parameter is $\gamma/\gamma^* \approx 1.0$. This approximated value obtained for non-rectangular girders, assures that the longitudinal stiffener remains straight and undeformed up to the critical shear load, and that either of the sub-panels with greater slenderness buckles before the whole panel. For values of γ/γ^* smaller than 1.0 the buckling wave develops across the whole web panel.

The shear force – out-of-plane displacement curves, registered in the central point of the weld line between the longitudinal stiffener and the web for both girders, are presented in **Figs. 4.14** and **4.15**.

In the first case (**Fig. 4.14a-b**), for values of γ/γ^* smaller than 1.0, it can be observed that the out-of-plane displacement starts at the central point of the web panel, where the longitudinal stiffener is welded. For the values of γ/γ^* greater than 1.0 (**Fig. 4.14c-d**) the buckling begins in the bottom sub-panel and longitudinal stiffener becomes undeformed.

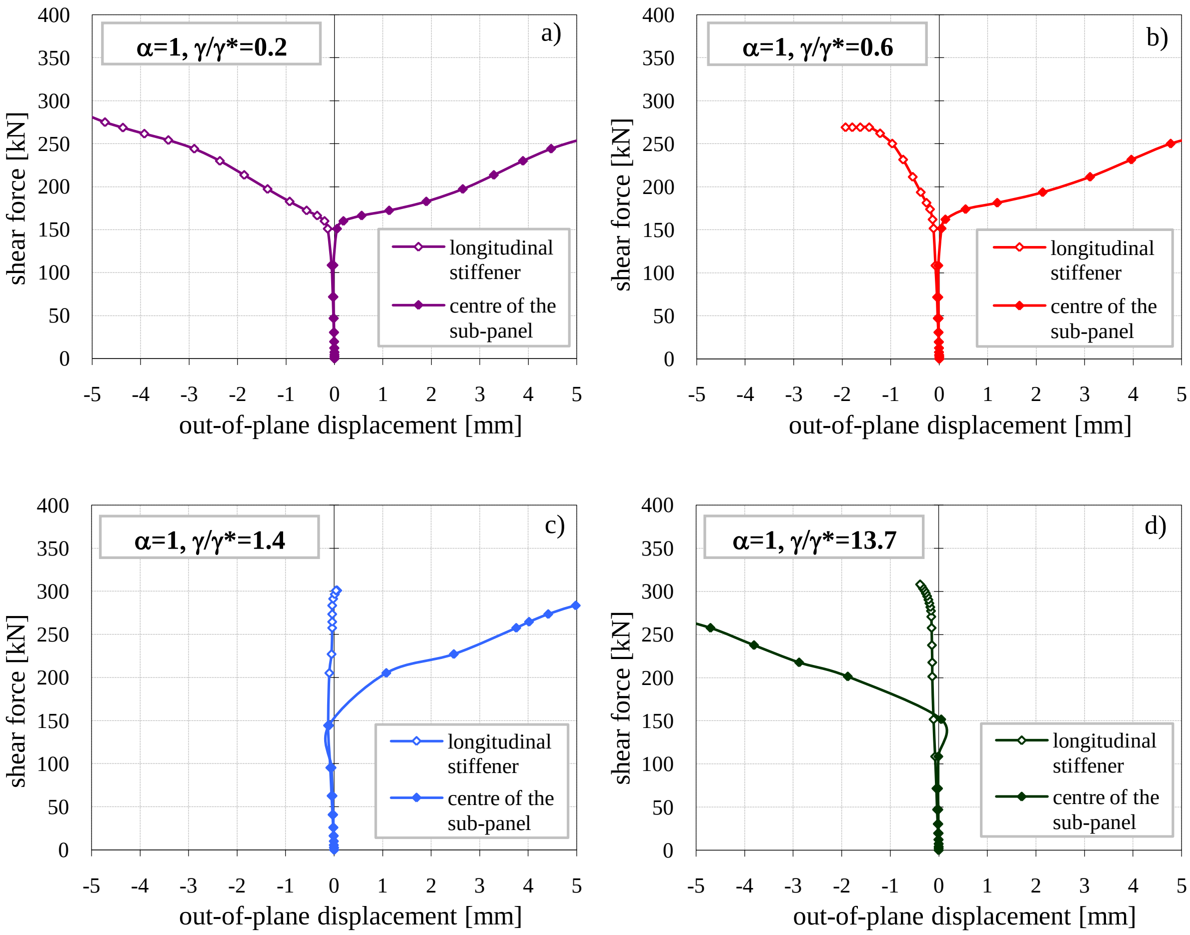

Fig. 4.14. Shear force-out-of-plane displacement curves for various ratios of γ/γ^* for girder A_600_1000_1000_3_180_15.

A similar situation is observed for girder B (**Fig. 4.15a**) where for the values of γ/γ^* smaller than 1.0, the longitudinal stiffener deforms before any sub-panel what confirms that the buckling wave develops along the whole web panel. Opposite situation takes place for $\gamma/\gamma^* > 1.0$ (1.35 and 1.96, **Fig. 4.15b-c**) where the stiffening remains practically straight when the critical shear force is reached and the buckle wave is formed in the bottom sub-panel.

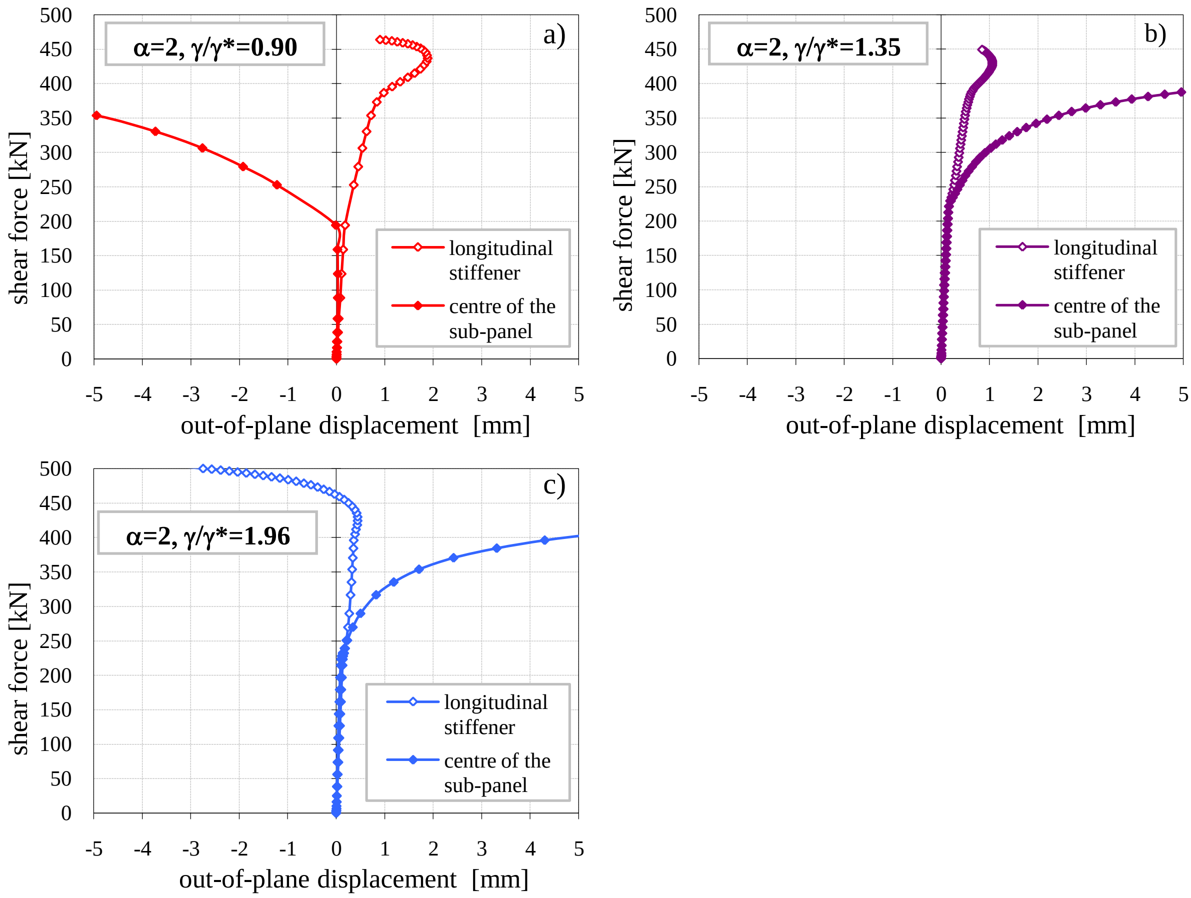

Fig. 4.15. Shear force-out-of-plane displacement curves for various ratios of γ/γ^* for girder B_800_1500_3000_4_220_25.

Fig. 4.16 shows the extreme situations of the deformed shape of the web panel when the buckling occurs. It is easy to see that the longitudinal stiffener in the first case ($\gamma/\gamma^* = 0.4$) is not enough rigid to avoid global buckling of the whole panel. For the second case ($\gamma/\gamma^* = 13.7$), buckling clearly starts within the lower sub-panel.

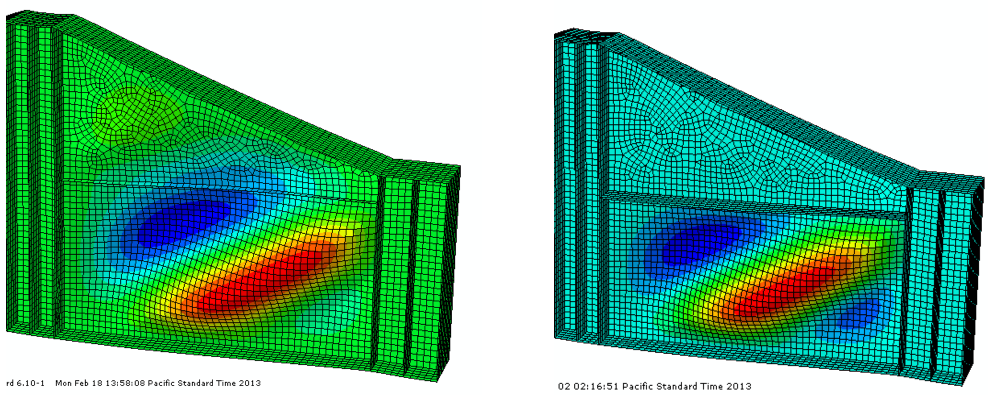

Fig. 4.16. Girder A_600_1000_1000_3_180_15. Out-of plane displacements at the moment of buckling: **a)** Global buckling of the whole web panel γ/γ^*=0.4 **b)** local buckling of the lower sub-panel γ/γ^*=13.7.

Results of this part of the research allow us to define the minimum rigidity of the longitudinal stiffener $(\gamma/\gamma^{*})_{min} \approx 1.0$, which avoids global buckling of the whole web panel. In the parametric studies on the optimal position of the longitudinal stiffener (section 4.6.3.), for all tested girders the value of γ/γ^{*} is always greater than that minimum $(\gamma/\gamma^{*})_{min}$.

4.6.3. Position of longitudinal stiffener

In the case of only one longitudinal stiffener, it is necessary to take into account the stress distribution to determine its optimal position. When the plate girder is subjected mostly to shear, the most efficient position for longitudinal stiffener would be at the mid-depth of the web, reducing the slenderness of the whole plate and dividing it into two sub-panels with similar slenderness. In fact, shear load always appears accompanied by bending and the interaction between these both internal forces should be considered. In the case of long plate girders (with aspect ratio α>>1), bending may play an important role and then the longitudinal stiffener should be able to resist the normal stresses in the compressed zone of the web panel. Therefore, the optimum position of such stiffener should be designed individually depending on the geometry of the plate.

In the numerical simulations, four different positions of the longitudinal stiffener are examined (cases I-IV, **Fig. 4.17**). Cases I and III have the longitudinal stiffener placed horizontally at the mid-height of the smallest h_0 and the largest depth h_1, respectively. In the case II the stiffener connects two points at the mid-heights of both depths. In the last case IV, the longitudinal stiffener is parallel to the inclined flange and welded at 2/3 of the largest depth h_1 measured from the bottom flange.

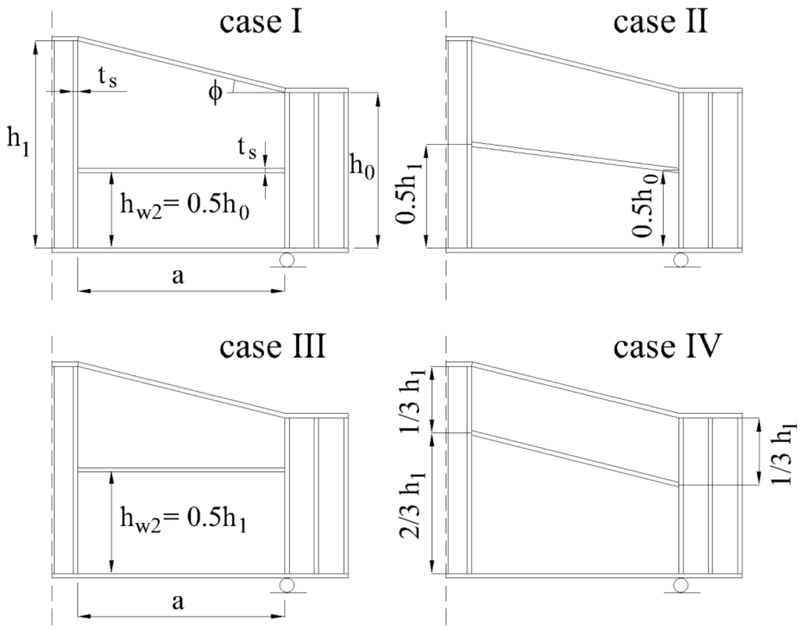

Fig. 4.17. Four cases (I-IV) of position of the longitudinal stiffener.

4.7. Numerical results vs. EN 1993-1-5

Three types of tapered plate girders with different aspect ratios $\alpha = 1$, 2, 3 are studied and denoted as A, B and C, respectively. Within each group of the girders with the same dimensions, four different positions of the longitudinal stiffener are considered and denoted as follows: I, II, III and IV (**Fig. 4.17**) and additionally, one girder without any longitudinal stiffener (called A0, B0, C0) is examined and used for comparison. For each aspect ratio three different girders with varied geometry are studied.

The main objective of this research is the extension of the existing rules in EN 1993-1-5 for prismatic longitudinally stiffened panels for non-rectangular members. In order to assess the correctness of the proposed procedure, the tested girders are examined in a wide range of geometric parameters such as the aspect ratio α, the web thickness t_w, the slope of the inclined flange $tan(\phi)$ and the rigidity of flanges and stiffeners. The notation of the girders includes its dimensions. The following example explains the notation: AIII_400_800_800_2_180_15 means a tapered plate girder with the longitudinal stiffener in position III, $h_0 = 400$ mm, $h_1 = 800$ mm, $a = 800$ mm, $t_w = 2$ mm, $b_f = 180$ mm and $t_f = t_s = 15$ mm. For all tested girders, a one-side flat stiffener is adopted, with the width $b_s = b_f/2$ and the thickness equal to the thickness of the flange in each studied case $t_s = t_f$.

Since for all tested girders the shear force is constant along their length, the numerical and analytical results of the ultimate shear strength are obtained with the presence of the maximum bending moment which appears at the mid-span. As it was mentioned before, the ultimate shear resistance V_u is calculated, according to EN 1993-1-5, assuming a simplified rectangular shape of the non-prismatic web panel and the upper sub-panel with its maximum depth h_1 or h_{w1}, respectively. Moreover, in calculations, non-horizontal longitudinal stiffener appearing in cases II and IV (**Fig. 4.17**) is approximated by the horizontal one; in that way, two rectangular sub-panels with depth h_{w1} and h_{w2} (**Fig. 4.13**) are created. Thus, the shear buckling coefficient $k_{\tau i}$ for each sub-panel is calculated according to the classic formulae for simply-supported rectangular plates simplifying their trapezoidal shape by rectangular one and assuming its largest depth h_{wi}.

The longitudinal open stiffeners are designed to fulfill the condition of the critical limit stiffness γ^* and assure their undeformed shape at least up to the instant when the critical shear load V_{cr} is reached. Due to the lack of analytical expression for γ^* for any position of the longitudinal stiffener, the condition concerning its minimal rigidity is checked only for girders with the stiffener placed in position III. Moreover, the expression given in **Eq. 4.8** is valid only for the girders with aspect ratio $0.5 \leq \alpha \leq 2$, so the parameter γ^* may be calculated only for girders A and B. Due to this difficulty in calculating γ and γ^* for all tested girders with aspect ratio $\alpha > 2$ and non-typical position of longitudinal stiffener, the requirement of the minimum rigidity of the longitudinal stiffener is checked according to the results shown in **Figs. 4.14** and **4.15**.

The most relevant results for the tested girders are given in **Table 4.7**. In the first three columns the numerical and analytical results of the ultimate shear resistance are presented and compared.

The parameters γ, γ^*, γ/γ^*, slenderness of the web panel and slenderness of the sub-panels can be found in the next columns, and in the last one, the increase of the numerical ultimate shear resistance for each longitudinally stiffened girder compared to the unstiffened one is presented.

Table 4.7. Numerical and analytical (EN 1993-1-5) results for V_u.

	Girder	FEM V_u	EN V_u	Diff. V_u [%]	γ	γ^*	γ/γ^*	$\bar{\lambda}$ panel	$\bar{\lambda}$ bottom sub-panel	$\bar{\lambda}$ upper sub-panel	V_u (FEM) increase vs. unstiffened panel [%]
$\alpha = 1$	A0_400_800_800_2_180_15	175.3	122.6	30.1	0.0	-	-	3.79	-	-	0.0
	AI_400_800_800_2_180_15	201.8	135.2	33.0	-	-	-	1.56	1.22	3.15	15.1
	AII_400_800_800_2_180_15	192.0	160.3	16.5	651.3	13.5	48.2	1.56	2.30	2.30	9.5
	AIII_400_800_800_2_180_15	309.9	160.3	48.3	651.3	13.5	48.2	1.56	2.30	2.30	76.8
	AIV_400_800_800_2_180_15	237.9	141.6	40.5	-	-	-	1.56	2.89	1.60	35.7
	A0_600_1000_1000_3_180_15	294.3	207.2	29.6	0.0	-	-	3.16	-	-	0.0
	AI_600_1000_1000_3_180_15	360.2	240.9	33.1	-	-	-	1.83	1.21	2.50	22.4
	AII_600_1000_1000_3_180_15	340.3	284.7	16.3	184.9	13.5	13.7	1.83	1.92	1.92	15.6
	AIII_600_1000_1000_3_180_15	335.5	284.7	15.1	184.9	13.5	13.7	1.83	1.92	1.92	14.0
	AIV_600_1000_1000_3_180_15	356.9	246.4	31.0	-	-	-	1.83	2.41	1.34	21.3
	A0_800_1500_1500_4_220_25	553.0	393.0	28.9	0.0	-	-	3.55	-	-	0.0
	AI_800_1500_1500_4_220_25	694.7	446.0	35.8	-	-	-	2.14	1.21	2.91	25.6
	AII_800_1500_1500_4_220_25	644.3	537.9	16.5	153.4	13.5	11.4	2.14	2.15	2.15	16.5
	AIII_800_1500_1500_4_220_25	722.7	537.9	25.6	153.4	13.5	11.4	2.14	2.15	2.15	30.7
	AIV_800_1500_1500_4_220_25	727.1	466.1	35.9	-	-	-	2.14	2.71	1.50	31.5
$\alpha = 2$	B0_400_800_1600_2_180_15	112.5	87.6	22.0	0.0	-	-	4.60	-	-	0.0
	BI_400_800_1600_2_180_15	160.6	102.9	35.9	-	-	-	2.26	1.24	3.57	42.8
	BII_400_800_1600_2_180_15	156.9	131.0	16.5	651.3	108.0	6.0	2.26	2.45	2.45	39.5
	BIII_400_800_1600_2_180_15	179.5	131.0	27.0	651.3	108.0	6.0	2.26	2.45	2.45	59.6
	BIV_400_800_1600_2_180_15	158.7	108.9	31.4	-	-	-	2.26	3.21	1.65	41.1
	B0_600_1000_2000_3_180_15	209.6	160.8	23.3	0.0	-	-	3.83	-	-	0.0
	BI_600_1000_2000_3_180_15	281.8	201.3	28.6	-	-	-	2.40	1.20	2.80	34.4
	BII_600_1000_2000_3_180_15	313.9	225.5	28.2	184.9	108.0	1.7	2.40	2.04	2.04	49.8
	BIII_600_1000_2000_3_180_15	250.1	225.5	9.8	184.9	108.0	1.7	2.40	2.04	2.04	19.3
	BIV_600_1000_2000_3_180_15	311.8	207.7	33.4	-	-	-	2.40	2.67	1.38	48.8
	B0_800_1500_3000_4_220_25	392.0	299.5	23.6	0.0	-	-	4.31	-	-	0.0
	BI_800_1500_3000_4_220_25	490.5	363.5	25.9	-	-	-	2.78	1.24	3.28	25.1
	BII_800_1500_3000_4_220_25	555.7	408.0	26.6	153.4	108.0	1.4	2.78	2.29	2.29	41.8
	BIII_800_1500_3000_4_220_25	476.0	408.0	14.3	153.4	108.0	1.4	2.78	2.29	2.29	21.4
	BIV_800_1500_3000_4_220_25	574.4	386.4	32.7	-	-	-	2.78	3.01	1.55	46.5
$\alpha = 3$	C0_400_800_2400_2_180_15	93.0	77.1	17.1	0.0	-	-	4.81	-	-	0.0
	CI_400_800_2400_2_180_15	134.7	93.0	31.0	-	-	-	1.56	1.25	3.67	44.8
	CII_400_800_2400_2_180_15	147.4	121.4	17.6	651.3	-	-	1.56	2.48	2.48	58.5
	CIII_400_800_2400_2_180_15	132.0	121.4	8.0	651.3	-	-	1.56	2.48	2.48	41.9
	CIV_400_800_2400_2_180_15	144.7	100.5	30.5	-	-	-	1.56	3.28	1.66	55.6
	C0_600_1000_3000_3_180_15	178.9	147.5	17.6	0.0	-	-	4.01	-	-	0.0
	CI_600_1000_3000_3_180_15	253.8	189.1	25.5	-	-	-	1.94	1.25	2.86	41.9
	CII_600_1000_3000_3_180_15	280.6	237.5	15.4	184.9	-	-	1.94	2.07	2.07	56.8
	CIII_600_1000_3000_3_180_15	227.2	237.5	-4.5	184.9	-	-	1.94	2.07	2.07	27.0
	CIV_600_1000_3000_3_180_15	297.8	195.5	34.4	-	-	-	1.94	2.73	1.25	66.5
	C0_800_1500_4500_4_220_25	336.2	272.4	19.0	0.0	-	-	4.51	-	-	0.0
	CI_800_1500_4500_4_220_25	450.9	338.2	25.0	-	-	-	2.30	1.25	3.37	34.1
	CII_800_1500_4500_4_220_25	533.4	439.8	17.5	153.4	-	-	2.30	2.32	2.32	58.7
	CIII_800_1500_4500_4_220_25	395.7	439.8	-11.1	153.4	-	-	2.30	2.32	2.32	17.7
	CIV_800_1500_4500_4_220_25	537.8	361.3	32.8	-	-	-	2.30	3.07	1.56	60.0

From the analysis of the results shown in **Table 4.7**, following conclusions can be pointed out:

1. The presence of the longitudinal stiffener increases the ultimate shear resistance up to 77 % comparing to the unstiffened one.
2. For girders C with the largest aspect ratio $\alpha = 3$, where the bending moments may achieve significant values, the most favourable positions of the longitudinal stiffener are II and IV. Shear-bending interaction causes additional compression in the upper sub-panel and makes it more susceptible for local buckling. Longitudinal stiffeners in position II and IV significantly reduces the slenderness of the upper sub-panel.
3. For the same girders with different aspect ratios, the greater aspect ratio, the smaller ultimate shear resistance, not depending on the position of the stiffener.
4. For all tested girders, the longitudinal stiffener designed with the ratio $\gamma/\gamma^* > 1$ avoids the global buckling of the whole web panel inducing local buckling within one of the sub-panels.
5. For the most cases the best approximation by EN 1993-1-5 is observed for girders where the longitudinal stiffener is in the position II (from 16.3 to 28.2 %) because the stiffener divides the whole panel into two quasi-rectangular sub-panels.
6. Extrapolation of EN 1993-1-5 rules is not suitable for girders with aspect ratio $\alpha > 2$ and longitudinal stiffener in position III, due to the overestimation of the ultimate shear resistance (differences between -4.5 % and -11.1 %).
7. For the other cases, the results obtained by using EN 1993-1-5 rules are on the safe side but some of them seem to be very conservative (up to 48.3 %).

4.8. Discussion and conclusions

This research is focused on the structural behaviour of tapered steel plate girders with one longitudinal stiffener subjected mainly to shear. All presented results obtained from both, experimental and numerical analyses allow for better understanding of the structural behaviour of longitudinally stiffened tapered steel plate girders subjected to shear and lead to some important conclusions which can be used in design of tapered panels.

A good agreement between the experimental and numerical results allowed verifying the numerical model used in the numerical analyses of this study.

The parametric study shows the complexity of the behaviour of tapered girders and the significant influence of their geometry and the position of the longitudinal stiffener on their ultimate shear resistance.

An important conclusion is about the extension of EN 1993-1-5 rules for the case of tapered steel plate girders with longitudinal stiffening. In general, the applicability of the rules included in EN 1993-1-5 for rectangular plates is possible for the most of cases of non-prismatic girders with one longitudinal stiffener in order to determine their ultimate shear resistance but is quite conservative.

Generally, the presence of the longitudinal stiffener always improves the ultimate shear resistance of the web panel compared to the unstiffened one. The level of this improvement depends on the geometry of the panel and on the position of the stiffener.

For the case of longitudinally stiffened tapered steel plate girders mainly subjected to shear, an inclined position of the stiffener connecting the two points at the mid-heights of both depths is the most favourable position. This solution leads to similar results when applying the numerical model and EN 1993-1-5 rules for prismatic members. In addition this arrangement also provides the highest shear resistances in most cases analyzed.

When bending effects are important, it is recommended to place the stiffener on the compressed zone of the tapered web panel, with a slope between the horizontal line and the angle of the inclined flange. Then both sub-panels may be assessed assuming them to be rectangular panels.

5. *Design proposal for ultimate shear strength of tapered steel plate girders*

5.1. Abstract

Previous studies conducted on the behaviour of tapered steel plate girders subjected to shear revealed existence of four different structural responses depending on the stress state of the inclined flange and the direction of the diagonal tension field. These structural responses are also influenced by Resal effect, where the vertical component of the axial force in the inclined flange may increase or decrease the ultimate shear capacity of tapered panel. Also it was demonstrated that the proposal for determining the ultimate shear resistance of prismatic plates included in EN 1993-1-5, applied for non-prismatic plates, may lead to unsafe assessment for some of them. In order to improve the existing approach for some geometries of tapered plate girders, a new simplified design proposal was presented.

The paper is focused on the further improvement of the design expressions for the ultimate shear strength of tapered steel plate girders. In the study four different behaviours of tapered panels and the corresponding Resal effect are taken into account.

As a result of this research, a new design proposal for calculating the ultimate shear resistance for tapered steel plated girders is presented. Its correctness and robustness is verified by numerical simulations conducted for a wide range of geometrical parameters.

Additionally, to assess the contribution of the Resal effect and study its influence on the ultimate shear strength of tapered plate girders, a new simplified mechanical model is developed.

***Keywords*:** tapered steel plate girders; Resal effect; mechanical model; critical shear load; ultimate shear resistance; shear-bending interaction; EN 1993-1-5 rules; design proposal;

5.2. Introduction

5.2.1. Previous studies

The behaviour of rectangular steel plates subjected to shear load was deeply studied in the last century. In conseqeunce, several theories to predict the ultimate shear capacity of such members were developed. Some of them were taken as a reference and evolved in time and other ones were implemented in design codes. The most important methods to be mentioned are: Basler's model (1960), Chern and Ostapenko (1969), the Rotated Stress Field Model developed by Höglund (1971, 1997) and the Tension Field Model developed in Cardiff and Prague by Porter et al. (1975) and Rockey and Škaloud (1972).

Almost all ultimate-shear-strength models for tapered plate girders proposed in literature are derived from the previous presented models for rectangular plates. Several models for tapered girders were developed by: Falby and Lee (1976), Davies and Mandal (1979), Takeda and Mikami (1987), Roberts and Newmark (1997), Zárate and Mirambell (2004) and Shanmugam and Min (2007). Recently, some other numerical studies have been published by Abu-Hamd M. and Abu-Hamd I. (2011). In most cases, the models are based on an assumption of a simply supported rectangular plate and do not consider either the actual boundary conditions existing in the flange–web–, stiffener–web– junctions or the geometry of the tapered steel plate girder. In the last years, some researchers, among others Lee et al. (1996), Mirambell and Zárate (2000) and Estrada et al. (2008) have proved the importance of these effects. The importance of the so-called „Resal effect" which appears in tapered plate girders was also explained in the other work of Zárate (2002).

Also some tests and design recommendations have been developed for stainless steel recently by Saliba and Gardner (2013) and Saliba et al. (2013).

On the other hand, the current European design norm - EN 1993-1-5 (2006) states that the design rules for the assessment of the ultimate shear resistance of prismatic members may be applied to non rectangular plate girders if the angle of the inclined flange does not exceed 10˚. For larger angles, panels may be assessed assuming it to be a rectangular panel based on the larger of depths of the panel. Previous research conducted by Bedynek et al. (2013) demonstrated that for some geometry of such panels, the ultimate shear strength results might be significantly overestimated.

The results obtained by Bedynek et al. (2013) also shown that tapered plate girders can be classified into four typologies. The differences among them consist in the direction of the diagonal tension field, which can develop on the shortest or the largest diagonal of the web panel and in the stress state in the inclined flange (tension or compression). These typologies are presented in **Fig. 5.1**. For the girders belonging to typologies I and III the diagonal tension field develops on the shortest diagonal of the web panel and the inclined flange is under compression or tension, respectively. For typologies II and IV the diagonal tension field appears on the longest diagonal of the web and the inclined flange is under tension or compression, respectively. Different behaviour observed within each typology of tapered panels also influences their ultimate shear resistance.

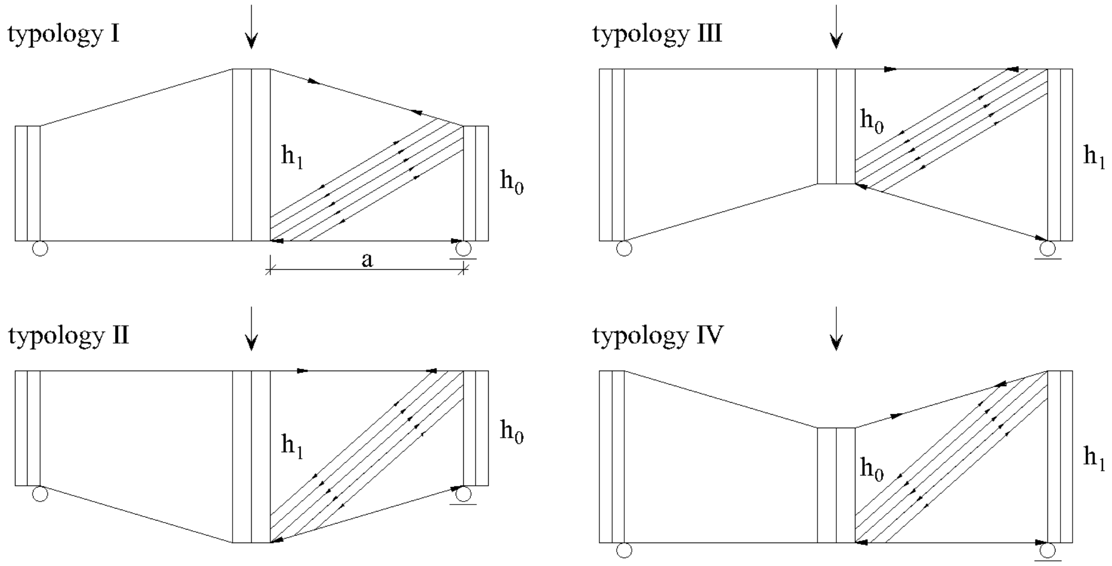

Fig. 5.1. Four typologies of tapered plate girders.

In this research an attempt of an extension of the existing design rules included in EN 1993-1-5 for non-prismatic panels were done. Within each typology of tapered plate girders various geometrical parameters such as: the aspect ratio of the panel, the slope of the inclined flange and the web and flange slenderness were taken into account. Moreover, a new mechanical model for assessing the influence of the Resal effect was developed and included in the final version of the proposal for calculating the ultimate shear resistance of tapered steel plate girders subjected to shear and shear-bending interaction.

5.2.2. Ultimate shear strength for plate girders

Different theories have been developed to analyze the behaviour of steel plated girders subjected to shear, and some of them are used nowadays in deign codes. The Rotated Stress Field Method (Höglund, 1997), is the one implemented in EN 1993-1-5. This method is based on the assumption that the web panel is under a pure shear stress state caused by a shear force in the slender web before buckling occurs (principal stresses are equal and opposite). Once buckling occurs, compression stress is close to the critical shear buckling stress and therefore, the increase of load is resisted by an increase of the principal tensile stress, until the moment that the yield criterion is fulfilled in the web. The inclination of the principal stresses varies as the load increases. The contribution of the flanges in the resistant mechanism is included considering that the tension band anchors in the flanges until a four hinge mechanism leads to the collapse of the girder (see **Fig. 5.2**). A more detailed explanation of the failure mechanism in plated girders subjected to shear can be found among others in the works of Johansson et al. (2007) or Maquoi and Skaloud (2000).

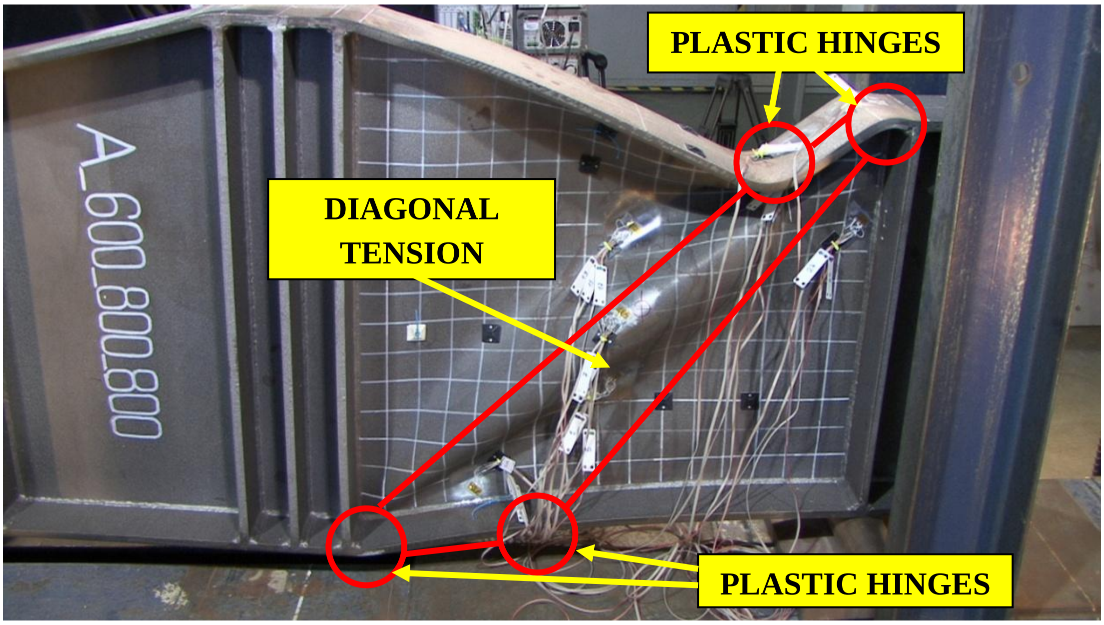

Fig. 5.2. Tapered plate girder failure.

5.3. Resal effect

5.3.1. General

Previous research conducted by Zárate and Mirambell (2004) confirmed that in tapered plate girders an additional vertical load derived from the axial force in the inclined flange appears and its influence on the ultimate shear resistance of the whole web panel should be taken into account. This phenomenon is known as Resal effect ((Samartín, 1993), (Florida Department of Transportation, 2008)) and may cause an increase or decrease of the ultimate shear resistance in tapered plate girders. Its positive or negative influence is strongly correlated with the typology of the web-panel. Graphical illustration of the Resal effect in all considered typologies is given in **Fig. 5.3**.

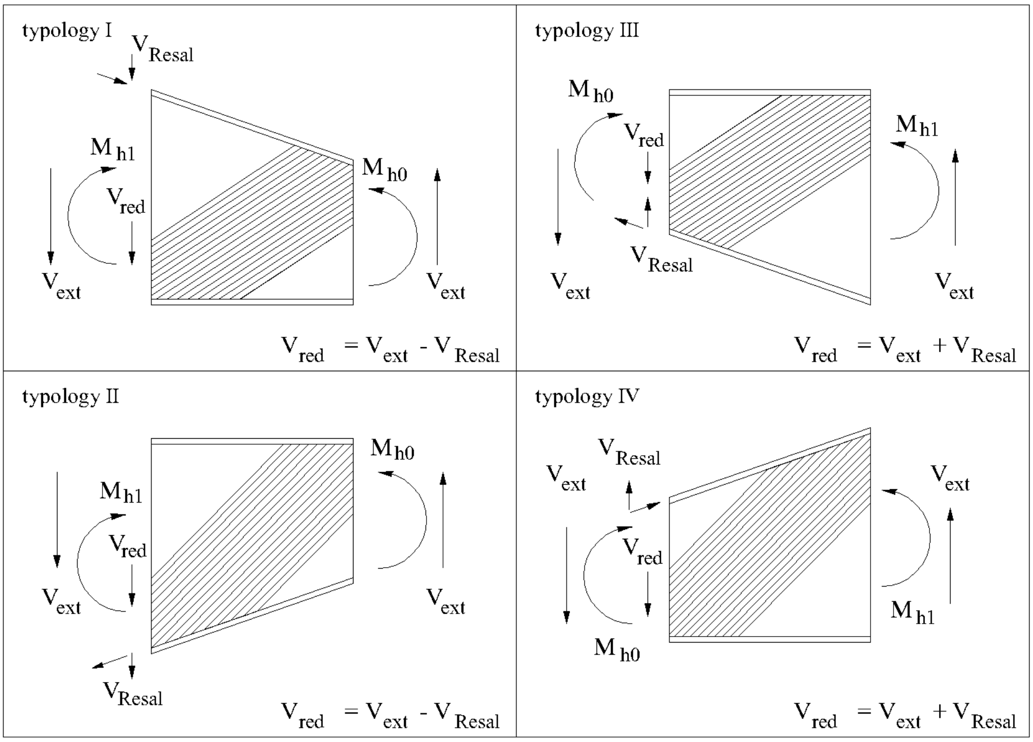

Fig. 5.3. Positive and negative influence of the Resal effect on V_u.

For these cases where the moment of inertia of the cross-section increases with the increase of internal forces (typology I and II), the vertical component of the Resal effect acts against shear force and reduces the shear force design value; in other words, consideration of the vertical component of the Resal effect increases the ultimate shear resistance of tapered girders (positive influence). For typologies III and IV the opposite situation is observed. Due to their smaller bearing capacity, these two typologies are not as common as typologies I and II, but sometimes might be required in a case of non-standard structural solutions where the geometry plays an important role.

5.3.2. Theoretical mechanical model

Since there is still observed a shortage in bibliography focused on the Resal effect in tapered steel plate girders, additional studies are needed to better understand its actual role.

The study on the influence of the Resal effect starts from defining a simplified two-dimensional mechanical model with simplified boundary conditions in some characteristic nodes (**Fig. 5.4**).

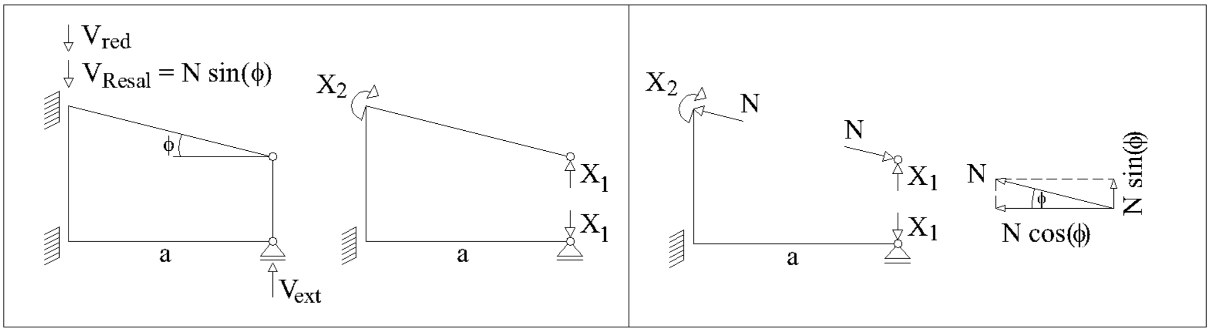

Fig. 5.4. Internal forces in the structural model.

The main objective of this section is to find a direct correlation between Resal force and the shear load acting on the girder. The model represents a rigid frame consisting of flanges and transversal stiffeners only. It is assumed that all the internal forces are transmitted only by surrounding rods of the frame (excluding contribution from the web). In fact, this simplification is used in order to find an approximated value of the Resal force, not its exact value. The boundary conditions reproduce the real ones: simply supported on the one end without bending moment along the shortest depth and with maximum constant bending moment along the rod representing the central cross-section (the largest depth for typologies I and II). Similar idea of simplification of tapered plate girder by rod structure (in that case by truss) was proposed by Davies and Mandal (1979).

Solving the hyperstatic frame with two unknowns X_1 and X_2, it is possible to find a contribution of the internal forces from the flanges and from the transversal stiffeners. Consequently, the axial force N (**Fig. 5.4**) in the inclined flange will be known. The Resal force is obtained directly by projecting the axial force N on the vertical axis.

Full procedure of determining the Resal force will be explained for the typology I, however, only the most important steps will be pointed out. Other typologies were analysed in the same way and their final expressions for calculating the Resal force will be presented.

Using the principle of virtual works, two unknowns X_1 and X_2 can be found and expressed by **Eqs. 5.1** and **5.2**:

$$X_1 = \frac{V_{ext}}{\left(1 + \frac{1}{\cos(\phi)}\right)} \tag{5.1}$$

$$X_2 = \frac{a\, V_{ext}}{\left(1 + \frac{1}{\cos(\phi)}\right)} \tag{5.2}$$

where a is a frame length and ϕ is an angle of the inclined flange (**Fig. 5.4**).

From the equilibrium of upper right hinge, the axial force N in the inclined flange can be found (**Eq. 5.3**):

$$N = \frac{V_{ext}}{\left(1 + \frac{1}{\cos(\phi)}\right)} \sin(\phi) \tag{5.3}$$

Next, the Resal force was calculated as the vertical component of axial force N and for all typologies is given by **Eq. 5.4**:

$$V_{Resal} = \frac{V_{ext}}{\left(1 + \frac{1}{\cos(\phi)}\right)} \sin^2(\phi) \tag{5.4}$$

As it was mentioned before, the Resal effect for tapered plate girders from typologies I and II is favourable. Thus, reduced shear force V_{red} should be calculated according to (**Eq. 5.5**):

$$V_{red} = V_{ext} - V_{Resal} \tag{5.5}$$

For typologies III and IV the Resal effect has a negative influence and V_{red} is given by (**Eq. 5.6**):

$$V_{red} = V_{ext} + V_{Resal} \tag{5.6}$$

5.4. Numerical study

5.4.1. General

Parametric studies were conducted on 85 tapered panels belonging to four typologies. The girders varied by geometric parameters such as: an aspect ratio $\alpha = a/h_1$, a slope of the inclined flange ϕ and a web thickness t_w. The range of dimensions for the studied models is presented in **Table 5.1**. Nomenclature used in girder's name is the following: 600_800_800_4_180_15 means: the smallest depth $h_0 = 600$ mm, the largest depth $h_1 = 800$ mm, a panel length $a = 800$ mm, a web thickness $t_w = 4$ mm, a flange width $b_f = 180$ mm and a flange thickness $t_f = 15$ mm (see **Fig. 5.1**). Due to the large amount of analysed cases, only selected results will be presented.

Table 5.1. Range of dimensions for the studied models.

variable	symbol	unit	range
web thickness	t_w	[mm]	2 to 8
smaller depth	h_0	[mm]	300 to 1235
larger depth	h_1	[mm]	700 to 3000
panel length	a	[mm]	800 to 8220
aspect ratio	α	-	1 to 4
tangent	$tan(\phi)$	-	0.0 to 0.5
angle	ϕ	[°]	0 to 26.6

5.4.2. Numerical model

In the initial part of the numerical study several nonlinear analyses were performed on the tapered plate girders with use of quad-dominant 4-node shell element S4R5. This finite element, with 5 degrees of freedom (in each node) and linear shape functions, is especially suitable for modelling shell surfaces where large rotations and displacements are expected. A convergence analysis allowed setting the mesh density with a mesh size of 20 mm for all modelled cases. The nonlinear analyses were conducted with the Modified Riks algorithm implemented in ABAQUS (2010). Due to the simple shape of the modelled tapered girders, the mesh used in the numerical model could be generated automatically.

All numerical simulations were done using the same bilinear material model with kinematic hardening: steel S275 with yield stress: $f_y = 275$ MPa, Young's modulus of $E = 210$ GPa and Poisson ratio $\nu = 0.3$.

The beams are modelled with a full 3D model for tapered plate girders to reflect the actual boundary conditions between web and flange panels in the continuous span of the girder. The numerical model is thought to be rigid end-post. The modelled girder is simply-supported on two edges and its boundary conditions are presented in **Fig. 5.5** and **Table 5.2**.

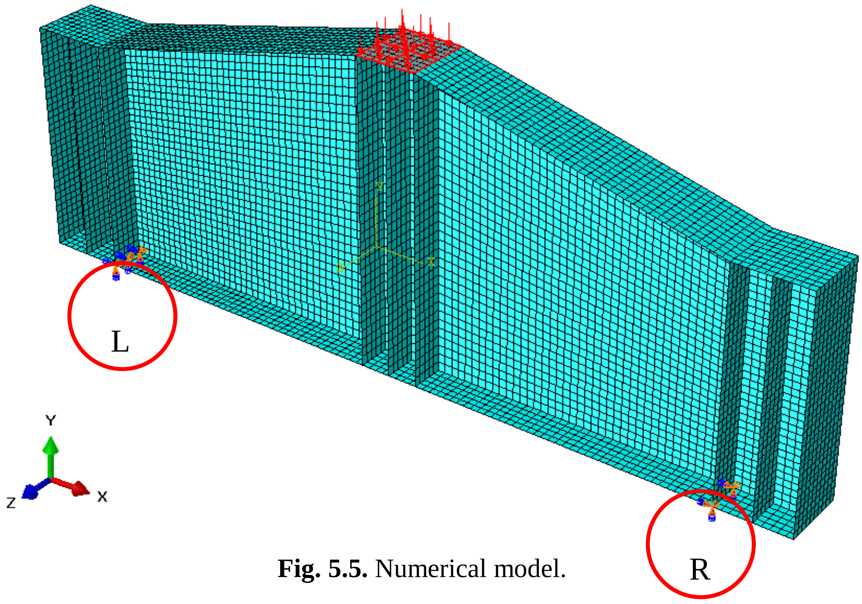

Fig. 5.5. Numerical model.

Table 5.2. Boundary conditions.

	u_x	u_y	u_z	θ_x	θ_y	θ_z
L	0	1	1	1	1	0
R	1	1	1	1	1	0

* 0 – free movement; 1 – restraint

Two different analyses have been considered in this study. First an eigen-value analysis to obtain the critical shear loads as the first eigen-value and to obtain the deformed shape for the critical shear load as the first eigen-vector. The second analysis is a geometric and material non linear analysis to reproduce the postbuckling behaviour of tapered plate girders up to failure. Geometric imperfections should be introduced in the model in order to develop the second order effects in the web panel. In this case, the deformation corresponding to the first eigen-mode was used.

The numerical model validation based on four experimental tests was presented in the paper of Bedynek et al. (2013). In the same paper the results from the analysis on the structural imperfections in tapered steel plate girders were shown. The studies proved that this kind of structures is not susceptible to the residual stresses and their consideration may decrease the ultimate shear resistance not more than 2%. For this reason only the geometrical imperfections derived from the deformed shape of the web-panel corresponding to the 1st positive eigen-value were used in the analysis. Also the magnitude of the geometric imperfections was scaled according to EN 1993-1-5, Annex C.5 what in practice means that the maximum amplitude was on the level of the 80% of the geometric fabrication tolerances.

5.5. Ultimate shear resistance according to EN 1993-1-5

5.5.1. Verification of existing design rules provided by EN 1993-1-5

EN 1993-1-5 suggests calculating the ultimate shear resistance of tapered panels treating them as rectangular ones with their largest depth $\boldsymbol{h_1}$. Unfortunately, for some particular geometries of non-rectangular plates this approach leads to significant overestimation of the results what means that the obtained values of the ultimate shear resistances do not fulfil the safety requirements. It happens especially for the typologies III and IV with larger slopes of the inclined flange. This situation can be partially caused by Resal effect, an additional vertical force derived from the axial force that appears in the inclined flange, which for typologies III and IV is unfavorable and should be taken into account. On the other hand, results obtained for typologies I and II are a bit conservative for some cases. Nevertheless, in general this approach gives a good estimation of the ultimate shear resistance of tapered panels with less than 18% difference between the analytical (EN 1993-1-5) and numerical solution (see **Table 5.3**).

Table 5.3. The critical shear buckling load and the ultimate shear resistance for analysed prototypes. Numerical (FEM) and theoretical results (EN 1993-1-5).

		girder	α	ϕ[°]	$tan(\phi)$	FEM		EN	Diff.$_{(1)}$ [%]	Proposal Bedynek et al. (2013) V_u [kN]	Diff.$_{(2)}$ [%]
						V_{cr} [kN]	V_u [kN]	V_u [kN]			
typology I	A	480_800_800_4_180_15	1.0	21.8	0.40	285.0	364.8	310.5	14.9	310.5	14.9
		600_800_800_4_180_15	1.0	14.0	0.25	238.0	366.9	310.5	15.4	310.5	15.4
		680_800_800_4_180_15	1.0	8.5	0.15	215.8	365.6	310.5	15.1	310.5	15.1
	B	600_1200_2400_4_250_25	2.0	14.0	0.25	177.9	368.4	305.4	17.1	305.4	17.1
		850_1200_2400_4_250_25	2.0	8.3	0.15	130.3	367.9	305.4	17.0	305.4	17.0
typology II	A	480_800_800_4_180_15	1.0	21.8	0.40	256.3	335.4	310.5	7.4	310.5	7.4
		600_800_800_4_180_15	1.0	14.0	0.25	217.3	351.3	310.5	11.6	310.5	11.6
		680_800_800_4_180_15	1.0	8.5	0.15	202.5	354.8	310.5	12.5	310.5	12.5
	B	600_1200_2400_4_250_25	2.0	14.0	0.25	180.0	355.2	305.4	14.0	305.4	14.0
		850_1200_2400_4_250_25	2.0	8.3	0.15	130.5	361.7	305.4	15.6	305.4	15.6
typology III	A	480_800_800_4_180_15	1.0	21.8	0.40	186.6	221.0	310.5	**-40.5**	186.3	**15.7**
		600_800_800_4_180_15	1.0	14.0	0.25	188.0	274.9	310.5	**-13.0**	232.9	**15.3**
		680_800_800_4_180_15	1.0	8.5	0.15	189.3	310.4	310.5	**0.0**	263.9	**15.0**
	B	600_1200_2400_4_250_25	2.0	14.0	0.25	95.4	186.9	305.4	**-63.4**	152.7	**18.3**
		850_1200_2400_4_250_25	2.0	8.3	0.15	95.5	263.5	305.4	**-15.9**	216.3	**17.9**
typology IV	A	480_800_800_4_180_15	1.0	21.8	0.40	161.6	202.7	310.5	**-53.2**	186.3	**8.1**
		600_800_800_4_180_15	1.0	14.0	0.25	168.7	263.3	310.5	**-17.9**	263.9	**-0.2**
		680_800_800_4_180_15	1.0	8.5	0.15	176.4	300.5	310.5	**-3.3**	232.9	**22.5**
	B	600_1200_2400_4_250_25	2.0	14.0	0.25	94.6	182.1	305.4	**-67.7**	152.7	**16.1**
		850_1200_2400_4_250_25	2.0	8.3	0.15	95.1	259.0	305.4	**-17.9**	216.3	**16.5**

In order to illustrate the differences when the ultimate shear resistance of tapered panels is calculated using EN 1993-1-5 simplification for tapered panels, results for some of the studied girders are presented in **Table 5.3**. In the column titled "Diff.$_{(1)}$", differences between the numerical (FEM) and analytical (EN 1993-1-5) values of the ultimate shear resistance V_u are shown. The aspect ratio of the girders "A" and "B" is $\alpha = 1$ and $\alpha = 2$, respectively.

New approach which gave better assessment of the ultimate shear resistance for typologies III and IV was presented by Bedynek et al. (2013). The ultimate shear resistance V_u calculated as for a rectangular plate was multiplied by a reduction factor h_0/h_1. Although that proposal is easy to apply and gives quite good agreement between the numerical (FEM) and analytical (EN) values of V_u (**Table 5.3**, last column "Diff.$_{(2)}$"), does not justify a new contribution from the web and flanges neither taking into account the Resal effect.

5.5.2. Proposal for the design shear resistance in tapered steel plates based on EN 1993-1-5

A new proposal for determining the design shear resistance for tapered steel plate girders based on the existing design rules in EN 1993-1-5 and considering the Resal effect obtained by the simplified model explained above is presented here.

The new proposal is valid for slender, rigid end-posted girders, whose slenderness parameter $\lambda_w > 1.8$. Moreover, in this part of the research according to the assumption made for the studied cases, the shear-bending interaction may be neglected. EN 1993-1-5 states that for the cases where the design bending moment M_{Ed} is smaller than the resistant moment of the cross-section consisting of the effective area of the flanges $M_{f,Rd}$, the shear-bending interaction can be omitted.

According to EN 1995-1-5 the design shear resistance $V_{b,Rd}$ for plate girders should be taken as:

$$V_{b,Rd} = V_{bw,Rd} + V_{bf,Rd} \tag{5.7}$$

where the contribution from the web is

$$V_{bw,Rd} = \frac{\chi_w\, f_{yw}\, h_w\, t_w}{\sqrt{3}\, \gamma_{M1}} \tag{5.8}$$

χ_w is the shear buckling reduction factor, f_{yw} - the yield stress of the flanges, h_w - the depth of the web panel, t_w – web thickness and γ_{M1} is the partial factor.

The contribution from the flanges is given by:

$$V_{bf,Rd} = \frac{b_f\, t_f^2\, f_{yf}}{c\, \gamma_{M1}} \left(1 - \left(\frac{M_{Ed}}{M_{f,Rd}}\right)^2\right) \quad \textbf{(5.9)}$$

where b_f is the flange width and t_f – the flange thickness.

In the last expression c is the distance between the plastic hinges in both flanges (**Eq. 5.10**):

$$c = a\left(0.25 + \frac{1.6\, b_f\, t_f^2\, f_{yf}}{t_w\, h_w^2\, f_{yw}}\right) \quad \textbf{(5.10)}$$

and f_{yw} is the yield stress of the web.

M_{Ed} is the design bending moment calculated in the central cross-section $M_{Ed} = a\, V_{Ed}$, and $M_{f,Rd}$ is the moment of resistance of the cross section consisting of the effective area of the flanges only.

Eqs. 5.11 and **5.12** show how to take into account the Resal effect when calculating the ultimate shear resistance of tapered plate girders. For typologies I and II the Resal effect is favourable and reduces the design value of the shear force V_{Ed}. Thus, the design shear resistance should be verified according to **Eq. 5.11**:

$$V_{Ed} - V_{Resal} < V_{b,Rd} = V_{bw,Rd} + V_{bf,Rd} \quad \textbf{(5.11)}$$

For typologies III and IV its influence is unfavourable increasing the external shear load (**Eq. 5.12**):

$$V_{Ed} + V_{Resal} < V_{b,Rd} = V_{bw,Rd} + V_{bf,Rd} \quad \textbf{(5.12)}$$

5.5.2.1. Contribution from the flanges

For tapered plate girders the depth h_w used to calculate the distance c in **Eq. 5.10** should be taken as the depth corresponding to the central cross-section when the design bending moment M_{Ed} is calculated. Consequently, for tapered plate girders from typologies I and II, the largest depth $h_w = h_1$ should be used and for typologies III and IV the smallest one $h_w = h_0$ (see **Fig. 5.1**).

5.5.2.2. Contribution from the web

For typologies I and II, the best assessment of their ultimate shear capacity is obtained when in **Eq. 5.8** for the contribution from the web, the depth h_w is substituted by the largest one $h_w = h_1$ (**Eq. 5.13**). The contribution from the web for typologies III and IV should be calculated using the smallest depth $h_w = h_0$ (**Eq. 5.14**).

$$V_{bw,Rd} = \frac{\chi_w \, f_{yw} \, h_1 \, t_w}{\sqrt{3}} \qquad \textbf{(5.13)}$$

$$V_{bw,Rd} = \frac{\chi_w \, f_{yw} \, h_0 \, t_w}{\sqrt{3}} \qquad \textbf{(5.14)}$$

From the comparison of the results given in **Table 5.4a** is easy to observe that ultimate shear resistance between various typologies of tapered plate girders may vary significantly. The ultimate shear strength V_u of girders belonging to typologies I and II is always higher than for the same girders from typologies III and IV. This difference can be caused by two important factors which are: the Resal effect, whose influence in case of typologies I and II is favourable and for typologies III and IV unfavourable, as well as the shear capacity of the web $V_{bw,Rd}$ (**Table 5.4a**).

Table 5.4a. Ultimate shear resistance for analysed prototypes. Pure shear.
Numerical results (FEM), results from the 1st proposal of Bedynek et al. (2013), results from the new proposal.

		girder	V_u (FEM) [kN]	Proposal Bedynek et al. 2013 V_u [kN]	Diff.(2) [%]	$V_{bw,Rd}$ [kN]	$V_{bf,Rd}$ [kN]	V_{Resal} [kN]	New proposal V_u [kN]	Diff.(3) [%]
typology I	A	480_800_800_4_180_15	364.8	310.5	**14.9**	268.4	42.0	20.6	331.0	**9.2**
		600_800_800_4_180_15	366.9	310.5	**15.4**	268.4	42.0	9.0	319.4	**12.9**
		680_800_800_4_180_15	365.6	310.5	**15.1**	268.4	42.0	3.4	313.8	**14.2**
	B	600_1200_2400_4_250_25	368.4	305.4	**17.1**	251.8	53.6	8.8	314.2	**14.7**
		850_1200_2400_4_250_25	367.9	305.4	**17.0**	251.8	53.6	3.2	308.6	**16.1**
typology II	A	480_800_800_4_180_15	335.4	310.5	**7.4**	268.4	42.0	20.6	331.0	**1.3**
		600_800_800_4_180_15	351.3	310.5	**11.6**	268.4	42.0	9.0	319.4	**9.1**
		680_800_800_4_180_15	354.8	310.5	**12.5**	268.4	42.0	3.4	313.8	**11.5**
	B	600_1200_2400_4_250_25	355.2	305.4	**14.0**	251.8	53.6	8.8	314.2	**11.5**
		850_1200_2400_4_250_25	361.7	305.4	**15.6**	251.8	53.6	3.2	308.6	**14.7**
typology III	A	480_800_800_4_180_15	221.0	186.3	**15.7**	177.5	39.3	14.4	202.4	**8.4**
		600_800_800_4_180_15	274.9	232.9	**15.3**	221.9	37.5	7.5	251.9	**8.4**
		680_800_800_4_180_15	310.4	263.9	**15.0**	251.5	38.9	3.2	287.2	**7.5**
	B	600_1200_2400_4_250_25	186.9	152.7	**18.3**	138.8	35.8	5.1	169.5	**9.3**
		850_1200_2400_4_250_25	263.5	216.3	**17.9**	196.6	45.3	2.5	239.4	**9.2**
typology IV	A	480_800_800_4_180_15	202.7	186.3	**8.1**	177.5	34.2	14.1	197.6	**2.5**
		600_800_800_4_180_15	263.3	263.9	**-0.2**	221.9	37.5	7.5	251.9	**4.4**
		680_800_800_4_180_15	300.5	232.9	**22.5**	251.5	38.9	3.2	287.2	**4.4**
	B	600_1200_2400_4_250_25	182.1	152.7	**16.1**	138.8	35.8	5.1	169.5	**6.9**
		850_1200_2400_4_250_25	259.0	216.3	**16.5**	196.6	45.3	2.5	239.4	**7.6**

The web contribution $V_{bw,Rd}$ for tapered plate girders has been evaluated by analysing the shear buckling factor χ_w for the reduction of the web from new 85 numerical simulations. The numerical values of χ_w have been obtained from **Eqs. 5.11** and **5.12**, subtracting from the numerical value of the ultimate shear resistance the contribution from the flanges (**Eq. 5.9**) obtained according to EN 1993-1-5. Thus, the expression for χ_w for typologies I and II stays unchanged (**Eq. 5.15**) and for typologies III and IV is given by **Eq. 5.16**.

$$\chi_w = \frac{1.37}{(0.7 + \bar{\lambda}_w)} \tag{5.15}$$

Here, it is important to point out that for all typologies of tapered plate girders, the slenderness parameter $\bar{\lambda}_w$, is always calculated as a simply supported rectangular panel with its largest depth, regardless of the typology.

Numerical results for the shear buckling factor are presented in **Figs. 5.6a-b** and compared with the actual proposal in EN 1993-1-5.

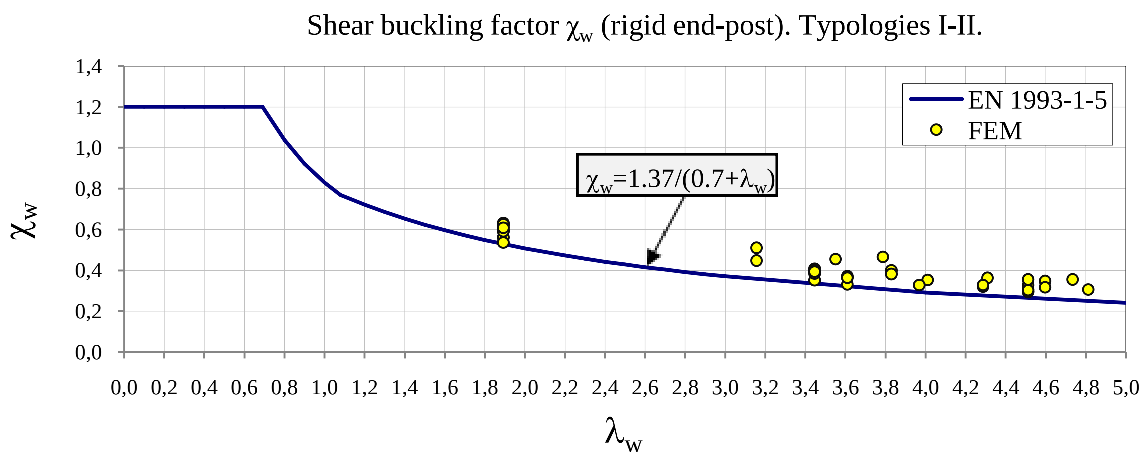

Fig. 5.6a. New proposal for the factor χ_w for end-posted, slender, tapered panels for typologies I-II.

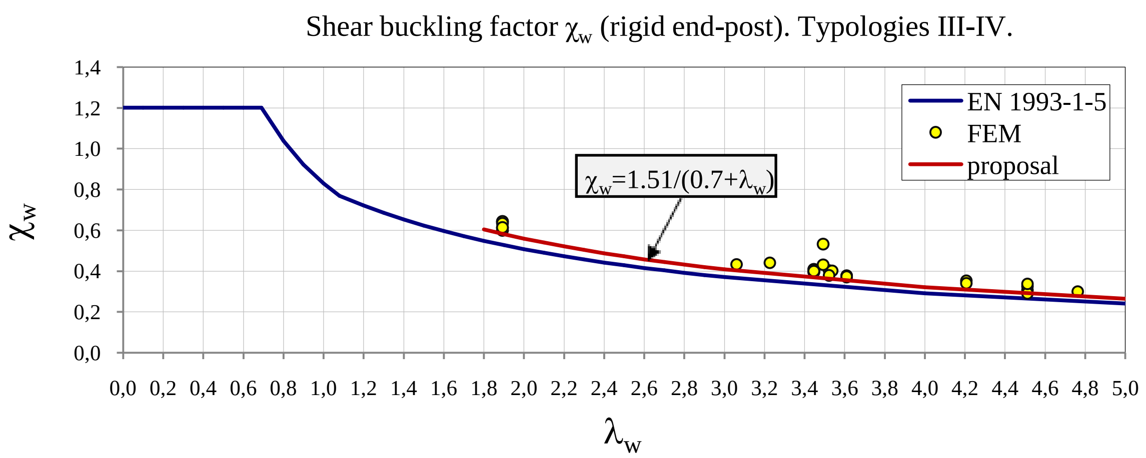

Fig. 5.6b. New proposal for the factor χ_w for end-posted, slender, tapered panels for typologies III-IV.

As it can be observed in **Fig. 5.6a**, the expression for calculating the reduction factor χ_w (**Eq. 5.15**) proposed in EN 1995-1-3 gives good approximation for end-posted tapered girders for typologies I and II whose slenderness parameter $\bar{\lambda}_w \geq 1.8$.

On the other hand, from the results shown in **Fig. 5.6b**, it is possible to find a better adjustment of the shear buckling factor χ_w for tapered plate girders belonging to typologies III and IV. From the numerical analyses of above 40 end-posted tapered plate girders with the slenderness parameter $\bar{\lambda}_w \geq 1.8$ belonging to typologies III and IV, it is concluded that better approximation (**Fig. 5.6b**) may be achieved by using the modified value of the shear buckling factor χ_w given by (**Eq. 5.16**):

$$\chi_w = \frac{1.51}{(0.7 + \bar{\lambda}_w)} \tag{5.16}$$

5.6. Analysis of the results

5.6.1. Shear

Based on the same examples of the girders presented in **Table 5.3**, the results for the ultimate shear resistance V_u obtained according to three different methods are compared in **Table 5.4a**. The values shown in the first column $V_{u\ (FEM)}$ come from the numerical analysis and they are compared with the proposal by Bedynek et al. (2013), in column "Diff. $_{(2)}$". The following columns represent the contribution from the web $V_{bw,Rd}$, contribution from the flanges $V_{bf,Rd}$ and the Resal effect V_{Resal} calculated according to the proposal. The final values of the ultimate shear strength can be found in the column called V_u (new proposal) and in the last one "Diff.$_{(3)}$" these values are compared with the numerical ones. The data from **Table 5.4a** refers only to several examples of the studied girders.

The results for the 85 girders obtained according to three methods: EN 1993-1-5, the proposal by Bedynek et al. (2013) and the new one are presented in **Fig. 5.7** and compared with the results derived from the numerical simulations.

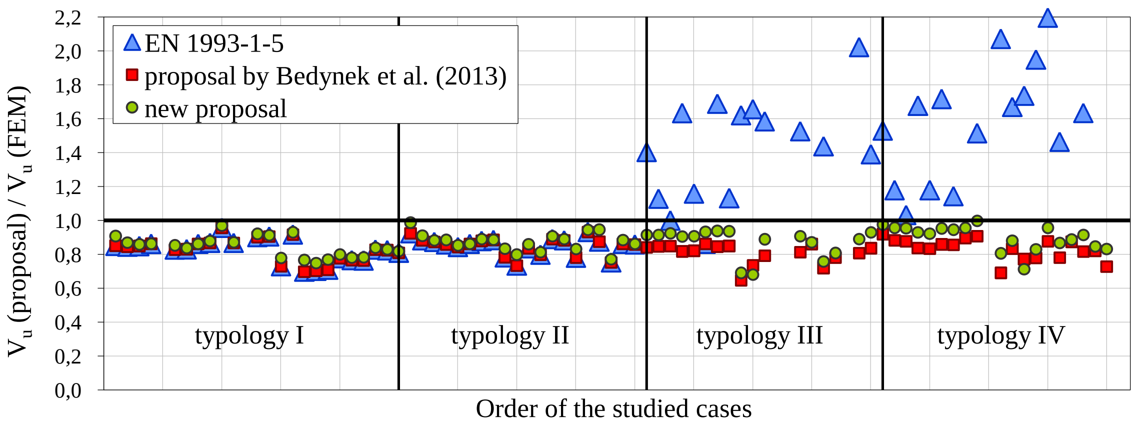

Fig. 5.7. Comparison of the results obtained according to EN 1993-1-5, the proposal by Bedynek et al. (2013) and the new proposal.

Significant improvement caused by applying the new proposal is especially noticeable for typologies III and IV. As it can be observed all values of the ultimate shear strength obtained according to the new proposal are on the safe side and show very good agreement with the numerical tests.

In **Fig. 5.8** a statistic distribution of the difference between the numerical results and those obtained according to the new proposal are shown. Almost for all cases these differences does not exceed 25%. Only for 3 from 85 studied girders (3.5% of all tests) the difference is greater than 25%, but always less than 35%. For 72% of studied girders the differences are smaller than 15% what confirms very good accuracy of the new proposal.

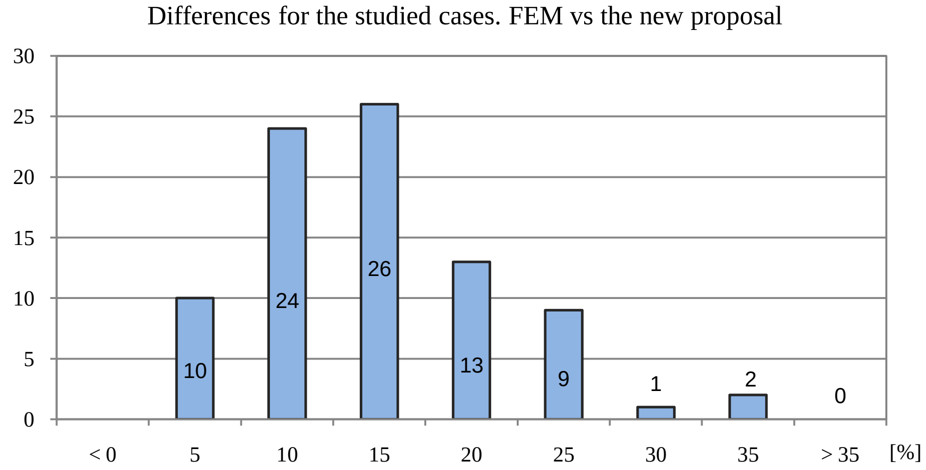

Fig. 5.8. Statistic distribution of the differences between the numerical results and those obtained according to the new proposal.

The verification of the new proposal also was conducted using the experimental data from three of the four tests under pure shear load presented in Bedynek et al. (2013). The results are presented in **Table 5.4b**, and the differences oscillate between 12.5-16.5%.

Table 5.4b. Ultimate shear resistance for analysed prototypes.Tests results and the new proposal.

	girder*	V_u (test) [kN]	$V_{bw,Rd}$ [kN]	$V_{bf,Rd}$ [kN]	V_{Resal} [kN]	New proposal V_u [kN]	Diff.(4) [%]
typ. I	600_800_800_3.9_180_15	392.0	271.4	46.9	9.2	327.5	**16.5**
	500_800_1200_3.9_180_15	320.5	244.9	27.7	7.9	280.5	**12.5**
	480_800_800_3.9_180_15	388.2	256.9	42.5	19.9	339.4	**12.6**

* All tested girders were made of steel S275.

5.6.2. Shear-bending interaction

5.6.2.1. EN 1993-1-5

For the cases where the design bending moment M_{Ed} is higher than the moment of resistance of the cross-section consisting of the effective area of the flanges $M_{f,Rd}$ and less than the plastic moment of the resistance of the cross-section $M_{pl,Rd}$ ($M_{f,Rd} < M_{Ed} < M_{pl,Rd}$), the shear-bending interaction should be considered. According to EN 1993-1-5, if $V_{Ed} > 0.5V_{bw,Rd}$ the combined effects of bending and shear in the web of a I girder should satisfy (**Eq. 5.17**).

$$\frac{M_{Ed}}{M_{pl,Rd}} + \left(1 - \frac{M_{f,Rd}}{M_{pl,Rd}}\right)\left(\frac{2V_{Ed}}{V_{bw,Rd}} - 1\right)^2 = 1 \qquad \textbf{(5.17)}$$

Some numerical analyses considering shear-bending interaction in tapered steel plate girders for the four different typologies studied in this research has been conducted and the results are presented in the next section.

5.6.2.2 Comparison of the results

In order to check the validity of the new proposal for tapered plate girders under shear-bending interaction, twelve new cases, three for each typology were examined. It is necessary to mention that the situation where influence of bending moment on the ultimate shear is significant and may lead to its reduction is not very common. It happens due the fact that design bending moment M_{Ed} derives from the vertical reaction in the one of supports (ultimate shear force) and in order to achieve its relevant level, tapered girders have to possess considerable length and relative low flexural resistance of the flanges which normally is not recommended from the design point of view.

In this section, the geometries of the studied girders were designed in order to fulfil condition about the design bending moment at the mid-cross-section (calculated as a distance *a* multiplied by V_u) which should be greater than the moment of resistance of the cross-section consisting of the effective area of the flanges, $M_{Ed} > M_{f,Rd}$ and $V_{cr} < V_u$.

The values of $V_{u\ red}$ (**Table 5.5**) were calculated with the same reduction factors as it has been explained before: $\chi_w = \frac{1.37}{(0.7+\bar{\lambda}_w)}$ for typologies I and II, and $\chi_w = \frac{1.51}{(0.7+\bar{\lambda}_w)}$ for typologies III and IV. Also the influence of the Resal effect V_{Resal} was considered.

In the first three columns of **Table 5.5** a comparison of the results obtained numerically $V_{u\ (FEM)}$ and those calculated according to unmodified method proposed in EN 1993-1-5 ($V_{u\ (EN)}$) are shown. Next, some extra data such as: the bending resistance of the flanges $M_{f,Rd}$, the design bending moment M_{Ed}, the contributions from the web $V_{bw,Rd}$ and flanges $V_{bf,Rd}$ and the

Resal force V_{Resal} were calculated according to the new proposal and are presented in the following columns. Finally, in the last two columns the reduced ultimate shear strengths $V_{u,red}$ are compared with their corresponding numerical values $V_{u\,(FEM)}$.

Table 5.5. Ultimate shear resistance for analysed prototypes. Shear-bending interaction.

typology	girder	V_u (FEM) [kN]	V_u (EN) [kN]	Diff.(1) [%]	New proposal $M_{f,Rd}$ [kNm]	M_{Ed} [kNm]	$V_{bw,Rd}$ [kN]	$V_{bf,Rd}$ [kN]	V_{Resal} [kN]	$V_{u\,red}$ [kN]	Diff.(3) [%]
I	600_1100_2500_5_180_15	336.5	327.6	**2.6**	707.5	819.1	332.0	0.0	6.2	333.9	**0.8**
	600_1000_4000_5_250_20	332.0	312.1	**6.0**	1198.5	1248.4	313.8	0.0	1.5	313.7	**5.5**
	800_1200_6000_6.5_400_25	545.0	511.9	**6.1**	2878.8	3071.7	516.8	0.0	1.1	513.1	**5.9**
II	600_1100_2500_5_180_15	336.6	327.6	**2.7**	707.5	819.1	332.0	0.0	6.2	333.9	**0.8**
	600_1000_4000_5_250_20	347.2	312.1	**10.1**	1198.5	1248.4	313.8	0.0	1.5	313.7	**9.7**
	800_1200_6000_6.5_400_25	549.5	511.9	**6.8**	2878.8	3071.7	516.8	0.0	1.1	513.1	**6.6**
III	1100_600_2500_5_180_15	190.5	327.6	**-72.0**	390.2	493.7	199.6	0.0	3.8	193.7	**-1.7**
	1000_600_4000_5_250_20	206.0	312.1	**-51.5**	728.5	823.1	207.5	0.0	1.0	204.7	**0.6**
	1200_800_6000_6.5_400_25	366.8	511.9	**-39.6**	1938.8	2249.1	379.8	0.0	0.8	374.0	**-2.0**
IV	1100_600_2500_5_180_15	219.0	327.6	**-49.6**	390.2	493.7	199.6	0.0	3.8	193.7	**11.5**
	1000_600_4000_5_250_20	236.2	312.1	**-32.1**	728.5	823.1	207.5	0.0	1.0	204.7	**13.3**
	1200_800_6000_6.5_400_25	426.5	511.9	**-20.0**	1938.8	2249.1	379.8	0.0	0.8	374.0	**12.3**

Relevant improvement for typologies III and IV is observed when the contribution from the web is calculated according to **Eq. 5.14** and when the Resal effect is taken into account. For typologies I and II this improvement is not so significant. Consideration of the Resal effect brings the values of $V_{u,\,red}$ closer comparing to the numerical solution for all examined cases.

In general, it can be observed that results obtained according to the new proposal give a very good agreement with the numerical ones, and only for typology III, the values of the ultimate shear resistance are slightly overestimated (not greater than 2%). When calculating $V_{u,red}$, the partial factor of the safety, normally included in design codes, was not taken into account, so its application may bring unsafe values of $V_{u,red}$ on the safe side.

In **Fig. 5.9** a graphical comparison of the obtained results is shown. As it was mentioned before for typologies I and II, the benefits from the application of the new proposal are observed in all cases, however the improvement is rather small (up to 2%).

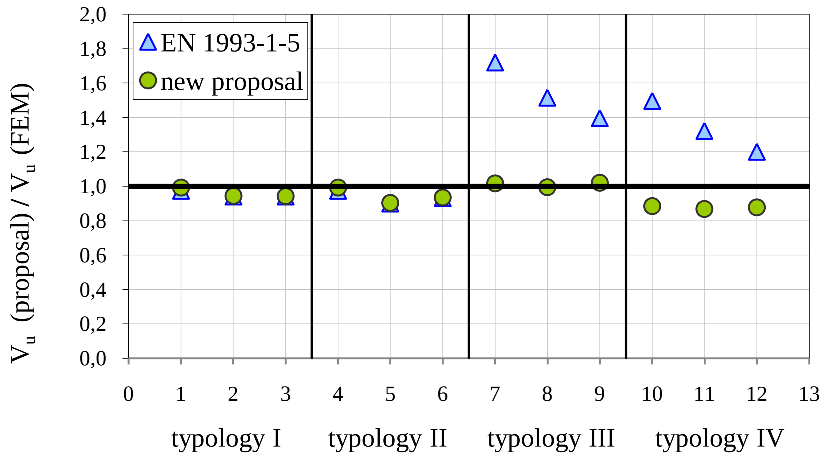

Fig. 5.9. Comparison of the results obtained according to EN 1993-1-5 and the new proposal.

On the other hand, for typologies III and IV the use of the new proposal improves the results and gives a good assessment for the ultimate shear resistance.

5.7. Conclusions

In this paper the structural response of tapered steel plate girders subjected to shear and shear-bending interaction has been studied. Numerical research has considered four different typologies of such girders which have been studied separately.

A new proposal for the assessment of the ultimate shear resistance of tapered steel plate girders on the existing design rules in EN 1993-1-5 and considering the Resal shear value obtained by a simplified model has been presented.

A simplified model to obtain the value of the shear load produced by the Resal effect has been presented, then the shear force acting in the web can be reduced in typologies I and II or increased in typologies III and IV when verifying the shear resistance of the web.

Based on the results obtained from 85 numerical simulations (approx. 20 for each typology) some modifications in expressions proposed by EN 1993-1-5 for rectangular plate girders were made for their application to tapered plate girders. First, the value of the depth used when determining the contribution of the web and used to calculate the distance c between two plastic hinges in the flange has been defined as $h_w = h_1$ for typologies I and II or $h_w = h_0$ for typologies III and IV.

Moreover, a new adjustment of the reduction factor χ_w has been presented for typologies III and IV.

A very good agreement between the results obtained according to the new proposal $V_{u\,(proposal)}$ and numerically $V_{u\,(FEM)}$ is observed. In the case where the shear-bending interaction is not considered, the differences between the values of the ultimate shear strength $V_{u\,(FEM)}$ and $V_{u\,(proposal)}$ do not exceed 33%, whereas in most cases these differences are less than 15%.

The same design proposal was applied for tapered steel plate girders subjected to shear-bending interaction. Due to presence of the significant bending moments at the central cross-section, an additional reduction of the ultimate shear resistance had to be done. Validation of the new proposal was carried out for 12 girders, 3 from each typology. Also here, a good agreement between the results obtained numerically and these calculated according to the proposal was observed. A significant improvement of the results was especially visible for typologies III and IV.

Presented design proposal not only provides a satisfactory tool for the assessment of the ultimate shear resistance of tapered steel plate girders but also reveals its physical interpretation and respects individual contributions of all parts. Therefore, with use of the proposed method all components of the ultimate shear strength of the whole girder such as: the contribution from the web and flanges or Resal force can be found. This improvement was possible especially thanks to division of tapered plate girders into four different typologies which required an individual analysis according to their geometry.

It is important to point it out that the main objective of this proposal is not thought to substitute or change the existing rules EN 1993-1-5 for rectangular plate girders, but only to give a simplified algorithm to assess an approximated value of the ultimate shear resistance of tapered members with considerable slope of the inclined flange. It is strongly recommended to treat the proposal as a reference and for the cases where the high precision is required an additional numerical study of specific girder is needed.

6. *Conclusions and future work*

6.1. General conclusions

In this chapter the most important conclusions derived from the thesis and future research lines are pointed out.

The main goal of this thesis was the development of a design proposal which could be useful in assessment of the ultimate shear capacity of tapered steel plate girders. Searching for coherent analytical solutions, it was important to find the optimal solution between two important factors which were: complexity and accuracy. In fact, the ideal solution would connect simplicity of the application with high satisfactory precision and safety.

The main aim of this research was to study tapered steel plate girders without longitudinal stiffeners, subjected to shear. It is important to clarify that pure shear practically does not occur in reality and shear force is always accompanied at least by bending moment derived from reaction force. Nevertheless, for all studied cases its value is very small, comparing to shear force, and according to EN 1993-1-5 its influence can be neglected.

All considerations and conclusions made in this work concern rigid end-posted slender ($\bar{\lambda}_w \geq 1.08$) tapered plate girders with aspect ratio $\alpha \geq 1.0$, whose critical shear load is smaller than the ultimate shear strength. These limitations are justified by the fact that this kind of girders is the most common among the real structural elements.

For purposes of the research a new realistic 3D finite element model was developed and after its validation against the experimental results, it was used for the parametric studies. Consequently, based on the numerical results and actual expressions for prismatic plates included in EN 1993-1-5, four new approaches for each typology of tapered steel plate girders were proposed. Moreover, a new physical model for assessment the Resal effect was developed and the influence of this phenomenon was taken into account in the final proposal for the ultimate shear resistance of tapered steel plates.

Numerous simulations and experimental tests confirmed a good accuracy of the proposal for any geometry of tapered panels. Suggested solution was developed according to actual design rules of EN 1993-1-5 which are based on the Rotated Stress Field Method. Therefore, the final product of this work was to provide a reliable and easy-to-use design procedure for all kinds of unstiffened non-prismatic web-panels in the above-mentioned range. Finally, it can be concluded that the principal aim of this thesis has been covered successfully.

6.2. Specific conclusions

Apart from the main objective, some different issues related to tapered steel plate girders were studied.

1. *Searching for shear buckling coefficient for tapered plates*:

Therefore, the content of the second paper is entirely focused on searching for shear buckling coefficients for different typologies of simply-supported tapered steel plates. The proposal, which consists of four analytical expressions, can be used in assessment of the critical shear load for non-prismatic simply-supported plates. Its estimation is often necessary in case of fatigue problems caused by web-breathing of very slender web-panels. In this study many geometric parameters such as: the aspect ratio, the slope of the inclined flange and the web thickness were taken into consideration. For simplification a numerical model of the web-panel without flanges was assumed. Instead of them, on both edges (bottom and upper) simply supported boundary conditions were assumed. Due to the weaker boundary conditions, this approach also may lead to underestimation of the critical shear load, however always gives results on the safe-side and they are much closer to their actual value comparing with the solution obtained for simply-supported rectangular plates. In this way, considering a real shape of tapered plate, proposed expressions allow for more realistic assessment of the critical shear load of non-prismatic members.

2. *Influence of structural imperfections (residual stresses) on the ultimate shear resistance of tapered steel plate girders*:

The following issue with secondary importance studied in this research was the influence of the structural imperfections such as residual stresses appeared during the fabrication process. For this purpose, one well know pattern of the distribution of initial stresses caused by flame cutting and welding was applied in various numerical models. Small differences (less than 2%) between ultimate shear capacities of girders with- and without structural imperfections allowed concluding that this kind of structure is not very susceptible to the influence of the residual stresses and their omission does not cause significant deviation of the results (the studies were carried out for slender tapered plate girders).

3. *Optimal position of the longitudinal stiffening and its minimum rigidity*:

Next point discussed in this work concerned studies on the position of the longitudinal stiffener and its minimum rigidity. To this end, four different positions of stiffening for various geometries of tapered plate girders were considered. The results derived from the numerical model were compared with those obtained for an unstiffened panel. It was concluded that the optimal position of the longitudinal stiffener may be different depending on the stress-state in the web-panel and is conditioned by influence of bending. Generally, it was observed that position of the longitudinal stiffener had not significant influence on the ultimate shear resistance of the analyzed girders. Also an approximated value for the minimum rigidity of the stiffening which can be used as a reference was established.

4. *Ultimate shear resistance model*:

The last and probably the most important issue studied in this research was the development of the analytical model for calculating the ultimate shear resistance of tapered plate girders belonging to any typology and with arbitrary geometry. There was make an effort to find reliable design tool which would be easy in use but with enough accuracy and fulfilling the safety requirements. Proposed model is based on the existing and currently valid method for prismatic plate girders. Modifications consist of the consideration of the trapezoidal shape of tapered panels and the Resal force appearing in the inclined flange of such tapered members.

6.3. Future work

In this thesis several important issues related to tapered steel plate girders are widely discussed and some new solutions are proposed. The main effort was done in order to understand differences in behaviour of prismatic and non-prismatic members and include them in design expressions. In the work, some studies on the second-rate topics were carried out and their development would be interesting and recommended.

Future research lines:

1. *Study on shear-bending interaction for larger values of the bending moment*:

In this research only several geometries of tapered plate girders were subjected to study. However, the ultimate shear strength obtained according to the proposal, developed for members only subjected to shear, seemed to be appropriate also for girders subjected to shear-bending interaction. In any case, it would be recommended to carry out an additional parametric study for wide range of the geometric parameters and various combinations of shear-bending. Eventually, for these cases whose resistance would be overestimated, a new adjustment of the presented method might be necessary.

2. *Extension of the proposal for tapered steel plate girders with* aspect ratio $\alpha < 1$:

All considerations included in the papers concerned tapered plate girders with aspect ratios $\alpha \geq 1$ which application in real structures is probably the most frequent. In order to cover remaining range of α, as a future line of research some experimental and parametric studies on the behaviour of shorter panels would be recommended and new analytical expressions for calculating their ultimate shear resistance could be developed.

3. *Design expressions for tapered steel plate girders with multiple longitudinal stiffeners subjected to shear*:

In the third paper some experimental and numerical studies on the position of the longitudinal stiffener and its rigidity were done. The numerical results were referred to the method proposed in EN 1993-1-5 and speaking more precisely to its interpretation for non-prismatic plates. Due to the excessive geometrical imperfections observed in two from four tested girders, full experimental results were obtained only for two of them which were less influenced by them. For this reason it could be interesting to conduct new experimental tests of tapered steel plate girders with multiple longitudinal stiffeners placed in various positions. Numerical studies in wide-range of geometric parameters would be useful in finding answers for unsolved issues related to longitudinal stiffening such as: optimal position of the longitudinal stiffeners, criterion for minimal required rigidity necessary to obtain an assumed improvement of the ultimate shear resistance or overall optimization of the geometry of tapered panel.

4. *Behaviour of plates which critical shear load is greater than ultimate shear resistance and slenderness smaller than* 1.8:

The content of this thesis is focused on a particular kind of tapered plate girders whose elevated slenderness allows observing specific behaviour of such members. The slenderness is strictly related to the capacity of tapered plate girders to develop a post-buckling resistance. Thus, to be able to observe this phenomenon, the geometries of all girders taken into consideration were designed so that the critical shear load would be always smaller than the ultimate shear resistance. Otherwise, completely different behaviour of tapered plate girders would be expected. A structural response of stocky plate girders was not a subject of this study.

For that reason it would be interesting to conduct a new research focused on the ultimate shear resistance of less slender tapered plate girders and at the same time to extend the existing expressions for any geometry.

References

Abu-Hamd M, Abu-Hamd I. 2011. Buckling strength of tapered bridge girders under shear and bending. In: Proceedings of the annual stability conference. Structural stability research council, Pittsburgh, Pennsylvania; 10–14 May, 2011.

Barth K, White D. 1998. Finite element evaluation of pier moment-rotation characteristics in continuous-span steel I-girders. Engineering Structures 20(8): 761–778.

Basler K. 1960. Strength of Plate Girders in Shear. Lehigh University, Bethlehem, PA, USA, Fritz Engineering Laboratory Report 251-320.

Bedynek A, Real E and Mirambell E. 2011. Tapered steel plate girders. Experimental and numerical investigation on shear and shear-bending interaction. Proceedings of 6th European Conference on Steel and Composite Structures, Budapest, Hungary (Dunai L et al. (eds)). ECCS, Brussels, Belgium, pp. 765–770.

Bedynek A, Real E, Mirambell E. 2013. Tapered plate girders under shear: Tests and numerical research. Engineering Structures 46: 350-358.

CEN (Comité Européen de Normalisation). 2006. EN 1993-1-5. Eurocode 3: Design of steel structures, Part 1-5. Plated structural elements. CEN, Brussels, Belgium.

CEN (Comité Européen de Normalisation). 2006. EN 1993-2. Eurocode 3: Design of steel structures, Part 2. Steel bridges. CEN, Brussels, Belgium.

Chern C and Ostapenko A. 1969. Ultimate Strength of Plate Girders Under Shear. Lehigh University, Bethlehem, PA, USA, Fritz Engineering Laboratory Report 328.7.

Cooper PB. 1967. Strength of longitudinally stiffened plate girders. Journal of Structural Division. Proceedings of the American Society of Civil Engineers. ST2. 67: 419-451.

Davies G and Mandal SN. 1979. The collapse behaviour of tapered plate girders loaded within the tip. Proceedings of the Institution of Civil Engineers, Part 2, 67(3): 65–80.

Dassault Systemes. 2010. Abaqus/Standard V.6.8. Simulia Products. Dassault Systemes S.A., Vélizy-Villacoublay, France.

Estrada I, Real E, Mirambell E. 2007a. General behaviour and effect of rigid and non-rigid end post in stainless steel plate girders loaded in shear. Part I: Experimental study. Journal of Constructional Steel Research 63(7): 15.

Estrada I, Real E, Mirambell E. 2007b. General behaviour and effect of rigid and non-rigid end post in stainless steel plate girders loaded in shear. Part II: Extended numerical study and design proposal. Journal of Constructional Steel Research 63(7): 12.

Estrada I, Real E, Mirambell E. 2008. A new developed expression to determine more realistically the shear buckling stress in steel plate structures. Journal of Constructional Steel Research 64(7–8): 737–747.

Estrada I, Real E, Mirambell E. 2008. Shear resistance in stainless steel plate girders with transverse and longitudinal stiffening. Journal of Constructional Steel Research 2008; 64: 1239-1254.

Evans HR. 1983. Longitudinally and transversely reinforced Plate Girders. Plated Structures, Stability and Strength, R. Narayanan, ed. Applied Science Publishers, London and New York.
1-37.

Evans HR, Tang KH. 1984. The influence of Longitudinal Web Stiffeners Upon the Collapse Behaviour of Plate Girders. Journal of Construction Steel Research, Vol. 4. 201-234.

Falby WE, Lee GC. 1976. Tension field design of tapered webs. Eng J, AISC: 11–17.

Florida Department of Tarnsportation. 2008. “New Directions for Florida Post-Tensioned Bridges”, Final report Volume 10 A, Load Rating Post-Tensioned Concrete Segmental Bridges.

Galambos TV, editor. 1998. Guide to stability design criteria for metal structures. J.Willey&Sons.

Günther HP and Kuhlmann U. 2004. Numerical studies on web breathing of unstiffened and stiffened plate girders. Journal of Constructional Steel Research 60(3-5): 549–559.

Höglund T. 1971. Behavior and Strength of the Web of Thin Plate I-girders. Division of Building Statics and Structural Engineering, Royal Institute of Technology, Stockholm, Sweden, Bulletin 93.

Höglund T. 1995. Strength of steel and aluminium plate girders – shear buckling and overall web buckling of plane and trapezoidal webs. Comparison with tests. Technical report no. 4 Stockholm: Royal Institute of Technology, Department of Structural Engineering.

Höglund T. 1997. Shear buckling resistance of steel and aluminium plate girders. Thin-Wall Structures; 29(1–4): 13–30.

Johansson B, Maquoi R, Sedlacek G. 2001. New design rules for plated structures in Eurocode 3. Journal of Constructional Steel Research; 57: 279-311.

Johansson B, Maquoi R, Sedlacek G, Müller C, Beg D. 2007. Commentary and worked examples to EN 1993-1-5 “Plated structural elements”. JRC Scientific and Technical Reports; 52-73.

Lee SC, Davidson JS, Yoo CH. 1996. Shear buckling coefficients of plate girder web panels. Comput Struct; 59(5): 789–795.

Maquoi R. and Skaloud M. 2000. Stability of plates and plated structures. General Report. Journal of Constructional Steel Research 55 (2000) 45-68.

Mirambell E and Zárate V. 2000. Web buckling of tapered plate girders. Proceedings of the Institution of Civil Engineers – Structures and Buildings 140(1): 51–60.

Pavlovčič L, Detzel A, Kuhlman U, Beg D. 2007a. Shear resistance of longitudinally stiffened panels – Part 1: Tests and numerical analysis of imperfections. Journal of Constructional Steel Research; 63: 337-350.

Pavlovčič L, Beg D, Kuhlman U. 2007b. Shear resistance of longitudinally stiffened panels – Part 2: Numerical parametric study. Journal of Constructional Steel Research; 63: 351-364.

Porter DM, Rockey KC and Evans HR. 1975. The collapse behavior of plate girders loaded in shear. The Structural Engineer 53(8): 313–325.

Real E, Bedynek A and Mirambell E. 2010. Numerical and experimental research in tapered steel plate girders subjected to shear. Proceedings of SDSS’ Rio 2010 International Colloquium on Stability and Ductility of Steel Structures, Rio de Janeiro, Brazil, pp. 747–754.

Roberts TM, Newmark CB. 1997. Shear strength of tapered aluminium plate girders. Thin-Wall Struct;29(1–4): 47–58.

Rockey KC, Evans HR, Porter DM. 1974. The ultimate shear load behaviour of longitudinally reinforced plate girders. Proceedings of the Symposium on Structural Analysis, Non-Linear Behaviour and Techniques, TRRL: 163-174.

Rockey KC and Škaloud M. 1972. The ultimate load behaviour of plated girders loaded in shear. The Structural Engineer 50(1): 29–47.

Saliba, N and Gardner L. (2013). Testing and design of lean duplex stainless steel plate girders. Engineering Structures. 46, 375-391.

Saliba N, Real E, Gardner L. (2013). Shear design recommendations for stainless steel plate girders. Engineering Structures. 59, 220–228.

Samartín A F. 1993. “Cálculo de estructuras de puentes de hormigón”. Editorial Rueda, Madrid, Spain, p.132-135.

Shanmugam NE, Min H. 2007. Ultimate load behaviour of tapered steel plate girders. Steel Compos Struct; 7(6): 469–486.

Skaloud, M. 1983. Optimum rigidity of stiffeners of webs and flanges, Plated Structures: Stability and Strength, Narayanan, R.ed., Applied Science Publishers, London. 103-134.

Takeda H, Mikami I. 1987. Ultimate strength of plate girder with varying depth loaded in shear. J Struct Eng; 33A: 115–126.

Ostapenko A, Chern C. 1971. Ultimate strength of longitudinally stiffened plate girders under combined loads. Proceedings colloquium on design of plate and box girders for ultimate strength: 301-313.

Zárate AV. 2002. PhD Thesis “Un modelo para dimensionamiento de vigas armadas de inercia variable de alma esbelta ”, Universitat Politècnica de Catalunya, Barcelona, Spain.

Zárate AV, Mirambell E. 2004. Shear strength of tapered steel plate girders. Proc Inst Civil Eng – Struct Build; 157(SB5): 343–354.